UNIVERSITY
COLLEGE
LONDON

INTERFEROMETRIC INVERSE SYNTHETIC APERTURE RADAR

Theodoros G. Kostis

Department of Electrical & Electronic Engineering

UNIVERSITY OF LONDON
University College London

Submitted to University College London in partial fulfilment of the requirements for the degree of Master of Science

DECLARATION

This report has been submitted for assessment towards a Master of Science Degree in Microwaves and Optoelectronics to the Department of Electronic and Electrical Engineering, UNIVERSITY COLLEGE LONDON, Torrington Place, LONDON WC1E 7JE.

T. Kostis

ACKNOWLEDGEMENTS

ΣΤΟΝ ΠΑΤΕΡΑ ΜΟΥ ΓΕΩΡΓΙΟ

ΤΗΣ ΔΙΚΑΙΟΣΥΝΗΣ ΗΛΙΕ ΝΟΗΤΕ
ΚΑΙ ΜΥΡΣΙΝΗ ΕΣΥ ΔΟΞΑΣΤΙΚΗ
ΜΗ ΠΑΡΑΚΑΛΩ ΣΑΣ ΜΗΝ ΛΗΣΜΟΝΑΤΕ ΤΗΝ ΧΩΡΑ ΜΟΥ.

ΑΕΤΟΜΟΡΦΑ ΤΑ ΕΧΕΙ ΤΑ ΨΗΛΑ ΒΟΥΝΑ
ΣΤΑ ΗΦΑΙΣΤΕΙΑ ΚΛΙΜΑΤΑ ΣΕΙΡΑ
ΚΑΙ ΤΑ ΣΠΙΤΙΑ ΠΙΟ ΛΕΥΚΑ
ΣΤΟΥ ΓΛΑΥΚΟΥ ΤΟ ΓΕΙΤΟΝΕΜΑ.

- ΟΔΥΣΣΕΑΣ ΕΛΥΤΗΣ.

Τον άντρα τον πολύτροπο πες μου, θεά, που χρόνια
παράδερνε, σαν πάτησε της Τροίας τ' άγιο κάστρο,
κι ανθρώπων γνώρισε πολλών τους τόπους και τη γνώμη
κι έπαθε πλήθος συμφορές στα πέλαγα, ζητώντας
πώς στην πατρίδα του ΑΒΛΑΒΟΣ να πάει με τους συντρόφους.

- *Ομήρου Οδύσσεια, Στίχος 1-5.*

This project would not have been possible without the consistent advice and constant support of Prof. Hugh Griffiths of University College London and Prof. Chris Baker of DERA Malvern.

My further appreciation to Dr. Goran Bezanov and Dr. Colin Lunn of South Bank University for providing me with strong foundations in order to be able to attempt engineering projects of considerable magnitude.

My gratitude to Maria Diakaki who changed the values of the TEST Model to come with the MORE Model in the simulations section. With her essential help productive results were ready by early August.

Special thanks go to my lifelong friends Pete Delimaras, George Koutsoulis, Kostas Pliakos and Kostas Kefalas.

Finally I wish to sincerely thank my father George, my mother Maria and my sister Lilla in Athens, Greece for being the wonderful people they are.

0. ABSTRACT

The aim of the project is to investigate methods of obtaining the height (third) dimension of a moving target scene. First the target height acquisition process using interferometric methods is evaluated. Then a two-dimensional plane representing the target extent is acquired using Inverse Synthetic Aperture Radar (ISAR) methodology. The challenge of the project is to associate the two methods above by combining their relevant parts leading to the Interferometric Inverse Synthetic Aperture Radar (InISAR) concept. Finally the image quality obtained by the InISAR method is analysed, simulated and documented.

The need for this project is connected with the ever demanding requirement for accurate target identification as friend or foe involving great distances between radar and target. Since this project finds better application in ship imaging the German battleship Bismarck laid down in 1936 and launched on the 14th February, 1939 by Blohm and Voss shipyards at Hamburg was used as the target structure. Trying to locate Bismarck in the Atlantic Ocean an air assault from H.M.S. Ark Royal aircraft was mistakenly made on H.M.S. Sheffield underlining the importance of correct target identification. Sixty years have passed since Bismarck was sunk by the British Royal Navy on the 27th of May, 1941.

1. CONTENTS

1.1. Index of Tables

1.2. Index of Figures

1.3. Index of Equations

2. INTRODUCTION

Griffiths [01] states that the concept of Synthetic Aperture Radar (SAR) is a significant airborne radar technology used for the generation of topographic maps of fine quality. Moreover these maps serve as a high resolution visual tool for remote sensing as details on the ground can be easily understood and can be further processed. On the other hand rotating targets cannot be clearly focused exactly because their rotational motion is counterproductive to the overall SAR concept. Stimson [07] (435) explains that the differential Doppler shifts involved are defocusing the synthetic array and result in a blurred or displaced from its actual position image.

Interferometric SAR (InSAR) as explained by Franceschetti [08] (167) is a method used to reconstruct the Digital Elevation Model (DEM) of the observed area. The same scene is simultaneously observed from two slightly different angles which provide a stereoscopic image. The main steps in the InSAR process is image registration, phase unwrapping and geocoding that lead to a DEM in applications like cartographic reference systems.

Baker [04] (1) states that Spotlight SAR is a limiting case of the SAR model. Now the region of interest is continuously tracked. The final resolution is dependent on the Dwell Time of the radar beam and not on the physical dimensions of the antenna.

Inverse Synthetic Aperture Radar (ISAR) as referenced by Baker [05] (190) is a well established SAR dual where the radar remains stationary and the target is in motion. Analytically this method is used to identify the reflectivity centres that synthesise the radar cross section (RCS) of airborne targets having a rotational motion.

Unfortunately there exist problems in forming a correctly focused ISAR image. Griffiths [01] states that there are two cases, co-operative ISAR where the target rotation is known and non co-operative ISAR in which the target motion is the unknown variable that needs to be estimated. In the latter case the task is further complicated by the degrees of freedom the target is using while rotating through a three-dimensional space.

ISAR provides very high spatial resolution only in the X (slant range) and Y (cross range) directions. In other words the major disadvantage of a 2D-ISAR process is that it cannot determine the height of each scattering centre on the target. Therefore with an ISAR process only a two-dimensional (2D) reflectivity map of the target's signature data, acquired as a function of frequency and azimuth angle, is projected on a plane determined by the rotation vector. And this project investigates the possibility of coupling extra interferometry data to the projected 2D-ISAR image to obtain the height information.

The availability of two-dimensional high resolution images allow for a better but not perfect visual identification of the target. The ideal solution would be a three-dimensional image that could lead to automatic positive target visualisation and classification, for example as friend or foe.

In conclusion ISAR gives a 2D projected image from single pulse correction methods in a plane determined by the rotation vector. Based on this information this project will assess the application of interferometry in the capacity to provide the missing height information.

Finally the short name of this project is FB16.

3. OBJECTIVES

3.1. To provide relevant theoretical foundations for the project.

- Project Relevant Radar Theory.
- Interferometry.
- Inverse Synthetic Aperture Radar (ISAR) systems.
- Research into the combination of the methods above for target height estimation.

3.2. To provide relevant experimental foundations for the project.

- Height information via the range profile leading to a pseudo 2D image for one pulse.
- Rotation vector measurement of the ship via the time sequence of the interferometric returns.
- Scaling and identification of the image projection from the Rotation Vector.
- Construction of a computing environment to investigate the above using MATLAB V6.0.
- Unified Modelling Language (UML) description of all relevant software.
- Possible actual field testing.

4. DELIVERABLES

- Two Interim Reports the first on the 29th of January 2001 showing the agreed line of action between the author and the supervisor and the second on the 11th of June 2001 reflecting on the current progress of the project.
- Simulation software source code and UML documentation in appropriate appendices.
- Proof that the program works as expected.
- Progress Logbook keeping a complete record of all work.
- Final Report.

5. ANALYTICAL RESEARCH DEFINITION

There follows the theoretical basis flow regime for the FB16 project.

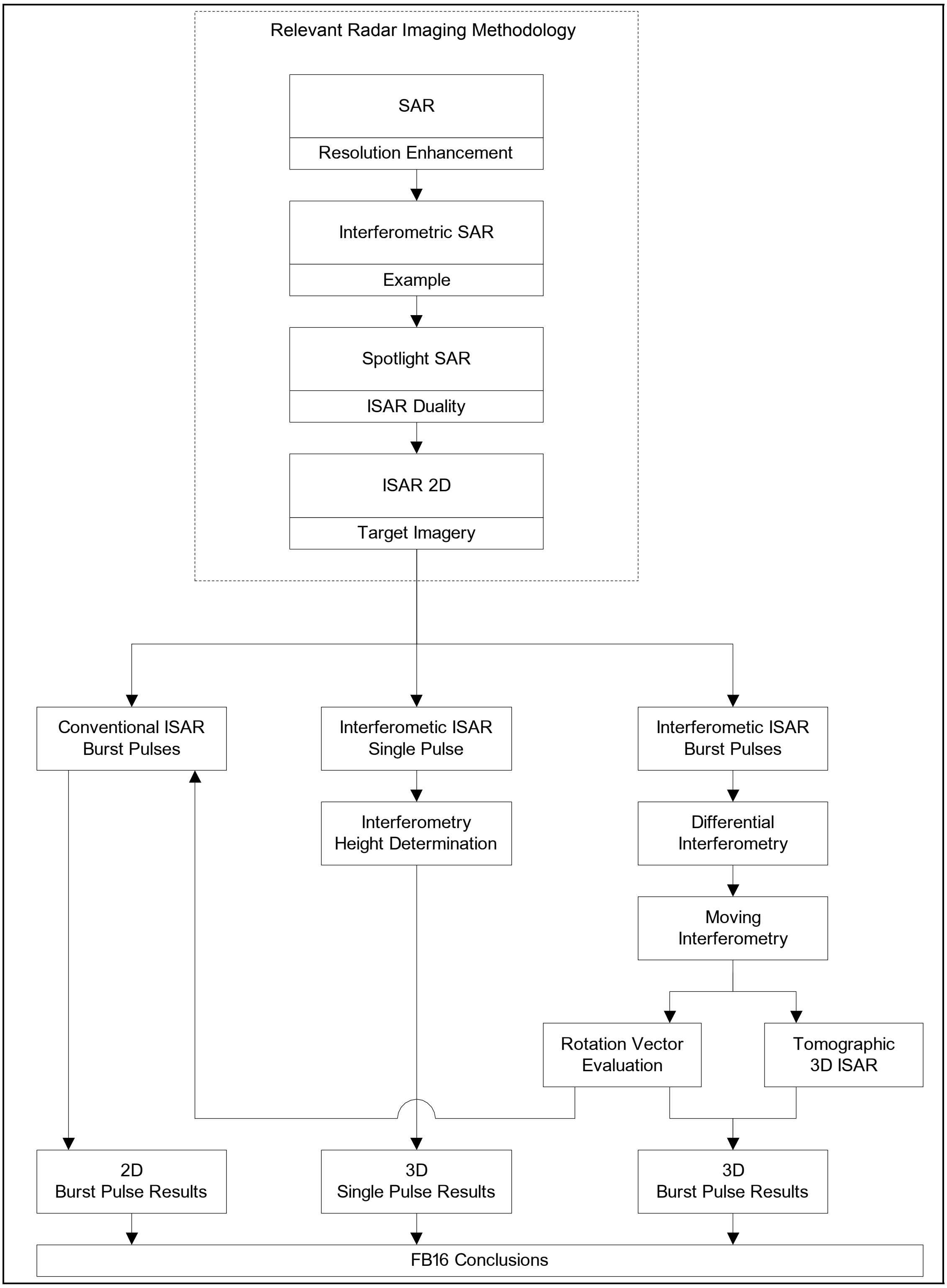

Figure 5.F1. Process Plan.

5.1. Radar Imaging

Rihaczek [22] (xviii) states that there is a significant difference between radar and optical imaging processes. For example at optical wavelengths the backscattering from a ship target is characterised by the same intensity. Therefore all the details of the target are visible to an observer assuming clear weather conditions and short observation distances. On the other hand at radar wavelengths the wave trapping features of a ship's superstructure exhibit small and large backscatter intensities. The above are summarised in table 5.1.T1.

	Optical Wavelengths	Radar Wavelengths
Backscatter Mode	Rough Scatterers	Coherent
Point Scatterer Intensity	Same	Different
Point Scatterer Center	Actual	Phase Dominated
Distance	Relatively Small	Very Large
Target Details	Very Recognisable	Difficult Recognition
Signal Processing	Low	Heavy

Table 5.1.T1. Comparison of Optical and Radar Vision.

5.1.1. The concept of Synthetic Aperture Antennas

A SAR system has an antenna aperture which is synthesised by the combination of relatable parts rather than the real dimensions of its physical antenna as shown in Figure 5.1.F1.

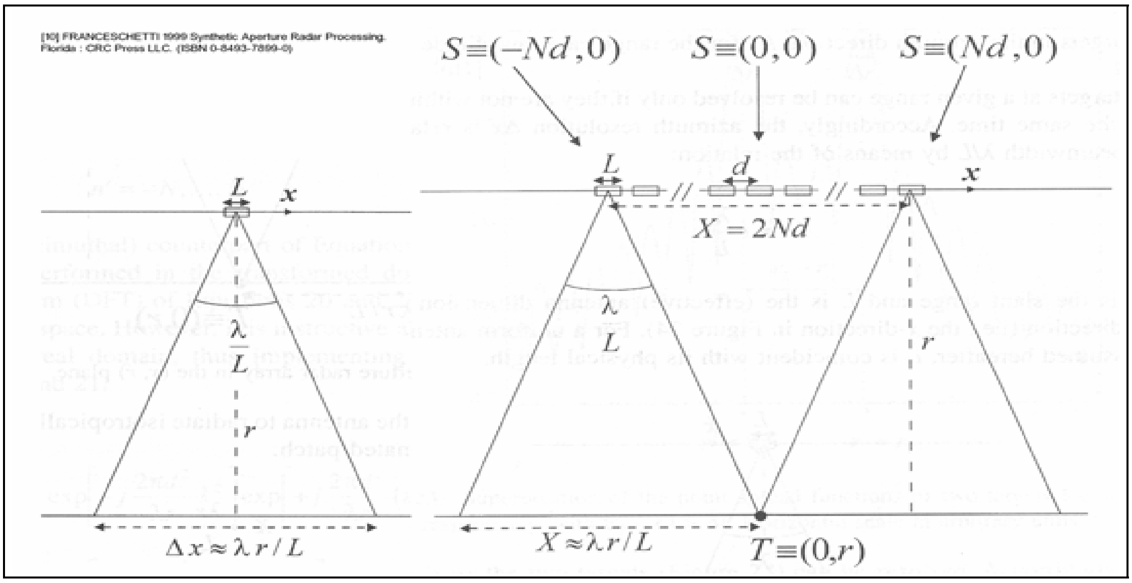

Figure 5.1.1.F1. Real Aperture Radar (RAR) vs Synthetic Aperture Radar (SAR).

The SAR imaging principle is based on two foundations :

- Coherence. Narrow Beamwidth. Linear array antennas.
- Sampling. The digitisation of continuous processes. The synthetic array is made up in a radar digital signal processor.

The basic SAR radar equation for a point target as taken from the MOE8 course notes on antennas and radar is shown in 5.1.E1

$$P_{RX} = \frac{P_{TX} G_{TX} G_{RX} \lambda^2 \sigma}{(4\pi)^3 R^4} \quad [5.1.1.E1]$$

where P_{RX} : Received Power
P_{TX} : Transmitted Power
G_{TX} : Received Power
G_{RX} : Received Power
λ : Operating Wavelength
σ : Radar Cross Section of the Target
R : Distance of Target from the Radar

The major advantage of SAR systems is much better cross range resolutions. The outcome is that the azimuth resolution becomes independent of the range resolution as with real antenna systems.

Now a numerical example will be utilised to illustrate all the above in much clearer terms. Starting with a conventional 10GHz radar with an antenna aperture of 3 meters looking down to a target 10 Km away, the cross range resolution is :

$$\Delta x = \frac{\lambda}{d} R = \frac{0.03}{3} 10000 = 100m \qquad [5.1.1.E2]$$

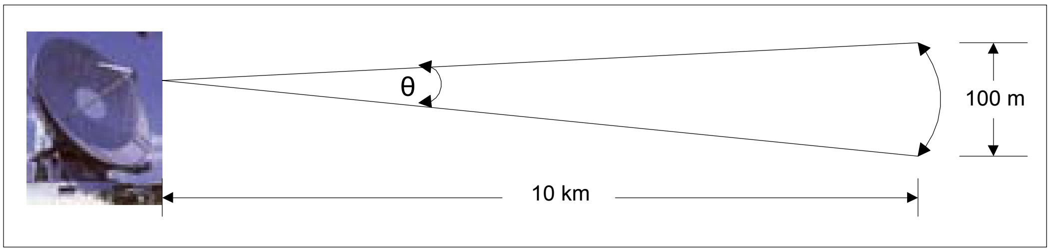

Figure 5.1.1.F2. Conventional Radar Angular Resolution.

This azimuth resolution is very low because a single resolution cell is illuminated at any one time. For example two ships less than 100 meters apart at the same range would appear as only one echo. Thus they cannot be resolved by the radar of figure 5.1.1.F1.

Now assuming stationary targets and employing an airborne SAR system at the same frequency and range the azimuth resolution $\Delta\chi$ can be brought from 100 meters down to 3 meters. The fly time should equal the distance of :

$$\Delta x = 3m = \frac{\lambda}{d} R \Rightarrow R = \frac{3d}{\lambda} = \frac{3*3}{0.03} = 300m \qquad [5.1.1.E3]$$

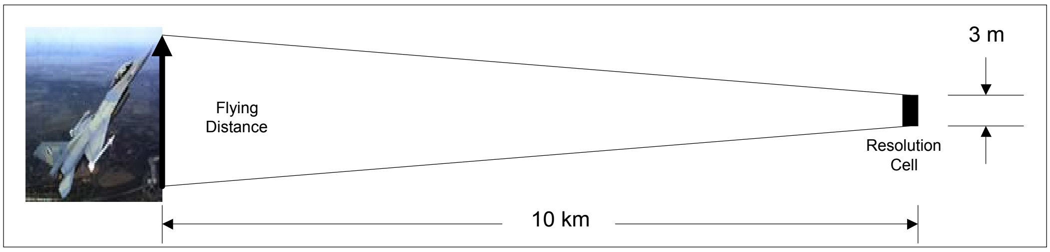

Figure 5.1.1.F3. Airborne SAR systems achieve higher azimuth resolutions.

Therefore when the airborne synthetic aperture system flies for 300 meters around or across the target the azimuth resolution becomes much finer at only 3 meters long.

Therefore SAR systems achieve incredible resolving power at great distances because with pulse compression many resolution cells are illuminated at any one time and their returns back at the radar are processed separately.

5.2. Synthetic Aperture Radar (SAR)

Ghiglia [18] (1) states that the SAR concept is based on coherent signal processing. This involves the aid of the phase attribute of signals in order to recreate their temporal and spatial domain equivalent exact representations. For example a plane wave exp(jωt-**kr**) signal representing an image of the earth's surface received back at the radar is initially in a two-dimensional Discrete Fourier Transform format as follows :

$$H_k = \sum_{n=0}^{N-1} h_n e^{-j2\pi k \frac{n}{N}} \longleftrightarrow h_n = \frac{1}{N}\sum_{k=0}^{N-1} H_k e^{j2\pi k \frac{n}{N}} \qquad [5.2.E1]$$

where h_n is the sample of h(t) with t = NT and H_k is the sample of H(ω) with ω = 2πk/NT.

$$H(\omega) = \int_{-\infty}^{+\infty} h(t) e^{-j\omega t} dt \longleftrightarrow h(t) = \frac{1}{2\pi}\int_{-\infty}^{+\infty} H(\omega) e^{j\omega t} d\omega \qquad [5.2.E2]$$

The magnitude spectrum |H| is the distribution of the absolute values of the frequency components of the image. For incoherent processing the intensity could be considered which is the square magnitude of H.

The phase spectrum [arctan(Im{H}/Re{H})] defines the relative position of each of the two dimensional complex exponential components from Equation 5.2.E1. SAR requires coherent processing and it is very important to always retrieve the correct phase spectrum of an image. Because coherence allows the synthesis of a much larger antenna aperture leading to higher image resolutions that these that would have been obtained by using the actual antenna on-board the surveillance aircraft as shown in Figure 5.2.F1.

Figure 5.2.F1. The E-8 JSTARS Surveillance aircraft uses the most advanced SAR equipment.

Analytically the returning signals have a precisely known phase because they can be referenced to their counterpart transmitted signals which were generated by a reference local oscillator again on-board the surveillance aircraft.

From the geometry of a SAR system as taken from the MOE8 course notes on antennas and radar and as shown in figure 5.2.F2 the range from the radar to the target is calculated as follows :

$$R^2 = Ro^2 + x^2 \Rightarrow R = \sqrt{Ro^2 + x^2} \Rightarrow R = Ro\sqrt{1 + \frac{x^2}{Ro^2}} \Rightarrow R = Ro\left(1 + \frac{x^2}{2Ro^2} + \ldots\right) \Rightarrow$$

$$R = Ro + \frac{x^2}{2Ro} \qquad [5.2.E3]$$

And the associated phase can be retrieved as follows :

$$\phi = -(\kappa * r) = -\frac{2\pi}{\lambda} 2R \Rightarrow \phi = -\frac{2\pi}{\lambda} 2\left(Ro + \frac{x^2}{2Ro} \right) = -\frac{4\pi}{\lambda} Ro - \frac{2\pi}{\lambda Ro} x^2 \Rightarrow$$

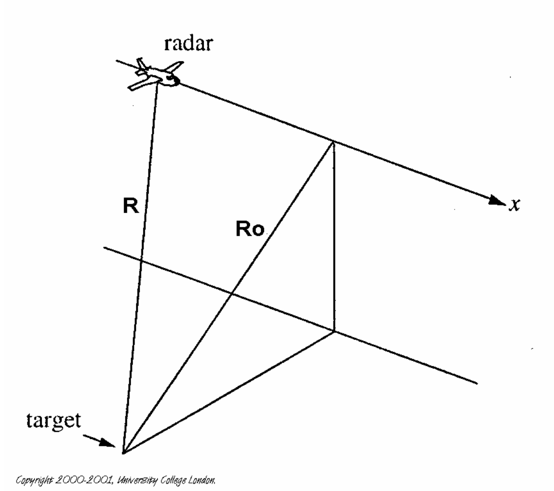

Figure 5.2.F2. SAR Geometry.

$$\phi = \phi_0 - \frac{2\pi}{\lambda Ro} x^2 \qquad [5.2.E4]$$

In the next chapter the phase associated with the height of the target will be computed without the need of the radar traversing the distance x above by applying the concept of interferometry.

Finally the associated Doppler Frequency is :

$$f_D = \frac{1}{2\pi}\frac{d\phi}{dt} = \frac{1}{2\pi}\frac{d}{dt}\left(\phi_o - \frac{2\pi x^2}{\lambda Ro} \right) = \frac{1}{2\pi}\frac{d}{dt}\left(-\frac{2\pi x^2}{\lambda Ro} \right) = -\frac{1}{2\pi}\frac{2\pi}{\lambda Ro}\left(\frac{d}{dt} x^2 \right) \Rightarrow$$

$$f_D = -\frac{1}{\lambda Ro}\frac{dx^2}{dx}\frac{dx}{dt} = -\frac{2xu}{\lambda Ro} \qquad [5.2.E5]$$

Finally SAR provides its own illumination method by using radio waves and thus can see through adverse weather and night conditions as shown in figure 5.3.F3. Stimson [09] (431)

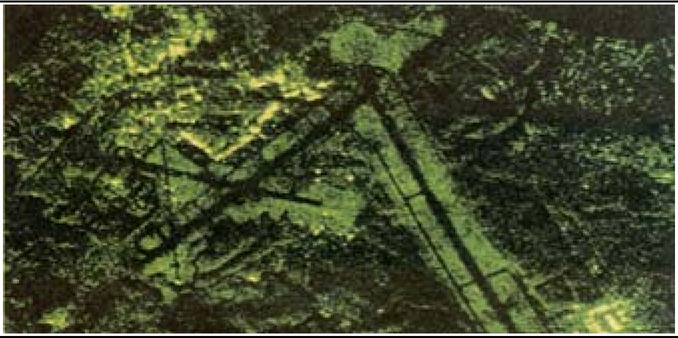

Figure 5.2.F3. Radar can clearly see from large distances and through all weather conditions.

5.3. Spotlight Mode SAR

Spotlight SAR is obtained as the radar antenna constantly tracks a particular target area of interest by squinting off in azimuth angle as shown in figure 5.3.F1.

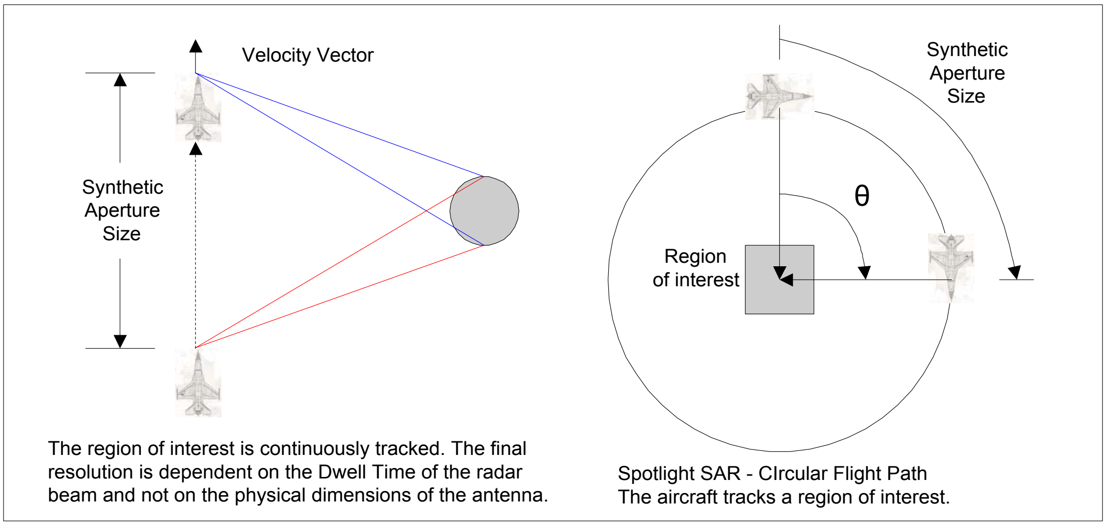

Figure 5.3.F1. Spotlight Mode SAR.

The cross range resolution is not limited by the size of the real aperture as in Side-Looking SAR but by the Dwell Time which is the time the radar beam is illuminating the target.

Wehner [10] (341) states that ISAR can be explained in terms of SAR by referring to the spotlight mode. Analytically after correcting for deviation from straight line motion a Spotlight SAR can be thought of as if the radar is flying an angular segment theta of a circle around the target area.

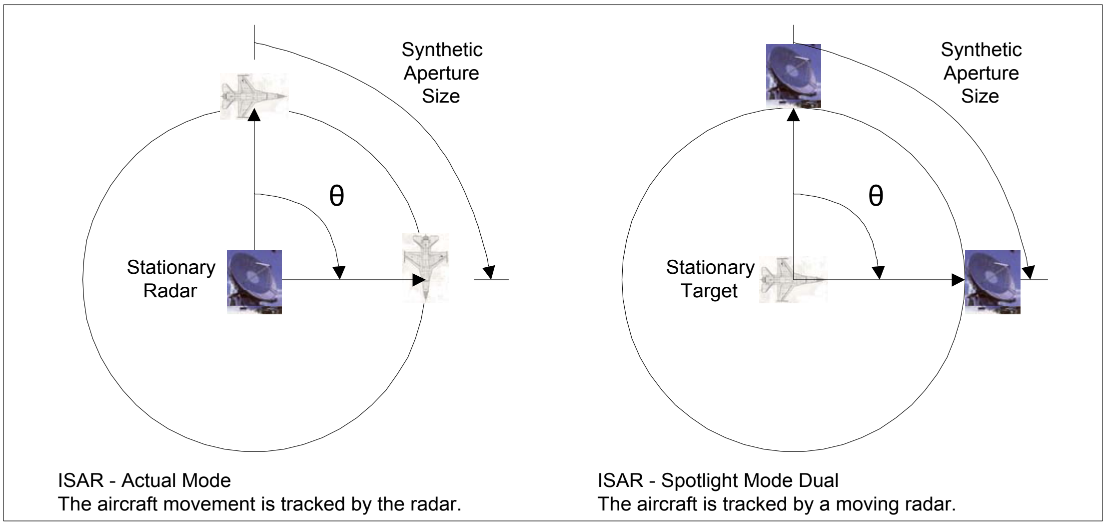

Figure 5.3.F2. ISAR and its Spotlight Mode SAR dual for a circular flight path.

Although the radar moves about the target the same data would be collected if the radar was stationary and the target area was rotated as shown in figure 5.4.F2. The aspect (viewing) angle θ of the target relative to the radar is used to generate the target map which is the target image as shown in figure 5.5.F2.

5.4. Interferometric SAR

Hecht [06] (377) explains that the phenomenon of interference is the interaction of two or more wave motions that create a disturbance pattern. This pattern corresponds to a resultant irradiance, which is the average energy per unit area per unit time, that is different from the sum of the component irradiances. In other words these two waves totally reinforce, partly reinforce or cancel each other resulting in an interference pattern. When the component motions are in phase the interference is constructive and the amplitude property could have a value much greater than any of the individual waves (constructive). And when the components are out of phase the interference is destructive and corresponds to a complete cancellation of the waves involved. The important condition for interference is that the two beams involved must have very nearly the same frequency (coherence).

Franceschetti [08] (171) states that Interferometric SAR systems are based on extracting the phase difference from two SAR images taken from the same scene. Then the two signal pair is properly focused to produce Single-Look Complex (SLC) images.

The Interferometric SAR process is summarised as follows :

- Generation of two SLC images relative to the same target scene.
- Registration of the images to extract the phase difference as an interferogram.
- Application of phase unwrapping algorithms to wrapped interferometric phases.
- Geocoding process completes the cartographic application and leads to a DEM (Digital Elevation Model) generation as shown in figure 5.4.F1.

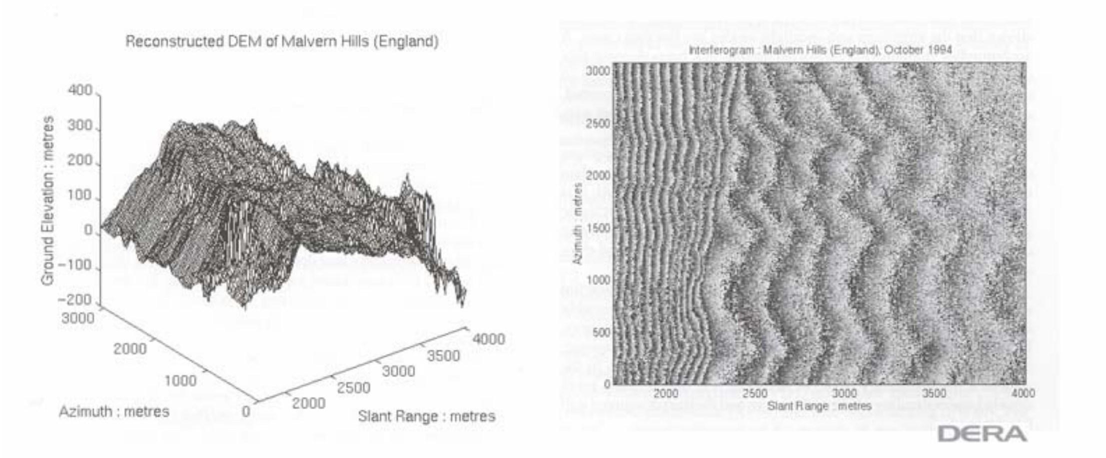

Figure 5.4.F1. The Digital Elevation Model and its corresponding interferogram.

From the geometry of an Interferometric SAR system in figure 5.4.F2 as taken from the notes of the MOE8 course notes on radar systems the following equations can be written :

$$R_1 = \sqrt{R^2 + (H - z)^2} \qquad [5.4.E1]$$

$$R_2 = \sqrt{R^2 + ((H + B) - z)^2} \qquad [5.4.E2]$$

For the simulations in appendices 10.1 and 10.2 equations 5.4.E1 and 5.4.E2 above are used.

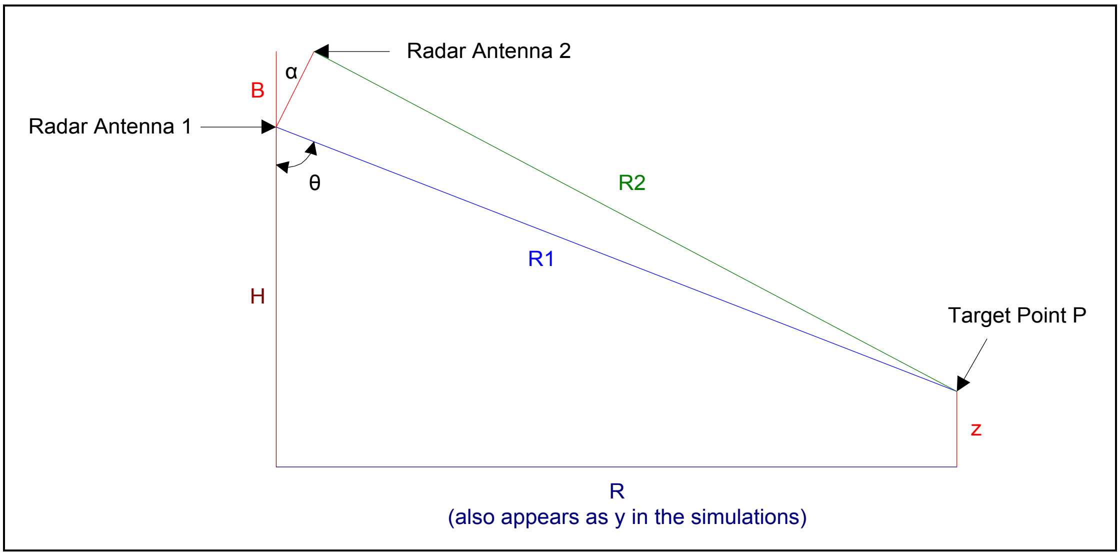

Figure 5.4.F2. Geometry of an Interferometric SAR system.

The height of the surveillance aircraft is a known parameter. For example it is continuously measured by an FM radar.

Also distances R1 and R2 are known. They are directly being measured by the radar equipment. Analytically for the ISAR and InISAR simulations in appendices 10.3 and 10.4 respectively the R1 and R2 distances are calculated by the geometry of figure 5.4.F2.

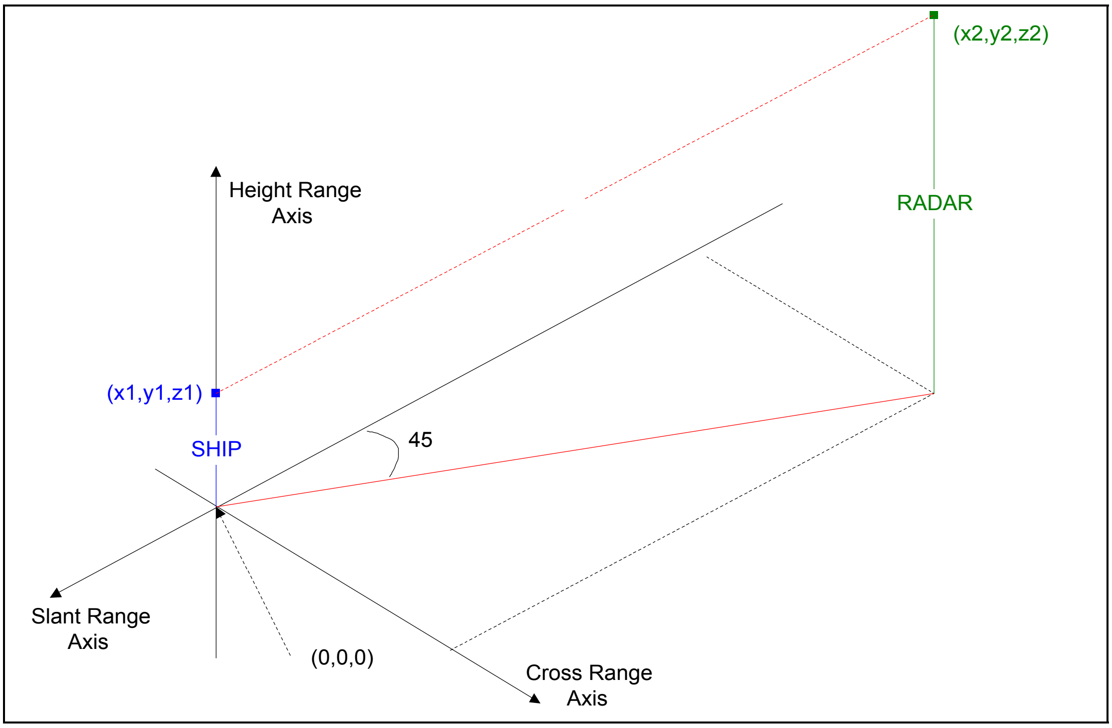

Figure 5.4.F3. ISAR-InISAR simulation geometry for the calculation of R1 and R2.

The distance between the point scatterer on the ship and the radar antenna is given by equation 5.4.E3.

$$R = \sqrt{(x2 - x1)^2 + (y2 - y1)^2 + (z2 - z1)^2} \qquad [5.4.E3]$$

All other radar functional parameters are shown in table 5.4.T1.

Description	Symbol
Slant Distance to Target from Lower Antenna	R1
Slant Distance to Target from Upper Antenna	R2
Interferometric Phase	φ
Radar Wavelength	λ
Antenna Baseline	B
Baseline Tilt with respect to Radar Height	α
Radar Height	H

Table 5.4.T1. Interferometric SAR known parameters.

The interferometric phase is derived by the registration of the two images produced by the two antennas and is calculated by equation 5.3.E4.

$$\phi = \frac{2\pi}{\lambda}\left(R_2 - R_1\right) \quad [5.4.E4]$$

In order to find the radar estimated target height and radar estimated target range the angle between the lower radar antenna and the lower slant range to target is then calculated as follows :

$$\theta = \cos^{-1}\left(\frac{R_2{}^2 - R_1{}^2 - B^2}{2BR_1}\right) - a \quad [5.4.E5]$$

With the angle θ known the radar estimated target height is as :

$$z = H - R_1 \cos\theta \quad [5.4.E6]$$

And the radar estimated target range is as :

$$y = \sqrt{R_1{}^2 - (H - z)^2} \quad [5.4.E7]$$

Therefore the unknown parameters that are calculated from the radar processor are :

Description	Symbol
Angle between the Lower Radar Antenna and the Lower Slant Range to Target	θ
Radar Estimated Target Height	z
Radar Estimated Target Range	y

Table 5.4.T2. Interferometric SAR calculated parameters.

Finally as referenced from Stimson [09] (517) the actual results obtained with the Interferometric SAR process is shown in figure 5.4.F3.

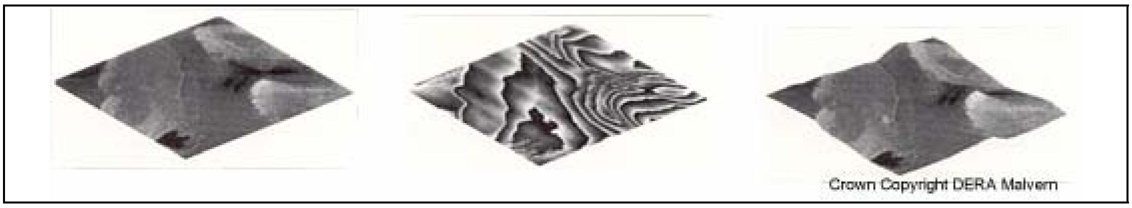

Figure 5.4.F4. Using DERA Malvern's C-band InSAR radar on a region in Wales.

5.5. Inverse Synthetic Aperture Radar (ISAR) Theory - Two Dimensional

ISAR uses a fixed beam that tracks the target's physical motion in order to integrate the synthetic aperture. The term synthetic aperture refers to the radar platform's cross range travel distance over which reflectivity data collected from the illuminated surface is coherently integrated to obtain higher cross range resolution. The result is the ISAR image which is a two-dimensional plane based on the target's rotation vector that reveals the slant range and cross range dimensions.

- The slant range resolution is determined by the pulse compression characteristics of the transmitted radar signal.

- The cross range resolution is dependent upon the Doppler frequency of the radar returning radar signals.

For ship targets the result is a marginally recognizable image at long ranges under all time and weather conditions.

Both SAR and ISAR can be explained in terms of processing a reflectivity dataset called Data Collection Aperture (DCA). And this process requires a change in the radar's viewing angle towards the target which translates to physical motion by either the radar or the target. This angle is the integration angle θ shown in figure 5.5.F1.

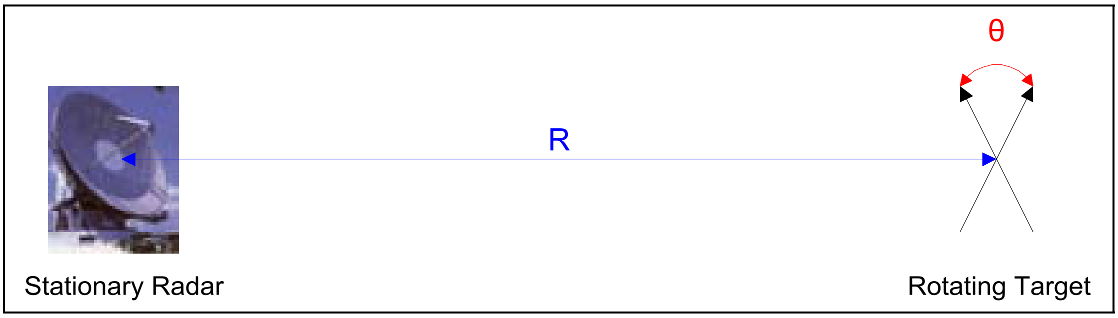

Figure 5.5.F1. 2D ISAR Model.

But now the rate of change of range and the Doppler frequency of the target are of great importance. Because from these the target's motion can be calculated giving the target's signature which is two-dimensional as shown in figure 5.5.F2 from Skolnik [15] (379).

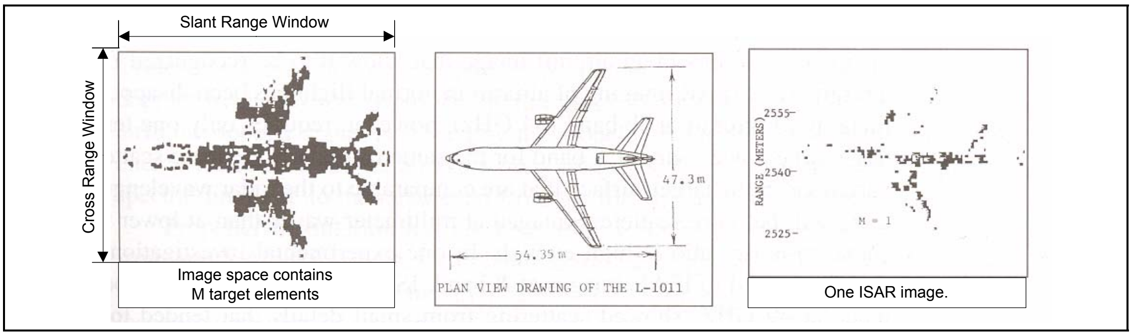

Figure 5.5.F2. The ISAR Image space is two-dimensional.

Stimson [07] (436) shows that ΔR is the incremental increase in range rate of points on the target separated by the Distance CRR normal to the radar's line of sight (LOS).

$$\Delta R = (CRR)\dot{\theta} \qquad [5.5.E1]$$

Description	Symbol
Slant Range Resolution	SRR
Slant Range Window	SRW
Cross-Range Resolution	CRR
Cross-Range Window	CRW
Angle traveled by the target with respect to the radar's Line of Sight (LOS). Also the angle the target has rotated during the integration time.	θ
Target's rate of rotation.	$\dot{\theta}$
Incremental increase in range rate of points on the target separated by the distance CRR normal to the line sight of sight from the radar.	ΔR
Integration time of the radar's Doppler Filters.	Tint

Table 5.5.T1. ISAR Parameters.

The resulting difference in the Doppler frequencies of the radar returns from successive points on the target is :

$$\Delta f_D = \frac{2\Delta R}{\lambda} = \frac{2(CRR)\ \dot{\theta}}{\lambda} \qquad [5.5.E2]$$

The minimum difference in Doppler Frequency the radar can resolve equals the 3dB bandwidth of its Doppler Filters.

$$B_{3dB} = \Delta f_D \qquad [5.5.E3]$$

The cross range dimension is not necessarily horizontal as with conventional SAR but perpendicular to the axis about which the target happens to be rotating. No image is formed if that axis is collinear with the radar's LOS or if the target has no rotational motion as observed from the radar.

The cross-range resolution distance is :

$$B_{3dB} = \frac{2(CRR)\dot{\theta}}{\lambda} \Rightarrow CRR = \frac{B_{3dB}}{2\dot{\theta}}\lambda \qquad [5.5.E4]$$

The integration time of the radar's Doppler filters is :

$$B_{3dB} = \frac{1}{t_{\text{int}}} \qquad [5.5.E5]$$

From equations 5.5.E3 and 5.5.E4 the Cross Range Resolution can be expressed as :

$$CRR = \frac{\lambda}{2\dot{\theta}}\frac{1}{t_{\text{int}}} = \frac{\lambda}{2\theta} \qquad [5.5.E6]$$

The above information describes the conventional ISAR processes that yields a two-dimensional image of the target. The axes involved are in slant range and in cross range as shown in figure 5.5.F2.

The modification that is proposed by this project is a two-dimensional image with different axes. Now the cross range axis is replaced with the height range axis as shown in figure 5.5.F3.

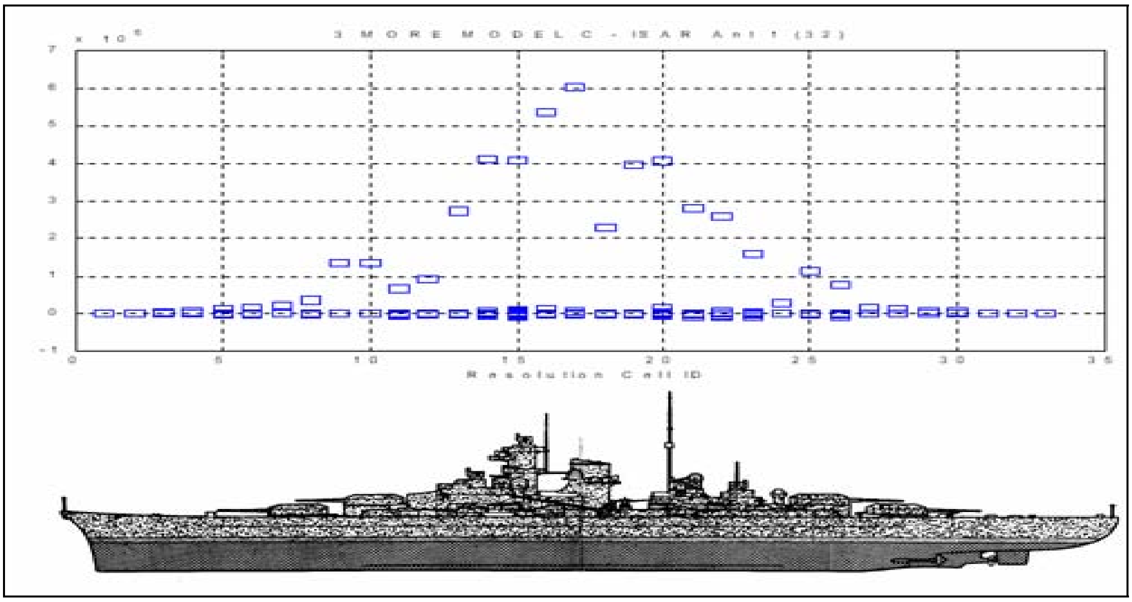

Figure 5.5.F3. Target height information through an ISAR process.

The contents of the corresponding cells are vertically integrated over the 32 milliseconds period of the radar's burst. The result is shown in figure 5.5.F3 where the Doppler frequency is proportional to the ship's height.

The complete analysis of this method is shown in chapter 6.

5.5.1. The ISAR Rotation Vector

The rotation vector is produced by the target's translational and rotational motions in a three-dimensional space. There follows in figure 5.5.1.F1 the approach path that leads to the acquisition of the rotation vector.

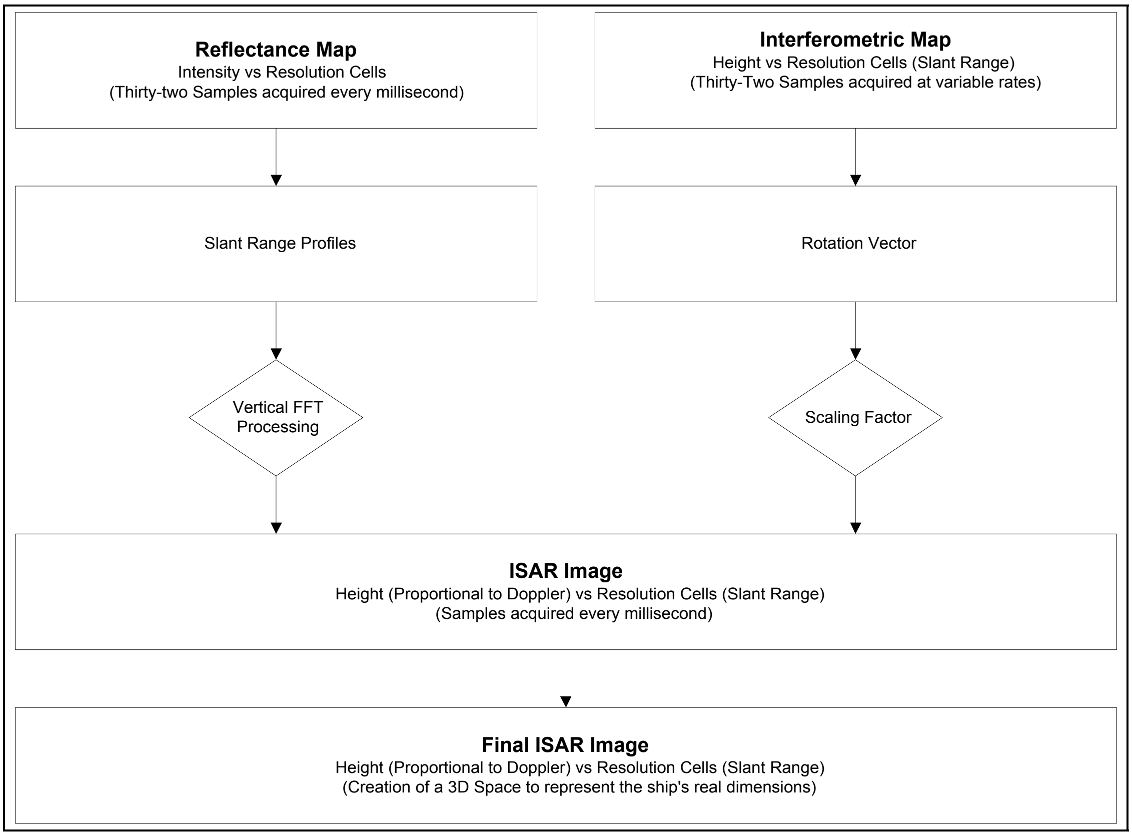

Figure 5.5.1.F1. InISAR Process Flow.

Theoretically the interferometric profiles should be able to reveal the rotation vector.

This approach path will be used to construct the ISAR simulation in part 6.4.

5.6. Inverse Synthetic Aperture Radar (ISAR) Theory - Three Dimensional

Seybold [09] classifies 3D-ISAR as an extension of the 2D-ISAR concept. The technique is based on frequency, waveform and target rotation absolute phase coherence. From at least two 2D-ISAR images obtained from different depression angles each x-y cell on the target is Fast Fourier Transform (FFT) transformed to generate the height profile of the image. Therefore it provides a complete RCS distribution in height for each x-y reflectivity map cell. On the other hand its major disadvantage is greater data collection and processing requirements.

Certain errors are involved in the process like near-field phase deviations. But 3D-ISAR can focus better and is not subject to the effects of glint. This is an advantage over the monopulse and InISAR methods.

Three dimensional imaging based solely on ISAR processes is not taken further in this report. The report baseline is focused on the combination of one pulse interferometry with a two-dimensional ISAR plane. If interferometry of a range profile gives a 2D image from one pulse then it has potentially very helpful advantages over sole ISAR methodologies.

5.7. Interferometric ISAR

Rihaczek [22] (xv) states that not enough information can be extracted form radar intensity images in order to be able to obtain high-resolution images of man-made targets leading to their positive identification. A solution would be to analyse the complex return image that contains the additional phase information. And for the ISAR part this is the method that is demonstrated in the simulation sections of this report.

As stated in the abstract the aim of the project is to investigate methods of obtaining the height (third) dimension of a moving target scene. In this project the target height acquisition process by means of interferometric methods is evaluated. These results can be seen in section 6.4.

Then a two-dimensional plane representing the target extent is acquired using Inverse Synthetic Aperture Radar (ISAR) methodology. These results can be seen in section 6.3.

The challenge of the project is to associate the two methods above by combining their relevant parts leading to the Interferometric Inverse Synthetic Aperture Radar (InISAR) concept. The model that will be used to draw out results is shown in figure 5.7.F1.

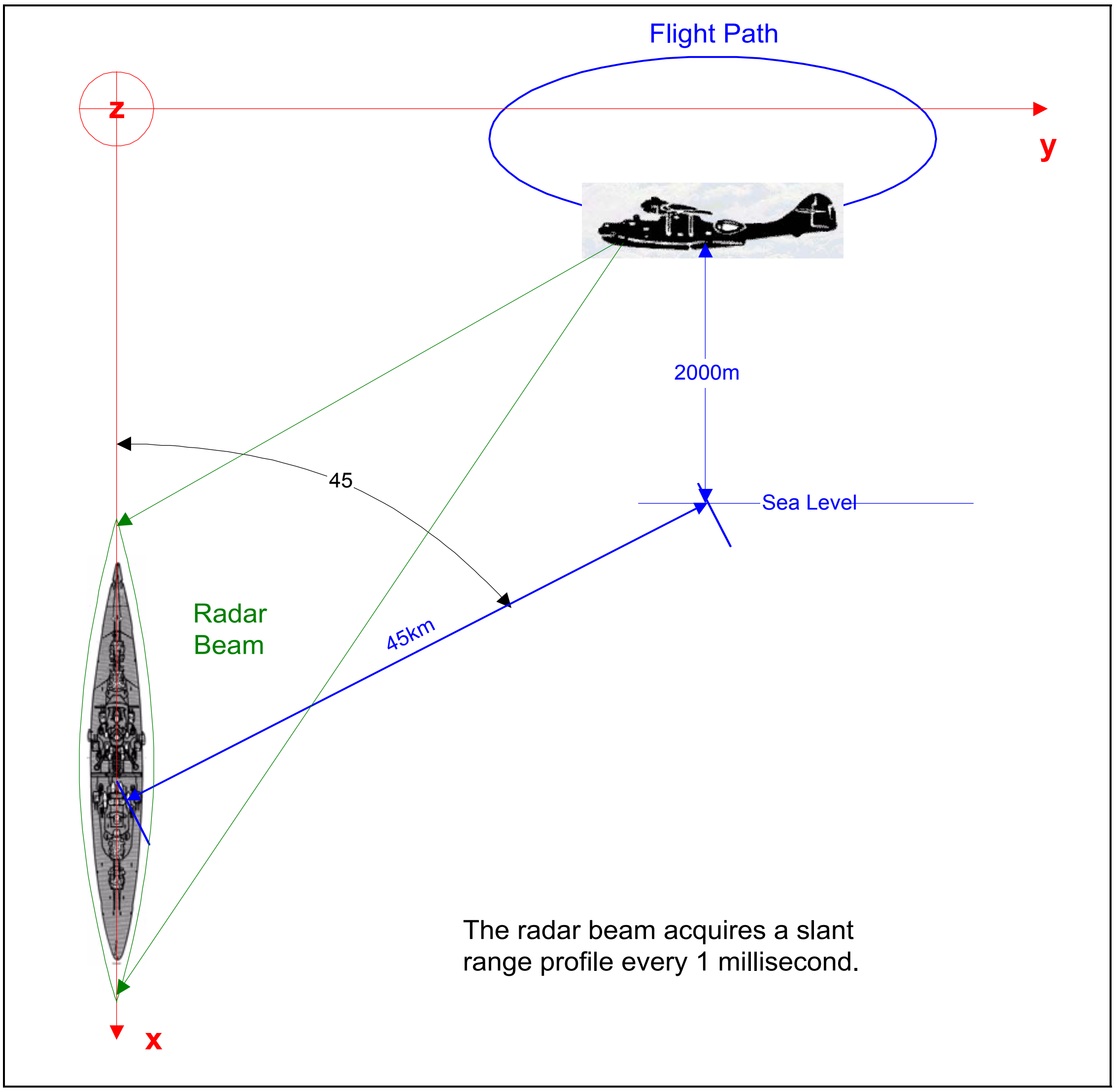

Figure 5.7.F1. Simulation Axes and Radar Aspect Angle.

The following assumptions were made :

- The imaging time corresponds to a certain type of motion which is taking place around a well defined x axis as shown in figure 5.7.F1. The simulation only traps a snapshot of the radar's motion but there is provision for incorporating a longer flying time.

- The airborne radar can track the vessel and thus acquire a certain viewing aspect angle as shown again in figure 5.7.F1. with no cell range migration. Therefore the slant range scale and cross range scale can both be definitely defined with respect to the radar position.

Problems associated with the above statements might be :

- Average height over actual resolution cell height.

- Phase Wrapping.

- Uncompensated relative rotational motion introduces distortion degrading image quality.

- Layover effects.

- Measurement of instantaneous height at current position instead of vertical height value.

- Non-linearities associated with the target motion may result in strange image projections.

This project is targeted to the investigation of these problems.

Finally the image quality obtained by the InISAR method is analysed, simulated and documented.

6. RESEARCH PROGRESS & TECHNICAL APPROACH

- Results are now available on interferometry and ISAR imaging. The ship model utilised was created using the MATLAB R12 environment.

- In this paper the basis of simulations rely on the observation of the same angle over different viewpoints as shown in figure 6.3.3.F2. in the next section. It is assumed that there is no cell range migration. Moreover the resolution quality is associated with the dwell time of thirty-two pulses (one burst) which in turn reveals the amount of angular rotation that has occurred via interferometry.

For example for a series of pulses guided through a Fourier Transform process the result is the different Doppler frequencies present in the spectra. And the Doppler frequencies can reveal radial velocity (u) information from equation 6.E1.

$$f_D = \frac{2u}{\lambda} \Rightarrow u = \frac{f_D \lambda}{2} \qquad [6.E1]$$

- All radar geometry is under the control of the human factor. This advantage allows for easier debugging of software results.

- For the first simulation part 6.1 (Interferometry Simulation with a Stationary Target) the accuracy of the phase difference obtained will reveal the correct height characteristics. For example for a very small change in height with a 2π phase change an ambiguity is introduced. It cannot be determined if the correct height is associated with the base 2π phase difference or a higher 2π multiple phase change. The steps to remove this important ambiguity (phase unwrapping) are outside the scope of this project.

- The second simulation part 6.2 (Interferometry Simulation with a Moving Target) resembles a ship's mast moving with a simple harmonic motion. The heights obtained will be associated with resolution cells which slice up the ship into different clusters.

- The third simulation part 6.3 deals with ISAR issues. The baseline is to provide an understanding for the ISAR operations. Particularly the ISAR 2D image will be extracted for a moving target. The term Doppler Frequency will be replaced for the term Target Height. Different heights in different range bins will reveal the profile of the ship.

- The final part is dealing with innovative research. Interferometric and ISAR information will be coupled to evaluate the quality of results. Moreover the merits of Differential Interferometry for this work will be considered.

The rotation rate of the ship will be known and the main purpose of the project will be to able to evaluate it from the other parameters.

Also another important point will be to assess if the information obtained from ISAR can be obtained by using an one pulse interferometric profile approach.

- Finally the target structure used for the FB-16 Second Interim Report was the German battleship Bismarck laid down in 1936 and launched on the 14th February, 1939. Bismarck was sunk by the British Royal Navy on the 27th of May, 1941, at 10:40, having sustained terrible damage. But before that an air attack from H.M.S. Ark Royal was mistakenly made on H.M.S. Sheffield underlining the importance of correct target identification.

The Bismarck was built by Blohm and Voss shipyards at Hamburg. The dimensions of the target can be found in Appendix 12.7.

6.1. Interferometry Simulation with a Stationary Target

The mast of the target was defined with five prominent scatterers and considered as stationary. The main results are as follows :

- **TARGET RANGE**
  The range of the target being tracked was tested at 3Km, 5Km, 7Km and 15Km. As a demonstration figure 6.1.F1. shows the results for the 15Km case. All other results were correct. Noticeable deviations in results can be located after 50Km from the radar.

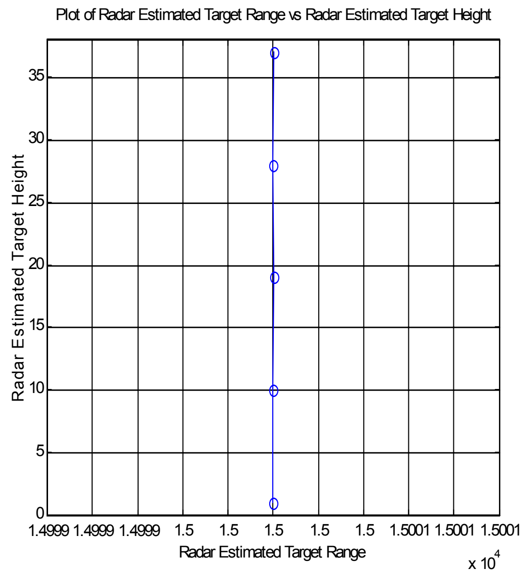

Figure 6.1.F1. Plot of Estimated Target Range vs Estimated Target Height.

The five different scatterers in figure 6.1.F1. have different corresponding radial velocities. The highest point is travelling faster than the lower as can be computed by equation 6.1.E1.

$$u = \omega * R \qquad [6.1.E1]$$

where u : Radial Velocity of a Scatterer
□ : Angular Velocity of a Scatterer
R : Radius (Height) of a Scatterer from the rotation centre.

The rotation centre can be either the bottom of the ship's mast as in this case or the centre of gravity of the vessel as in the simulations section.

From equation 6.E1 and equation 6.1.E1. it may be possible to compute the rotation vector of the vessel. This is one of the main endeavours of this project.

- **RADAR BASELINE**
  The baseline parameter at 0.5m, 1.0m and 2.0m leaves all other results unaffected and correct. For information purposes any baseline longer than 1micrometer produces correct height and range estimation.

- **RADAR HEIGHT**
  The height of the airborne radar was tested from 2km as an airborne radar up to 36000 Km as a geostationary satellite radar. All results of target height and range estimation were correct from all radar heights.

- **TARGET HEIGHT**
  The Target Height was a mast of 50m height approximated by five scatterers located at 1.0, 10.0, 19.0, 28.0 and 37 meters. The radar was able to resolve the scatters at all permutations of target range, radar baseline and radar height.

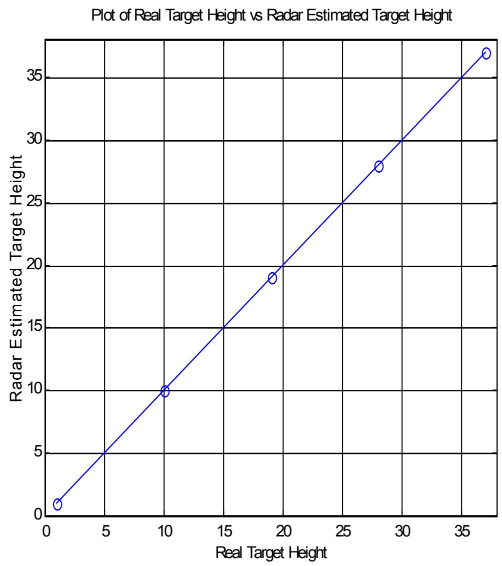

Figure 6.1.F2. Plot of Real Target Height vs Estimated Target Height.

The complete static interferometry results and corresponding software listings can be seen in Appendix 12.2.

6.2. Interferometry Simulation with a Moving Target

A simple harmonic motion is started where an interferometric sample is taken every 1msec. Therefore every time interval is associated with a corresponding height. From the geometry of the simulation the height parameter is known. Moreover the interferometric routine of part 6.1 can calculate it with high accuracy.

Now the time element introduced and dictates the motion. So an attempt is made to derive the rotation rate of the ship's mast from the sequence of the height measurements in time. In other words the speed of the mast is the unknown factor in this simulation block.

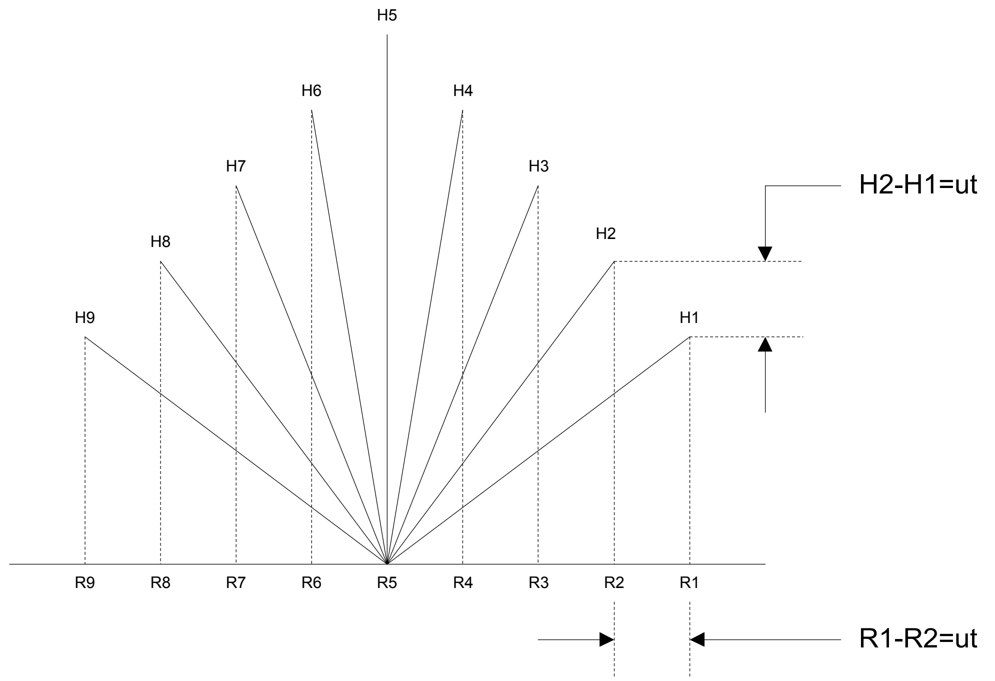

Figure 6.2.F1. Interferometry on the ship's moving mast reveals the height and range.

Taking a part of figure 6.2.F1 a vector can be drawn from point H1 to pointH2 as shown in figure 6.2.F2.

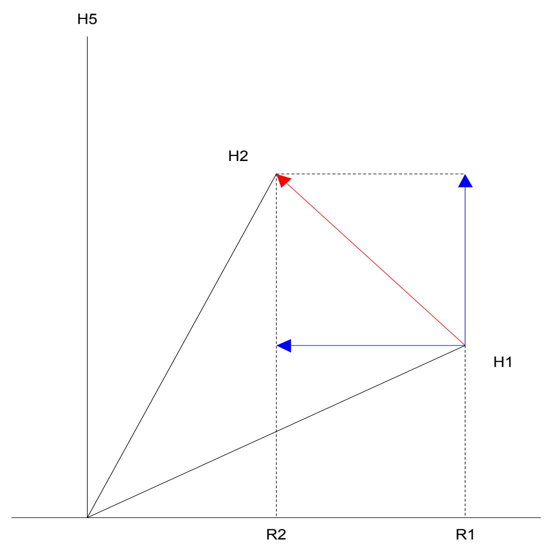

Figure 6.2.F2. Different mast points reveal the rotation vector.

A simulation for introduction and intuition purposes was completed by the second interim report. The software listings can be found in appendix 12.3.1. and the results are shown in figure 6.2.F3.

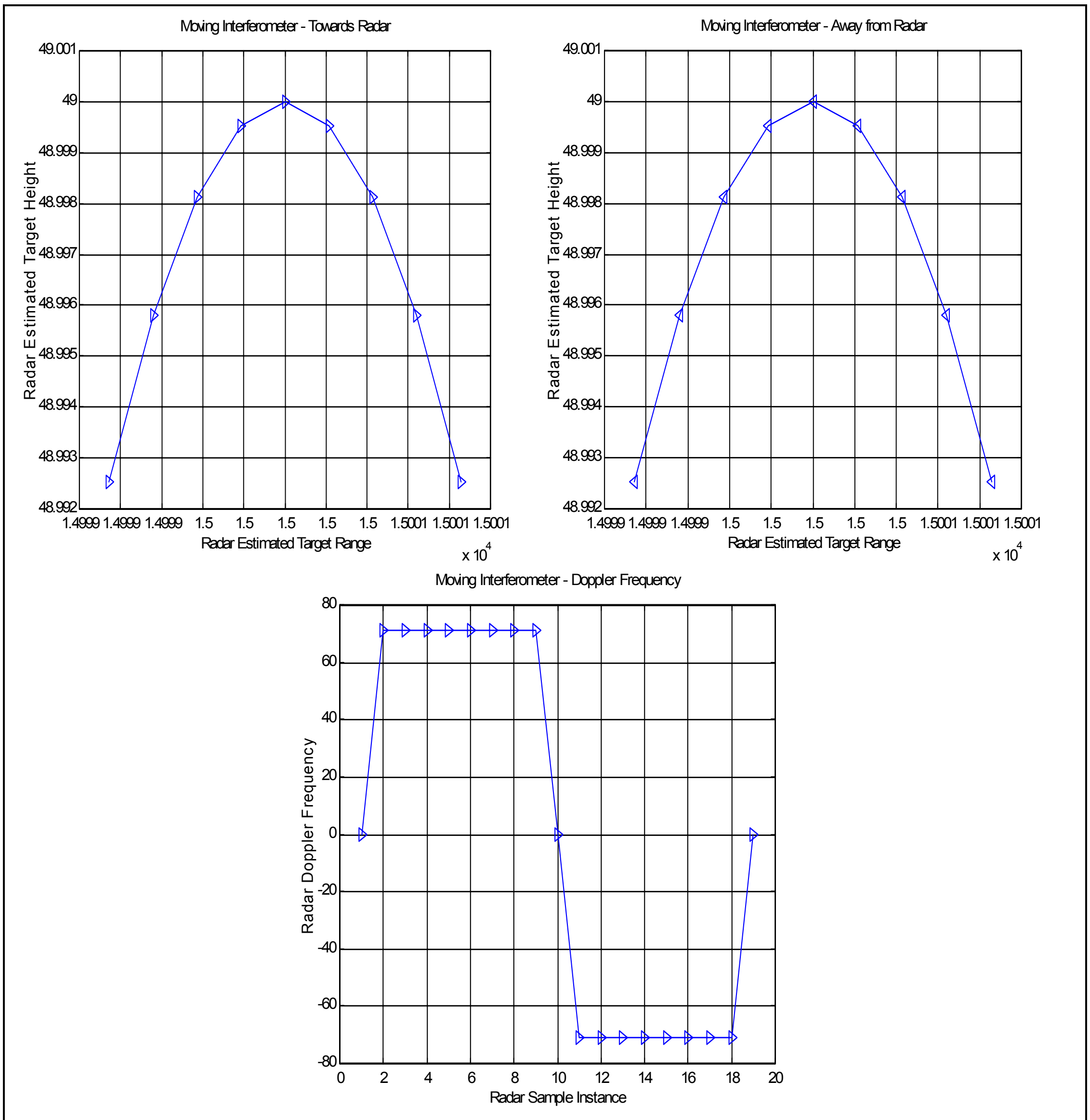

Figure 6.2.F3. Interferometry can track a rotating target in both range and height.

This simulation exercise set up the foundations for the project software in sections 6.3 and 6.4.

6.3. ISAR Simulation

A part of a simple harmonic motion is simulated of a ship's mast having a period of one second as shown in figure 6.3.F1.

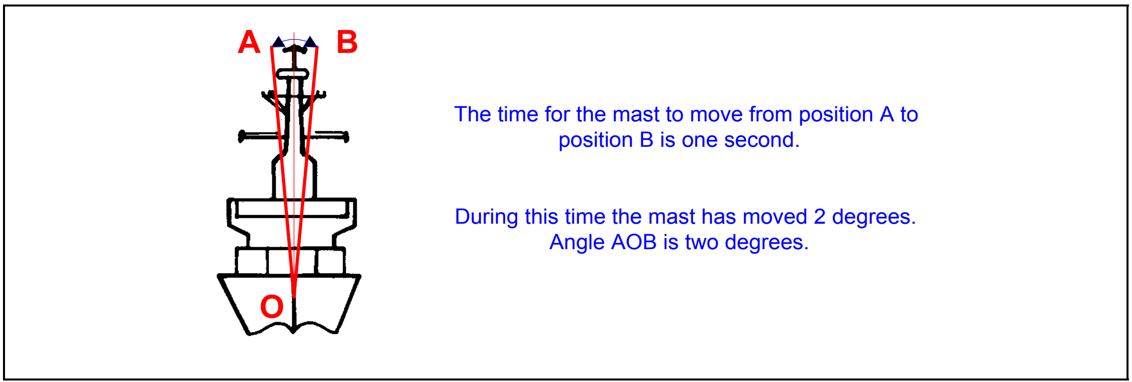

Figure 6.3.F1. The complete ship movement.

The radar scans this motion one thousand times every second as stated in equation 6.3.E1. (Pulse Repetition Frequency) and equation 6.3.E2. (Pulse Repetition Interval).

PRF = 1000 Hz [6.3.E1]

PRI = 1 msec [6.3.E2]

Figure 6.3.F2. is a representation of the complete simulation process which is analysed in section 7.

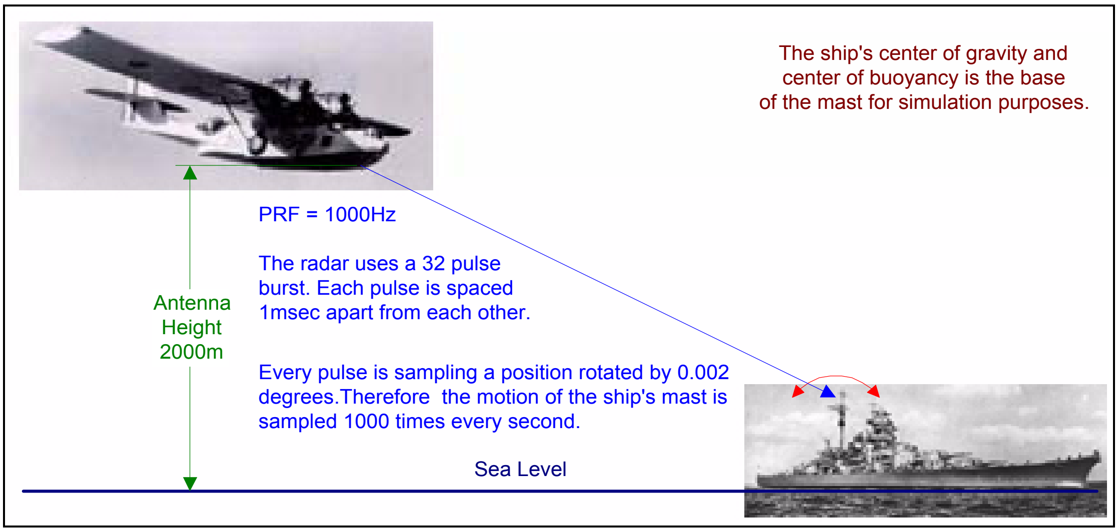

Figure 6.3.F2. ISAR data acquisition.

Part of this motion will be scanned for simulation purposes by the radar waveform of section 6.3.1.

6.3.1. Radar Waveform

The radar waveform is a burst of 32 pulses as shown in figure 6.3.1.F1. Therefore the radar acquires a thirty-two millisecond history of the position of the mast.

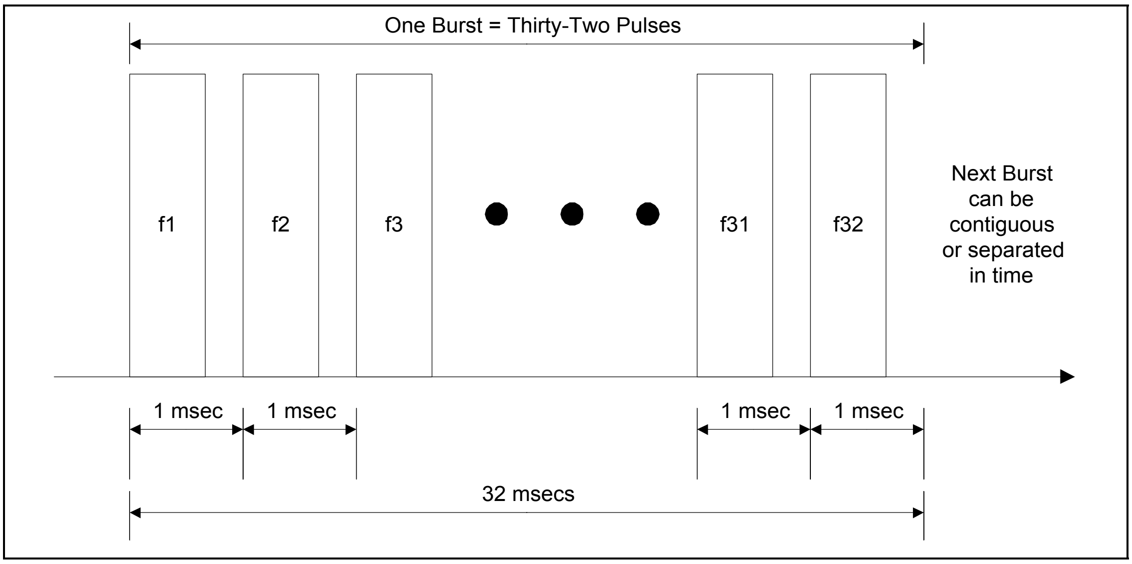

Figure 6.3.1.F1. Waveform used in ISAR imaging.

For achieving higher resolution the above pulse can be transmitted as shown in figure 6.3.1.F2.

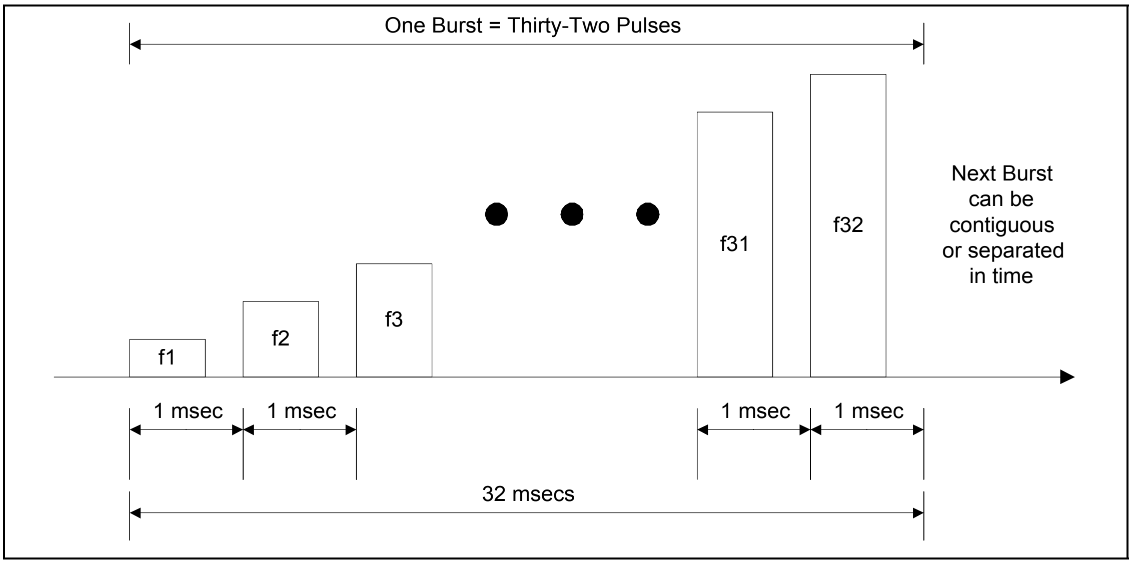

Figure 6.3.1.F2. Enhancing slant range resolution in ISAR imaging.

By using the waveform of figure 6.3.1.F2. the slant range resolution can be adjusted as required by the project requirements. A thorough analysis is found in the following section 6.3.2.

6.3.2. Computational Analysis

A burst of 32 pulses is used to image the target's current position which is shown in figure 6.3.2.F1. The duration of each pulse is one millisecond. Therefore the radar's Doppler filters integration time corresponds to 0.032 seconds.

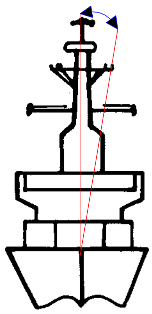

Figure 6.3.2.F1. The simulation ship movement.

And the Doppler bandwidth taken from equation 5.5.E4. is :

$$B_{3dB} = \frac{1}{t_{\text{int}}} = \frac{1}{0.032\sec} = 31.25Hz \qquad [6.3.2.E1]$$

The target is rotating with one degree every half a second. The conversion in rad is shown in Equation 6.3.2.E2.

$$RotationRate = \frac{\pi}{180} rad / 0.5\sec onds = 0.035 rad/\sec \qquad [6.3.2.E2]$$

From equation 5.5.E3. then the Cross Range Resolution is 26.78m at 5GHz as the target is rotating with 0.035 rad/sec as shown in Equation 6.3.2.E3.

$$CRR = \frac{B_{3dB}}{2\dot{\theta}}\lambda = \frac{31.25}{2\dot{\theta}}(0.06) = \frac{0.9375}{\dot{\theta}}[m] = \frac{0.9375}{0.035}[m] = 26.786m \qquad [6.3.2.E3]$$

For simulation purposes the cross range resolution is brought down to eight (8) meters. Using this convention a resolution cell can take the shape of a square as shown in figure 6.3.3.F2. in the next section. This attribute is used in the several versions of the *ResCells* function in the simulation sections. The actual improvement method in cross range resolution to match the above information is outside the scope of this project. Relevant information can be found in the paper by Zheng [43] (645) which states that high cross range resolution is possible by coherently processing the target's Doppler phase history.

On the other hand the slant range resolution can be easily set to the required 8 meters as shown in equation 6.3.2.E4.

$$SRR = \frac{c}{2B} \Rightarrow B = \frac{c}{2(SRR)} = \frac{3*10^8}{2(8)} = 18.750MHz \qquad [6.3.2.E4]$$

6.3.3. Simulation Model Range-Doppler Analysis

A simple reflectance model is used where the ship is divided into one hundred and forty-five (145) square equal cells. Each of these cells produces an echo back at the radar which is modelled as a complex number (amplitude and phase) as shown in equation 6.3.3.E1.

Reflectance Cell = $RF\,e^{jIP}$ [6.3.3.E1]

where RF is the Reflectance Amplitude and IP is the Reflectivity Initial Phase of a reflectance cell on the target. All reflectance cells form the complete reflectance model which is shown in figure 6.3.3.F1.

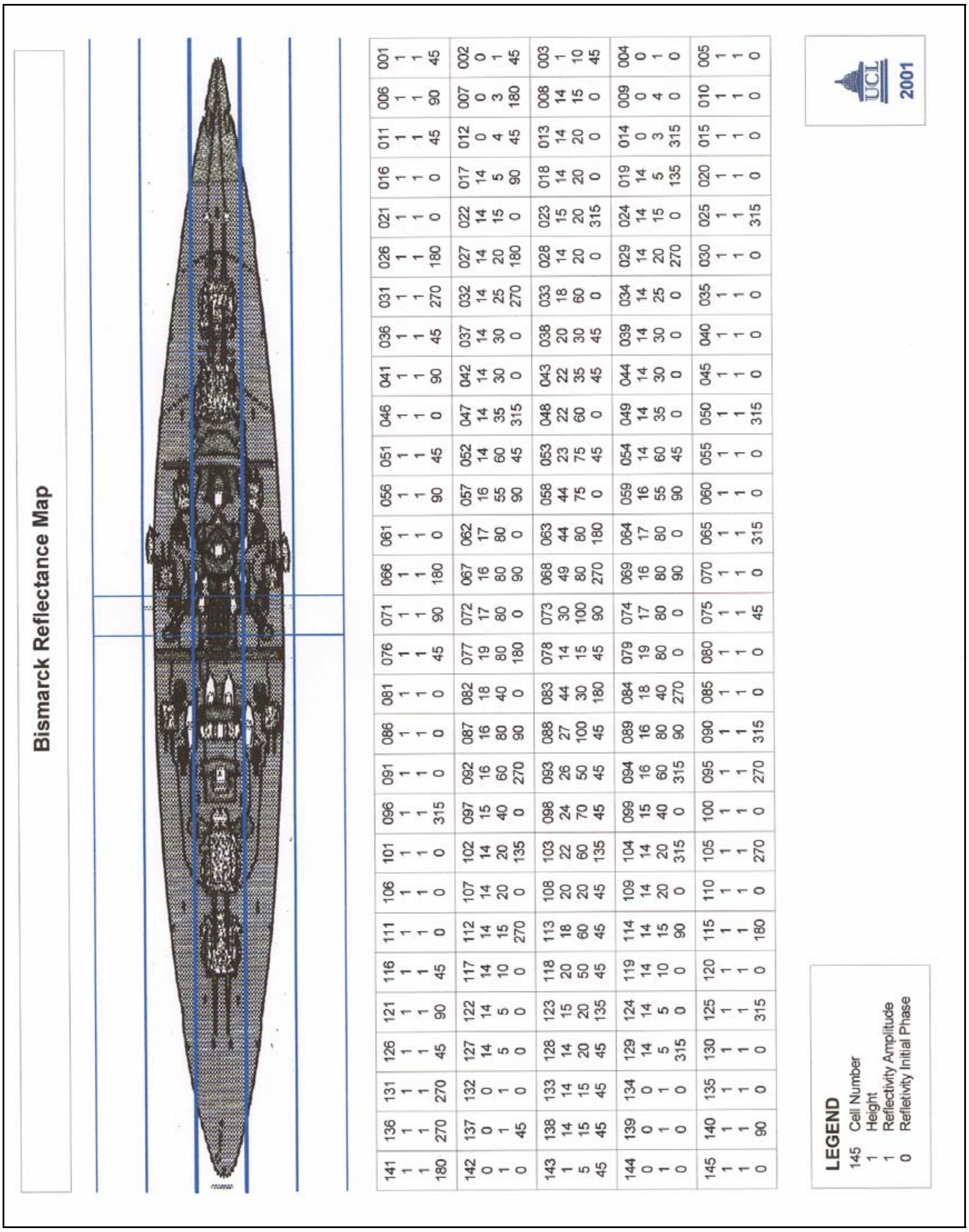

Figure 6.3.3.F1. KMS Bismarck Reflectance Map.

The radar is placed at 45 degrees from the vessel. The resolution is set as to create thirty-three resolution cells that contain one to five reflectors as shown in figure 6.3.3.F2.

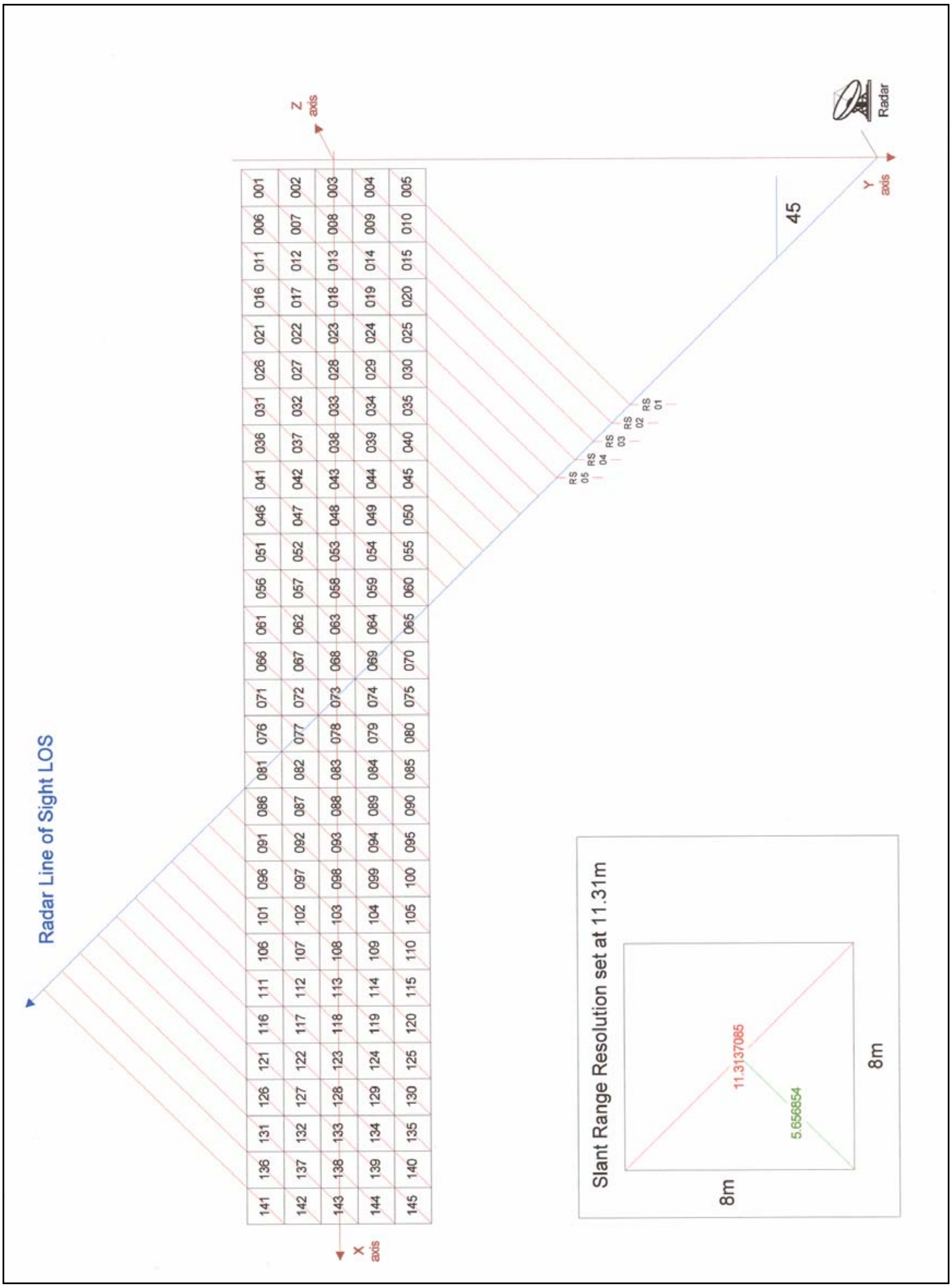

Figure 6.3.3.F2. Radar Aspect Angle and Resolution Cell Definition for ISAR.

Based on the information given by figure 6.3.3.F2. five ship models were compiled as shown in table 6.3.3.T1.

Simulation Section	Model ID	Ship Levels	Scatterer Amplitude	Scatterer Initial Phase	Range Dependent
6.3.3.1.	TEST	0	All 1	All 0	No
6.3.3.2.	TEST	0	All 1	All 0	Yes
6.3.3.3.	MORE	0	Geometry	Random	Yes
6.3.3.4.	MORE	0	Geometry	All 0	Yes
6.3.3.5.	MULT	5	Geometry	Random	Yes

Table 6.3.3.T1. Model permutations.

The response of the above thirty-two slant range profiles is processed by thirty-three vertical FFT operations as explained in figure 6.3.3.F3.

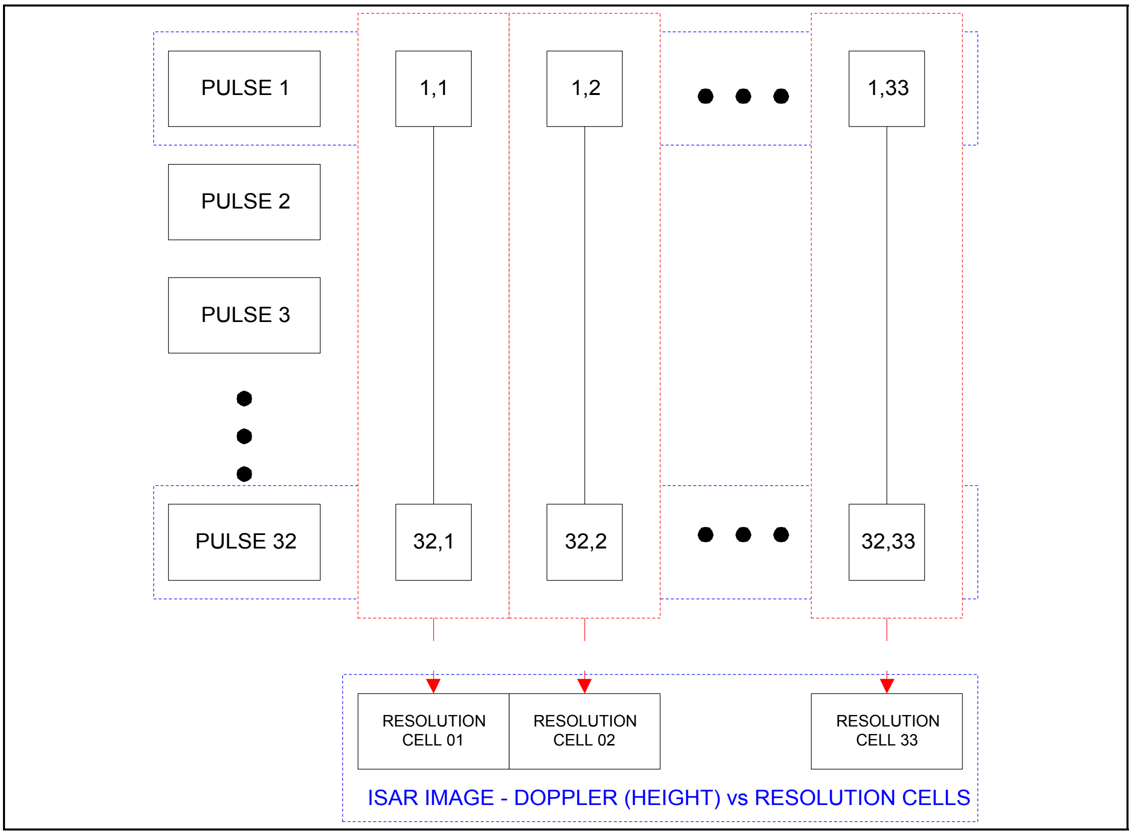

Figure 6.3.3.F3. The Range-Height Process used in the simulations.

The above process associates the Doppler information with the height of the target.

6.3.3.1. Test (TEST) Model - Ideal Parallelogram.

In order to test the validity of the ship model at an early stage and with high accuracy a test model was first implemented. In this model all amplitudes are 1 and all initial phases are 0. Moreover the phase is not dependent on the range from the radar. Then the results showed the expected perfect parallelogram as shown in figure 6.3.3.1.F1.

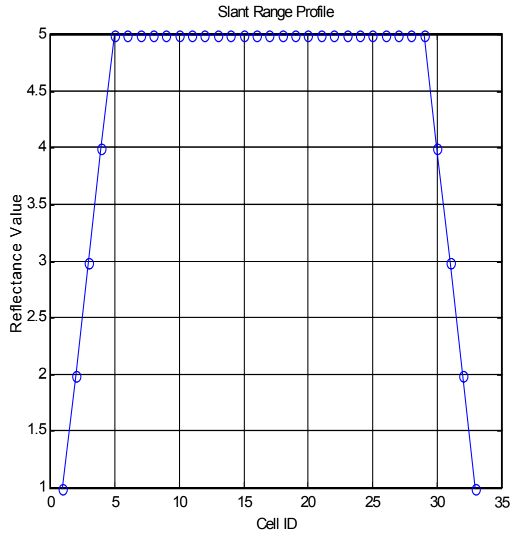

Figure 6.3.3.1.F1. Test Model Perfect Parallelogram.

Therefore the software was working as expected. The complete results for the Permutation 1 Test Model are shown in appendix 12.4.1.1. And the resulting Doppler frequencies will correspond to the height of the ship as shown section 6.3.3.3.

6.3.3.2. Test (TEST) Model - Range Dependent.

The second step involved the introduction of the phase dependent on radar range from the target. The results showed the expected disturbance from the previous ideal model as shown in figure 6.3.3.2.F1. The complete results of the Permutation 2 Test Model are shown in Appendix 12.4.1.2.

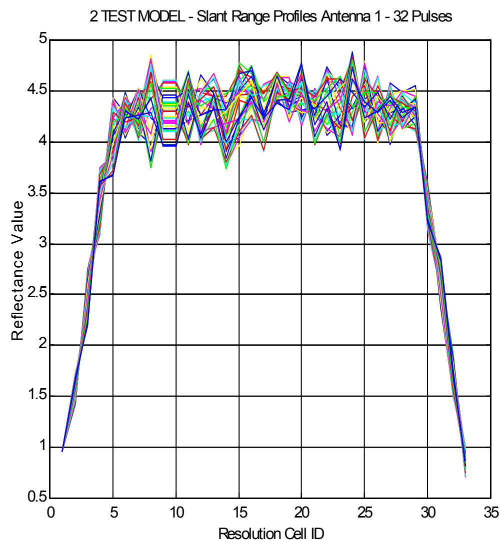

Figure 6.3.3.2.F1. Test Model Perfect Parallelogram with distance related phase dependence.

6.3.3.3. More Realistic (MORE) Model - Complete.

The third step is to introduce a more realistic model in which the amplitudes and phases of the reflectors correspond to the actual physical dimensions of the model ship.

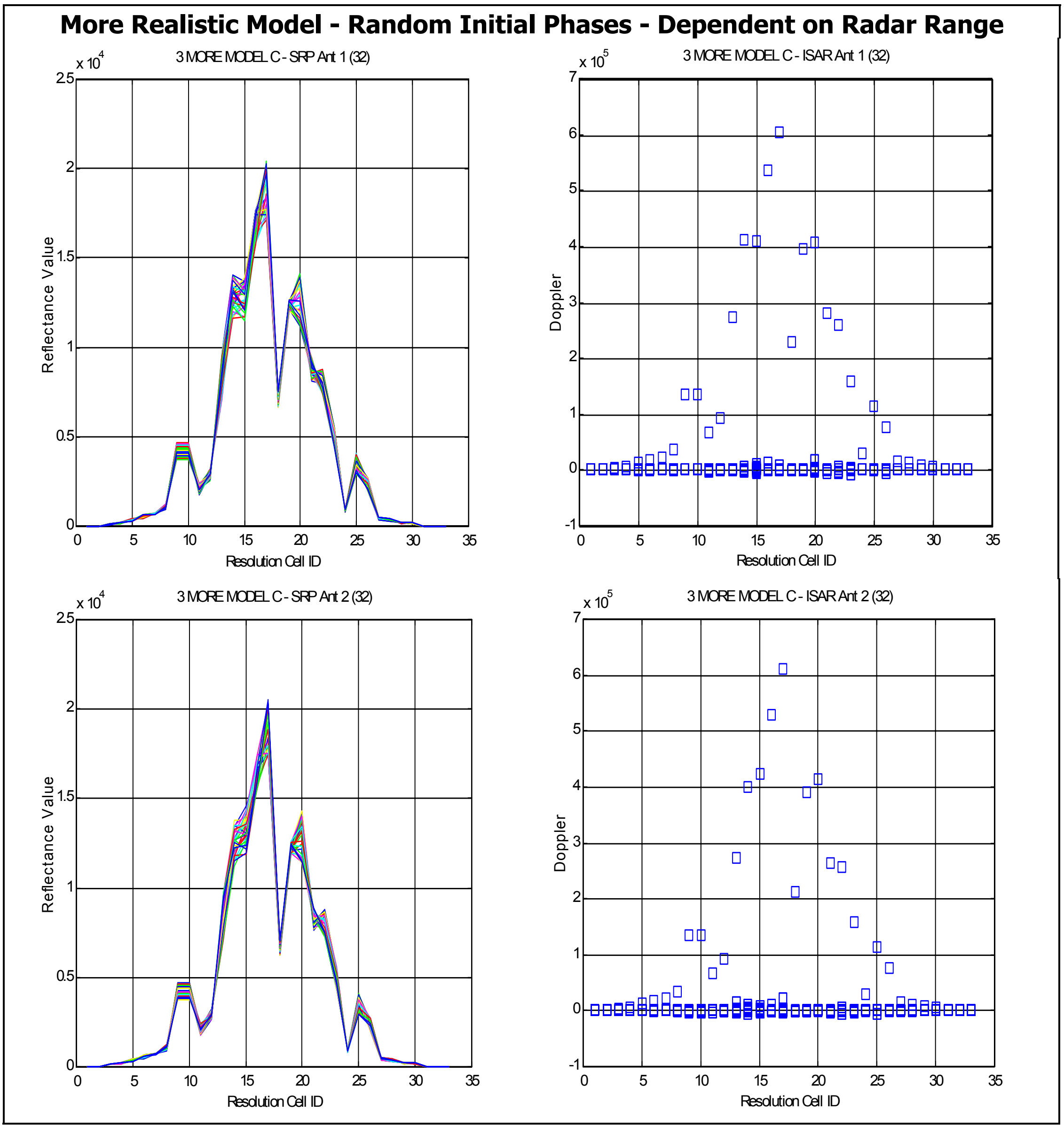

Figure 6.3.3.3.F1. Permutation 3 More Model Complete - Dependent on range from radar.

In figure 6.3.3.3.F1. the first and last peaks correspond to the Bismarck's cannon turrets. The middle and higher peak corresponds to the main superstructure. And the third peak accounts for a significantly lower superstructure that has the highest point on the ship. Figure 6.3.3.3.F2 is a profile version of the Bismarck for identification assistance purposes.

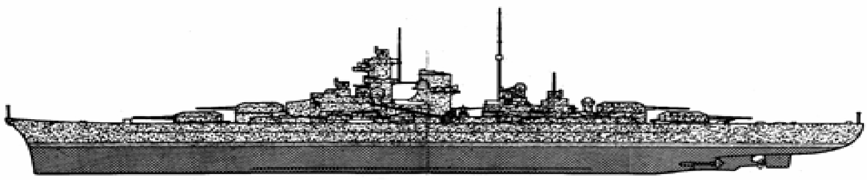

Figure 6.3.3.3.F2. KMS Bismarck Left Profile as seen by the simulation software.

6.3.3.4. More Realistic (MORE) Model - Reflector Initial Phases Zero.

A final basic model was made in which the initial reflectors phases are all 0 whereas the reflectors amplitudes are the same as those in the permutation 3 model. The phase is still dependent on range. This model was compiled for verification purposes and its details are shown in appendix 12.4.1.4.

6.3.3.5. Multi-Layer Model

A more realistic ship model is the one shown in figure 6.3.3.5.F1. There are multiple scatterers at different heights in the middle section of the superstructure. Also an additional scatterer has been added to the giant front and back gun turrets.

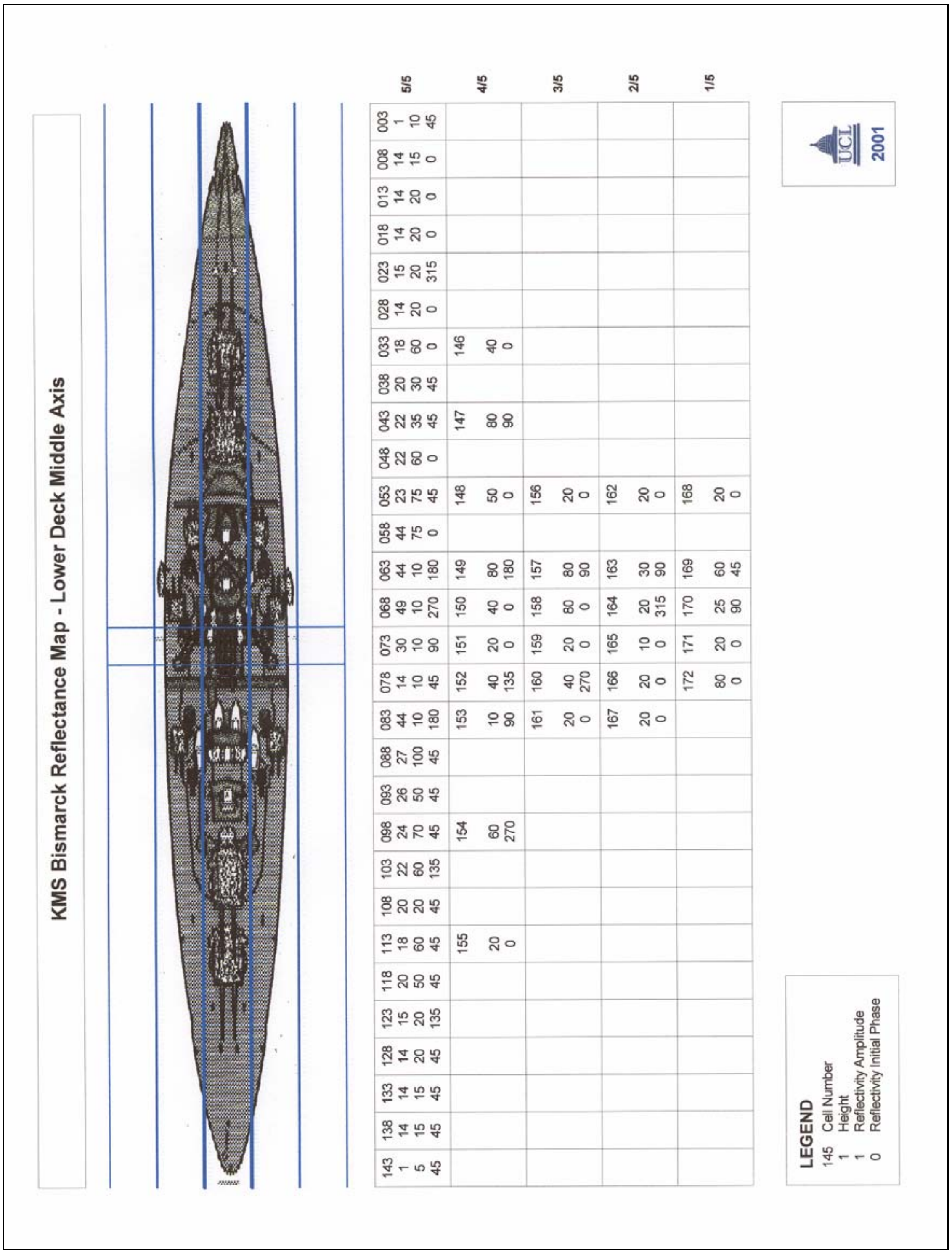

Figure 6.3.3.5.F1. KMS Bismarck Reflectance Map - Multiple Layer Model.

The information shown in figure 6.3.3.5.F1 complements the complete model of figure 6.3.3.F1. The results are shown in section 7.1.1.

6.4. Interferometry and ISAR Correlation Simulation

The ISAR part is the same as in section 6.3 but now another antenna is added to the surveillance aircraft as shown in figure 6.4.F1. Both antennas perform the ISAR function and both are needed to acquire the interferometric reference.

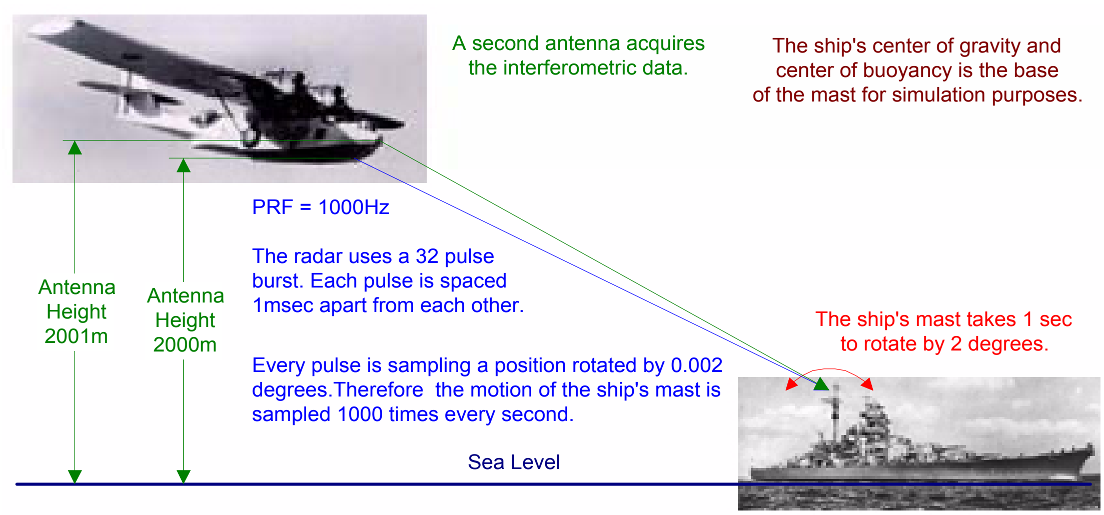

Figure 6.4.F1. Interferometric ISAR data acquisition.

6.4.1. Interferometrically Acquired Ship Profile with no Glint Effects

First the middle line of the ship was interferometrically examined. This will assist in the comparison with the ISAR results from the previous section.

As set out in the simulation sections the real values of the ship's profile is shown in figure 6.4.1.F1.

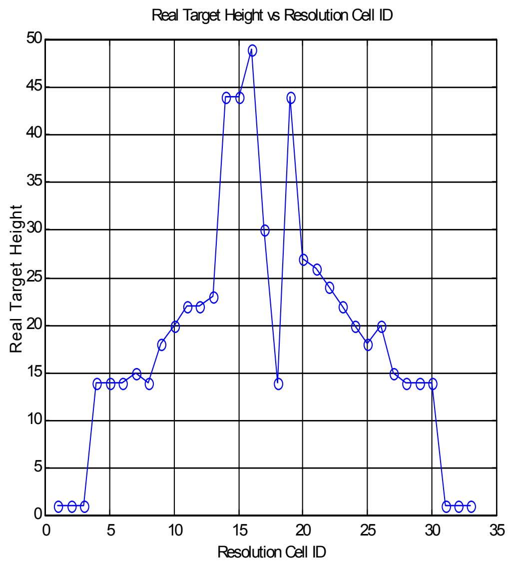

Figure 6.4.1.F1. Real observation of the ship's middle axis.

The interferometer follows the middle axis of the ship as it can be seen with an aspect angle of forty-five degrees. This is the explanation for the three low points in the beginning and the end of the profile in figure 6.4.1.F1.

Now the same motion as used for the ISAR simulations will be used with the interferometer software referenced in appendix 12.3.2.

In figure 6.4.1.F2. the rotation angle is 0.002 degrees per millisecond. Although there are actually thirty-two profiles only the last one can be seen in green since the change in height is very small and they overlap.

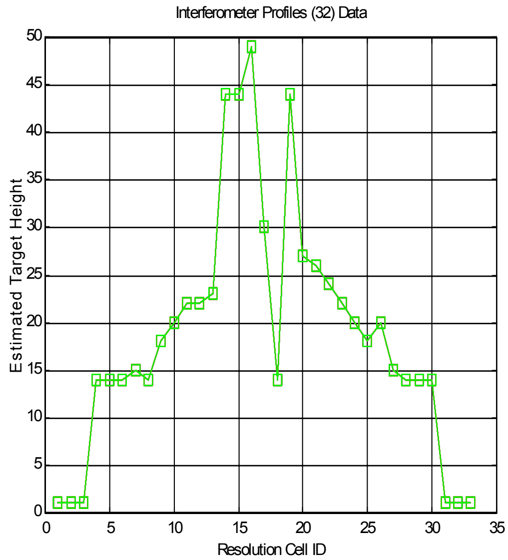

Figure 6.4.1.F2. Interferometric observation of the ship's middle axis.

The results shown in figure 6.4.1.F2. exhibit no glint effects. In order to be able to compare the interferometric and ISAR methods a glint situation has to be constructed. It is shown in section 6.4.2.

6.4.2. Interferometrically Acquired Ship Profile with Glint Effects

The height of the ship's superstructure that can be seen by the interferometer is shown in figure 6.4.2.F1. Scatterers close to each other should start to confuse the interferometer.

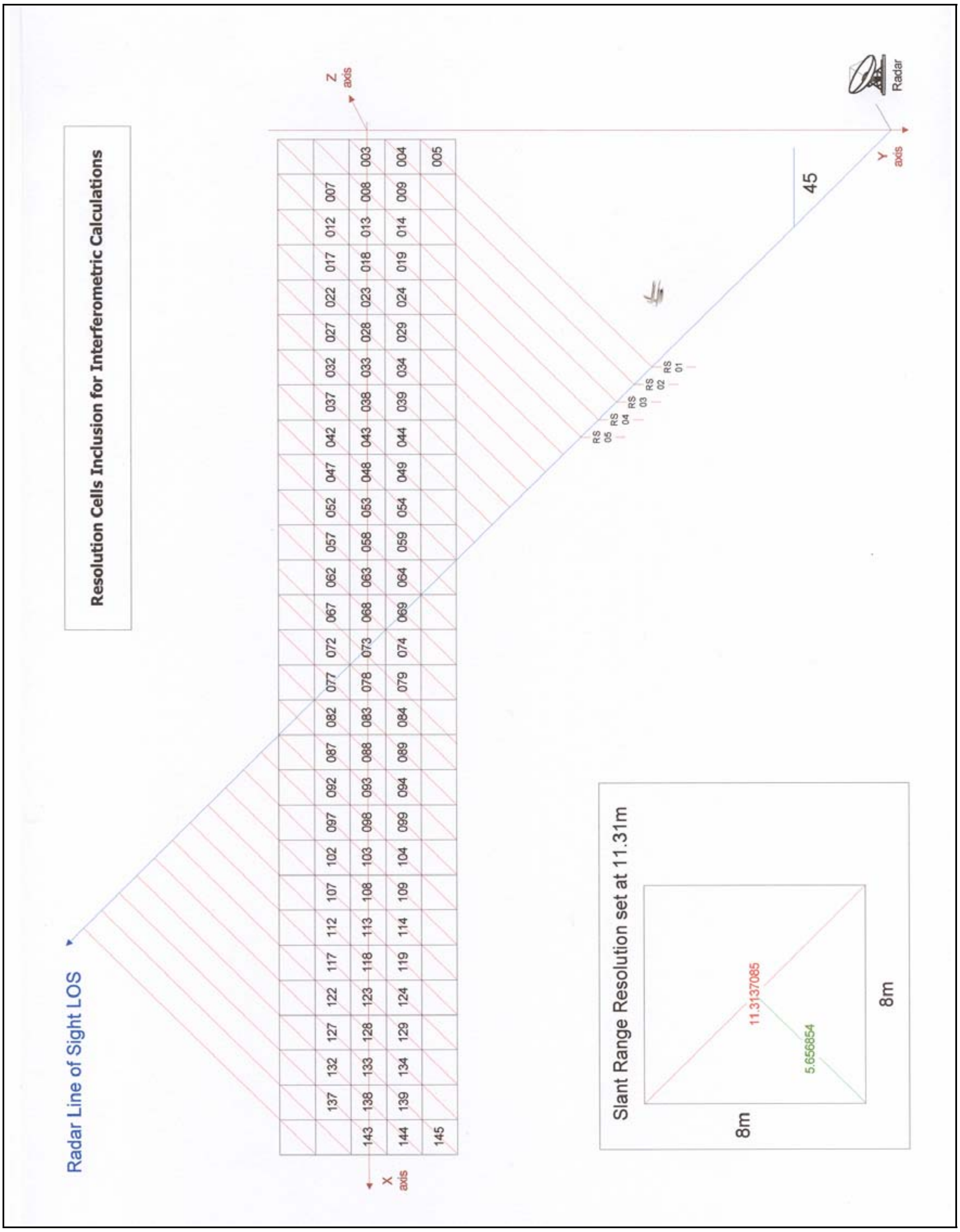

Figure 6.4.2.F1. Radar Aspect Angle and Resolution Cell Definition for Interferometry.

The complete analysis on interferometric results is shown in the experiments section 7.4.

Now that the ship's profile has been established by both ISAR and interferometric methods the analysis part of the project using selected experiments can commence.

7. RESULTS & DISCUSSION

Experiments based on the Derived ISAR Ship Model

The course of action regarding experiments based on the above derived ship model was set on the 1st August, 2001, and is as follows :

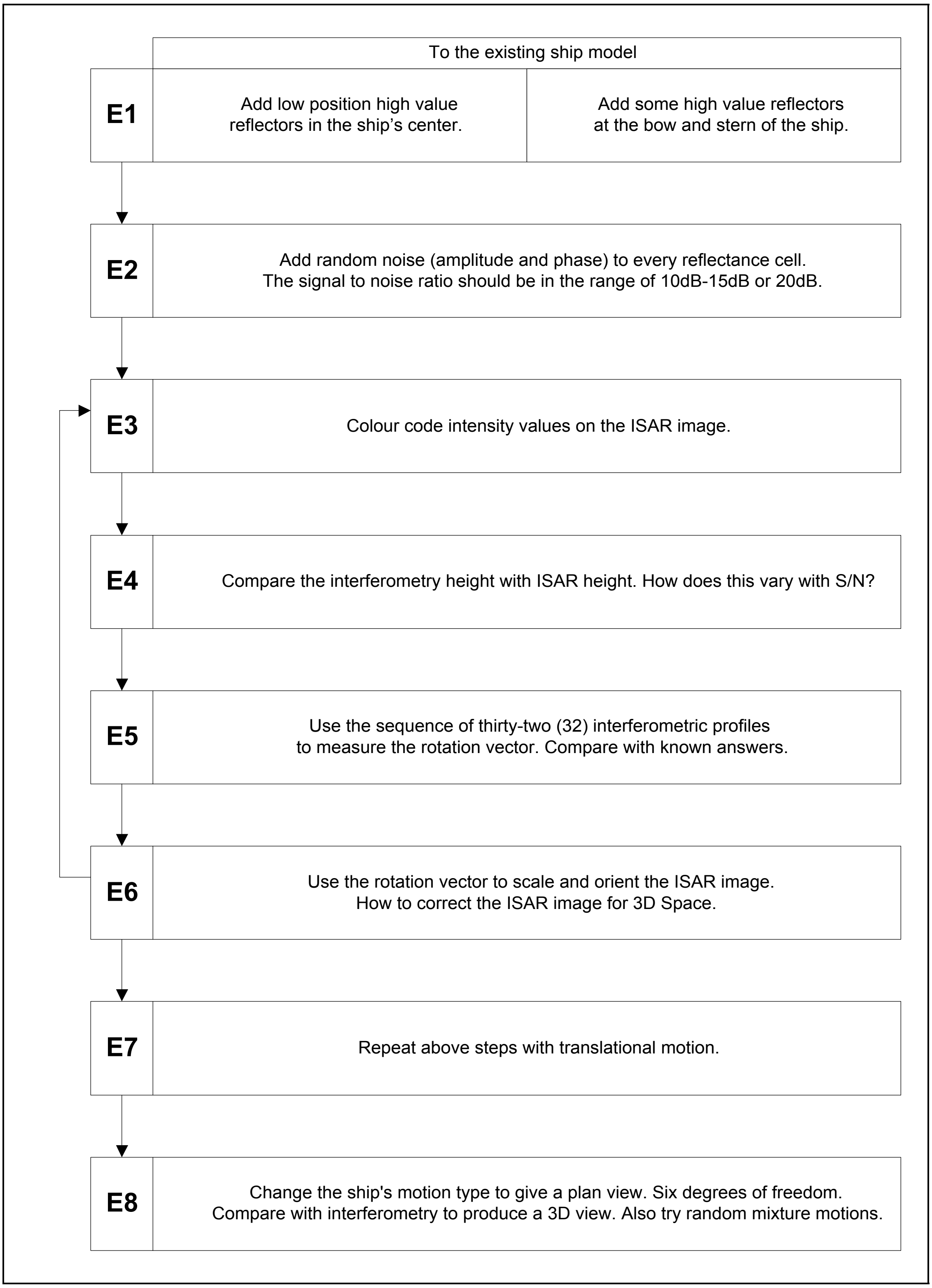

Figure 7.F1. Experiments based on the Derived ISAR Ship Model.

7.1. Experiment 1 Results - Multi-Layer/Bright End Reflectors Ship Model

7.1.1. Experiment 1 Results - Multi-Layer Ship Model

These are the results for the ship model with scatterers in different heights within the same coordinates.

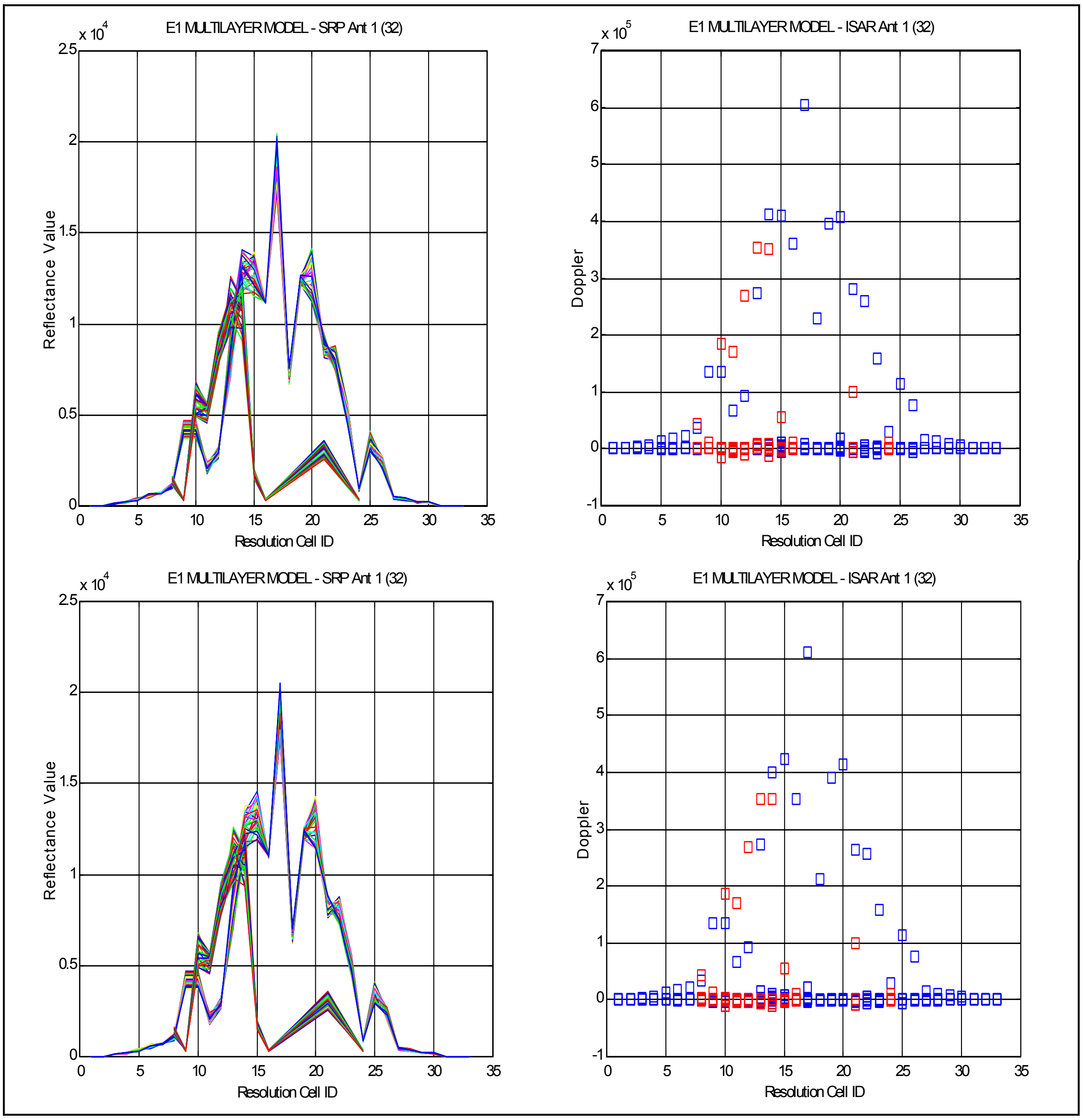

Figure 7.1.1.F1. Multi-Layer Ship Model Results.

As shown in figure 7.1.1.F1., when comparing the two slant range profiles, the glint effect is distorting the shape of the vessel.

7.1.2. Experiment 1 Results - Bright End Reflectors Ship Model

Also another model was created that had high value reflectance in lower heights ship coordinates. The results for this model can be found in appendix 12.5.1.

7.2. Experiment 2 Results - Noise

Discussion of the effects of the amount of noise compared to the level of the radar signal.

7.2.1. Noise level at 10dB

An observable distortion starts at 10db. Other results at 15dB and 20dB leave the results unaffected and can be seen in appendix .

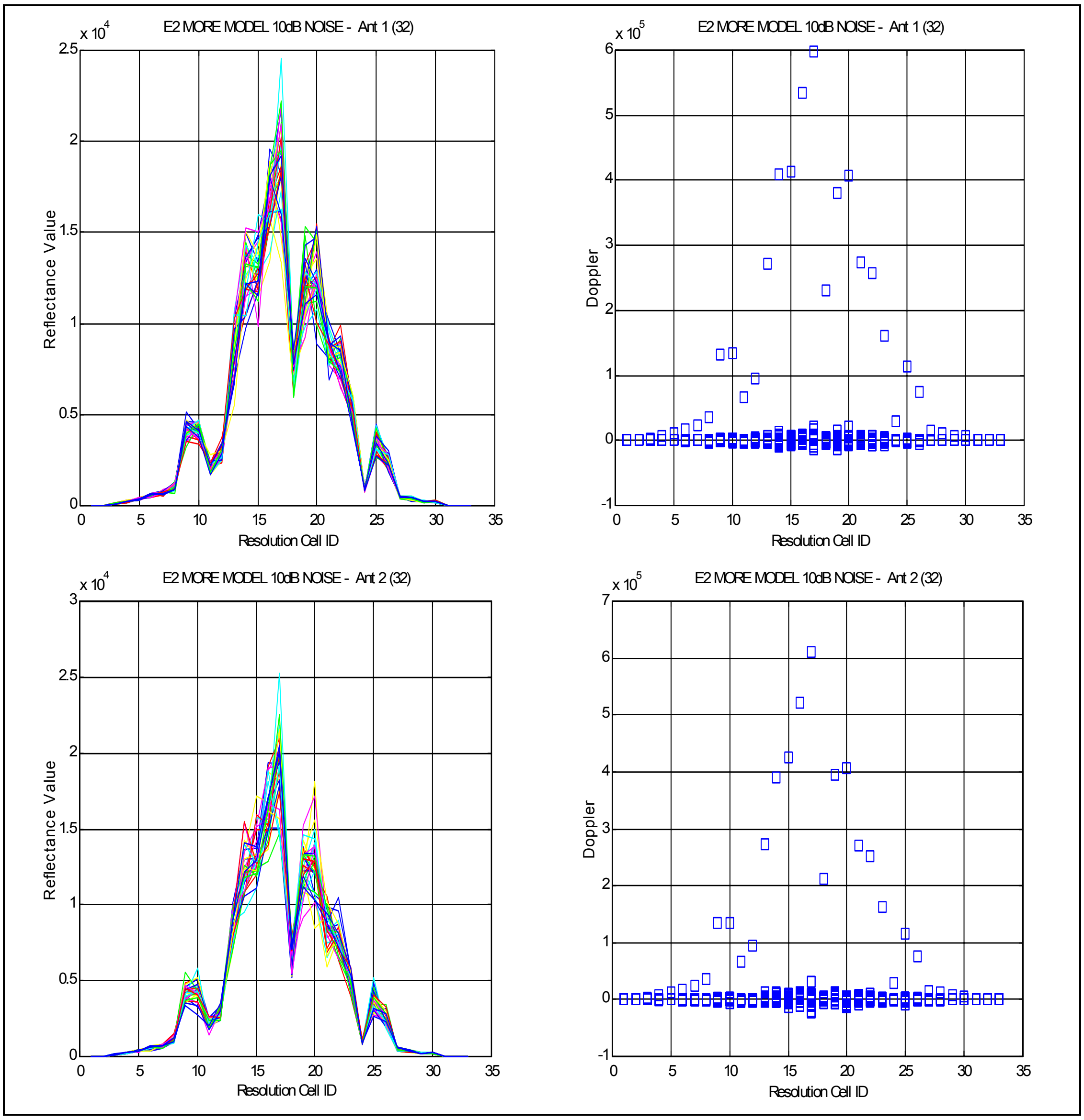

Figure 7.2.1.F1. Noise is becoming a problem at 10dB.

7.3. Experiment 3 Results - ISAR Image Colour Coding

Due to time restrictions the results for this section are not available. Although considerable work has been done towards their acquisition which can be found in the accompanying cd-rom under subdirectory E3.

7.4. Experiment 4 Results - Interferometry & ISAR Height Comparisons

Due to time restrictions the results for this section are not available. Although considerable work has been done towards their acquisition which can be found in the accompanying cd-rom under subdirectory E3.

This part is very close to completion and results may be available as a compendium on the 25th of September during the viva presentation.

7.5. Experiment 5 Results - Rotation Vector Estimation via Interferometry

Due to time restrictions the results for this section are not available.

7.6 Experiment 6 Results - ISAR Image Scaling & Correction in 3D Space

Due to time restrictions the results for this section are not available.

7.7 Experiment 7 Results - Translational Motion Considerations

7.7.1. Translational Motion at 30 Knots.

3 MORE REALISTIC MODEL - COMPLETE WITH PHASES - DEPENDENT ON RADAR RANGE

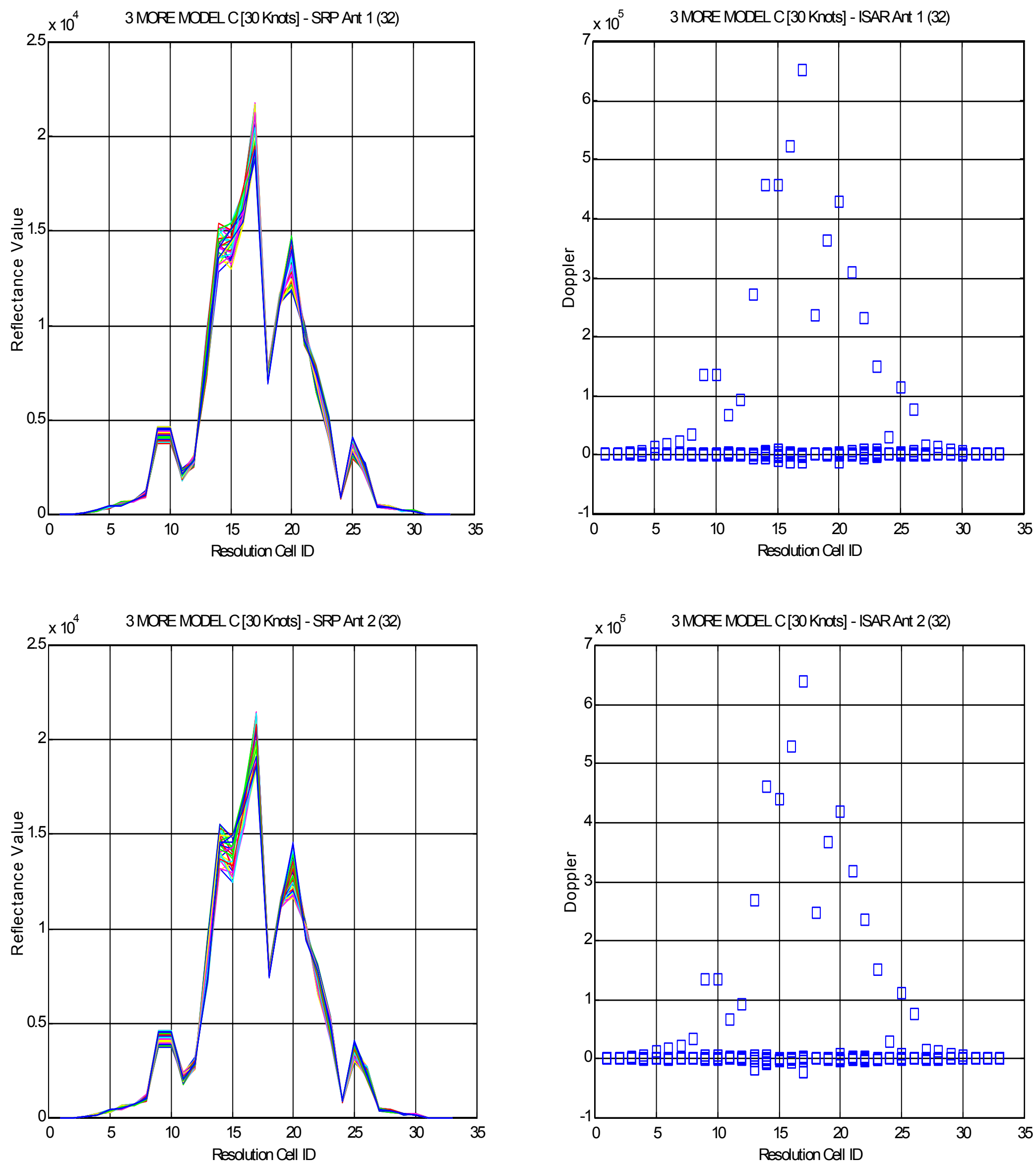

Figure 7.7.1.F1. Bismarck's top speed was thirty knots.

7.8. Experiment 8 Results - Composite Translational Motion Considerations

Due to time restrictions the results for this section are not available. Although considerable work has been done towards their acquisition which can be found in the accompanying cd-rom under subdirectory E8.

The main line for the creation of composite motion with the MORE Model is in the xrotation function. For the simple rotation around the x-axis of the ship the function has the form of equation 7.8.1.

New Coordinates = Movement Matrix * Old Coordinates [7.8.E1]

Analytically the parameters in equation 7.8.E1. are shown in equations 7.8.E2., 7.8.E3 and 7.8.E4.

x(new) = +[x(old)*cos(rotation angle) + y(old)*sin(rotation angle)] [7.8.E2]

y(new) = - [x(old)*sin(rotation angle) + y(old)*cos(rotation angle)] [7.8.E3]

z(new) = +[z(old)] [7.8.E4]

Therefore the movement matrix has the form shown in equation 7.8.E5.

$$MovementMatrix = \begin{matrix} \cos(rotationangle) & \sin(rotationangle) \\ -\sin(rotationangle) & \cos(rotationangle) \end{matrix} \qquad [7.8.E5]$$

In order to provide a more complicated motion the movement matrix needs to be multiplied by matrices that have different parameters from equation 7.8.E5. always according to the required rotation action.

Excellent references that fully explain the above are Abrash [49] (931) and Biran [29] (225).

8. CONCLUSIONS

The major research topic evaluated in this project is an overall assessment of interferometric processes as applied to Inverse Synthetic Aperture Radar (ISAR) image focusing techniques. The final product can bear the title Interferometric Inverse Synthetic Aperture Radar (InISAR).

Simulation emphasis will be given to the results provided by the interferometric approach for high resolution images of moving targets. Therefore the experimental point of the project is an overall efficient and well documented software system. MATLAB 6.0 as a mathematical package is used.

From all current work progress the following conclusions are now available :

- Interferometric ISAR will be able to provide three-dimensional information about a moving ship target. There is still considerable work between the theoretical approach and a realisation model. But the simulation of the physics of this subject seem very promising towards a working observation instrument.

- Glint effects from multiple dominant scatterers will distort the ship's profile. This result is attributed to the comparison of the Single-Layer and the Multi-Layer ship models.

- Noise problems are evident below or around 10dB.

- Translational motion will blur the image and needs to be compensated.

Finally it should be noted that most current work involving interferometry as a three-dimensional radar viewing implementation is still at an early stage.

9. RECOMMENDATIONS FOR FURTHER WORK

There are two types of recommendations :

- Theoretical enhancements that are analysed in section 9.1.

and

- Real Data Collection and Analysis Project Stage which is covered in section 9.2.

9.1. FB16 Military Simulation Model Enhancements

- Intelligent radar beam function that senses the complete domain of a 3D space.
- The ISAR imaging part needs the function that plots the different colours that correspond to intensity values.
- Rotation Vector Estimation via Interferometry section needs to be discussed.
- Composite motion results extraction.
- Several permutations that lead to the better understanding of the related physics principles.
- Finally a reflectivity model for the HMS Hood shown in figure 8.1.F1. could be compiled and compared to the existing Bismarck model.

Figure 9.1.F1. The HMS Hood.

The program should be able to automatically calculate which ship is viewed in its radar beam from all operator defined viewing angles.

9.2. Real Data Collection and Analysis Project Stage

- Actual data should be obtained for example by a stationary radar on a shore or an airborne radar. Then a model should be implemented to process the information according to the recommendations and conclusions laid out in this project.

10. REFERENCES

[01]. GRIFFITHS 2001 MOE8 Antennas & Radar Lecture Notes.
London : University College London.

[02]. GRIFFITHS 1995 Interferometric Synthetic Aperture Radar (InSAR).
London : IEE Electronics & Communication Engineering Journal Volume 7 Number 6.

[03]. GRIFFITHS 1999 High-Resolution Radar Ship Signature Classification.
London : University College London, Departmental Review 1998-1999, page 43.

[04]. BAKER 1995 High Resolution 3D Radar Imaging.
Malvern : DRA, Worcs WR14 3PS, UK.

[05]. BAKER 1995 Hybrid Stripmap - Spotlight SAR.
Malvern : DRA, Worcs WR14 3PS, UK.

[06]. BAKER 2000 Short Range Surveillance Radar Systems.
London : IEE Electronics & Communication Engineering Journal August 2000.

[07]. KOSTIS 2000 Frequency Synthesis for Modern Communications Systems.
London : South Bank University (BEng Thesis).

[08]. HECHT 1998 Optics.
Harlow : Addison Wesley. (ISBN 0-201-83887-7)

[09]. STIMSON 1998 Introduction to Airborne Radar.
New Jersey : SciTech Publishing. (ISBN 1-891121-01-4)

[10] FRANCESCHETTI 1999 Synthetic Aperture Radar Processing.
Florida : CRC Press LLC. (ISBN 0-8493-7899-0)

[11]. SEYBOLD 1996 3D-ISAR Imaging Using a Conventional High-Range Resolution Radar.
IEEE Radar Conference Proceedings, May 1996, p.309-314.

[12]. WEHNER 1995 High-Resolution Radar.
London : Artech House. (ISBN 0-89006-727-9)

[13]. SOUMEKH 1999 Synthetic Aperture Radar Signal Processing.
London : Artech House. (ISBN 0-471-29706-2)

[14]. CARRARA 1995 Spotlight Synthetic Aperture Radar.
London : Artech House. (ISBN 0-89006-728-7)

[15]. SKOLNIK 2001 Introduction to Radar Systems.
New York : McGraw Hill. (ISBN 0-07-118189-X)

[16]. MAHAFZA 1998 Introduction to Radar Analysis.
London : CRC Press. (ISBN 0-8493-1879-3)

[17]. COLE 1992 Understanding Radar.
Oxford : Blackwell Scientific Publications. (ISBN 0-632-03124-7)

[18] WALKER Range Doppler Imaging of rotating objects.
IEEE.

[19]. CHAPMAN 2000 MATLAB Programming for Engineers.
California : Brooks-Cole Publishing Company. (ISBN 0-534-95151-1)

[20]. GHIGLIA 1998 Two-Dimensional Phase Unwrapping.
New York : John Wiley & Sons. (ISBN 0-471-24935-1)

[21]. BANKS 1998 Handbook of Simulation.
New York : Engineering & Management Press. (ISBN 0-471-13403-1)

[22]. RIHACZEK 2000 Theory & Practice of Radar Target Identification.
Massachusetts : Artech House. (ISBN 1-58053-081-8)

[23]. H.M.S. HOOD ASSOCIASTION Internet Presence.
HMS Hood Association Internet Site (www.hmshood.com).

[24]. K.M.S. BISMARCK Internet Presence.
Bismarck Memorial Internet Site (www.battleshipbismarck.hypermart.net/index.htm).

[25]. SCHWEBER 1999 Electronic Communications Systems.
New Jersey : Simon & Schuster. (ISBN 0-13-780016-9)

[26]. RAO 1991 Engineering Electromagnetics.
New Jersey : Prentice Hall. (ISBN 0-13-251604-7)

[27]. BLAKE 1997 Comprehensive Electronic Communication.
Minnesota : West Publishing Company. (ISBN 0-314-20140-8)

[28]. SOMMERVILLE 1996 Software Engineering.
Essex : Addison Wesley. (ISBN 0-201-42765-6)

[29]. BIRAN 1999 MATLAB 5 For Engineers.
London : Prentice Hall. (ISBN 0-201-36043-8)

[30]. BIRD 1996 Engineering Mathematics.
Oxford : Newnes. (ISBN 0-7506-3121-X)

[31]. SON 2001 Range-Doppler Radar Imaging & Motion Compensation.
London : Artech House. (ISBN 1-58053-102-4)

[32]. MUSMAN 1996 Automatic Recognition of ISAR Ship Images.
IEEE. (0018-9251/96)

[33]. LUC 2000 Multi-Look Autofocus in High Resolution Inverse SAR Imaging.
IEEE. (0-7803-6293-4/00)

[34]. VOLES 1993 Resolving Revolutions : Imaging & Mapping by Modern Radar.
IEEE Proceedings-F, Vol. 140, No. 1, February 1993.

[35]. CURRIE 1991 Synthetic Aperture Radar.
Electronics & Communications Engineering Journal, August 1991.

[36]. RODRIGUEZ 1992 Theory & Design of Interferometric SAR Radars.
IEEE Proceedings-F, Vol. 139, No. 2, April 1992.

[37]. HOHMANN 1990 An Adaptive SAR/ISAR Processing Algorithm.
Institute of Remote Sensing Applications, Joint Research Center, 21020 Ispra, ITALY.

[38]. SOUMEKH 1996 Automatic Aircraft Landing using Interferometric ISAR Radar Imaging.
IEEE. (1057-7149/96)

[39]. CHEN 1999 Radar Signal & Image Processing.
IEEE Signal Processing Magazine, March 1999.

[40]. ZHENG 2000 Principles & Algorithms for ISAR Radar Imaging of Maneuvering Targets.
IEEE International Radar Conference. (0-7803-5776-0/00)

[41]. ZHENG 1996 An Effective Autofocus Algorithm for ISAR Imaging.
EE Research Institute, Xidian University, Xi'an, 710071, P.R. CHINA. (0-7803-2914-7)

[42]. ZHENG 1998 A New Method for ISAR Range Instantaneous Doppler Imaging.
EE Research Institute, Xidian University, Xi'an, 710071, P.R. CHINA. (0-7803-4325-5/98)

[43]. ZHENG 1998 One-Dimensional Cross-Range Imaging and Methods to Improve the Resolution of Low Resolution Radar Targets.
Key Laboratory for Radar Signal Processing, Xidian University, Xi'an Shaanxi, P.R. CHINA.

[44]. MENSON 2000 ISAR Inversion Methods for Complex Range Response Data.
IEEE. (0-7803-6359-0/00)

[45]. SATO 1999 Shape Estimation of Space Debris using Single-Range Doppler Interferometry.
IEEE . (0196-2892/99)

[46]. BJORKLUND1999 DBT - A MATLAB Toolbox for Radar Signal Processing.
Stockholm : (www.s2.chalmers.se/~athley/)

[47]. IEE REVIEW The Black Art of Project Management.
London : Institute of Electrical Engineers. (www.iee.org.uk)

[48]. EXE 1999 Requirements for success.
London : EXE, The Software Developers Magazine Volume 13 Issue 12. (www.exe.co.uk)

[49]. ABRASH 1999 Graphics Programming Black Book.
Albany : Coriolis Group Books. (ISBN 1-57610-174-6)

[50]. MILLER 1999 Modern Electronic Communication.
New Jersey : Prentice Hall. (ISBN 0-13-927237-2)

[51]. BANKS 2001 Interferometric Synthetic Aperture Sonar.
London : University College London, London Communications Symposium 2000.

11. TIME MANAGEMENT

11.1. Action Plan

ID	Task Description	Prec	Days	Start	Finish
01	**The FB16 Project**		**305d**	**Fri 17/11/00**	**Mon 17/09/01**
02	First Report		60d	Fri 17/11/00	Mon 15/01/01
03	Second Report		190d	Fri 17/11/00	Fri 25/05/01
04	Final Report		305d	Fri 17/11/00	Mon 17/09/01
05	**Project Planning - Phase I**		**73d**	**Fri 17/11/00**	**Sun 28/01/01**
06	Initial Research & Goal Setting		18d	Fri 17/11/00	Mon 04/12/00
07	Requirements Analysis	6	19d	Tue 05/12/00	Sat 23/12/00
08	Feasibility Analysis	6	12d	Mon 11/12/00	Fri 22/12/00
09	Interim Report Authoring	8	17d	Sat 23/12/00	Mon 08/01/01
10	Supervisor Acknowledge	9	0d	Wed 10/01/01	Wed 10/01/01
11	First Interim Report to UCL	10	0d	Mon 29/01/01	Mon 29/01/01
12	MOE0 Final Exam		0d	Wed 17/01/01	Wed 17/01/01
13	**Project Planning - Phase II**	**5**	**134d**	**Mon 29/01/01**	**Mon 11/06/01**
14	Work Progress Control Plan - Checkpoint 0		0d	Mon 29/01/01	Mon 29/01/01
15	Work Progress Control Plan - Checkpoint 01	14	16d	Mon 29/01/01	Tue 13/02/01
16	Work Progress Control Plan - Checkpoint 02	15	13d	Wed 14/02/01	Mon 26/02/01
17	Work Progress Control Plan - Checkpoint 03	16	14d	Tue 27/02/01	Mon 12/03/01
18	Software-Algorithm Design	17	53d	Tue 13/03/01	Fri 04/05/01
19	Work Progress Control Plan - Checkpoint 04	17	14d	Tue 13/03/01	Mon 26/03/01
20	Work Progress Control Plan - Checkpoint 05	19	0d	Fri 30/03/01	Fri 30/03/01
21	Work Progress Control Plan - Checkpoint 06	20	12d	Fri 30/03/01	Tue 10/04/01
22	Final Exams Preparation		25d	Wed 25/04/01	Sat 19/05/01
23	Last Draft to both Supervisors		0d	Tue 29/05/01	Tue 29/05/01
24	Work Progress Control Plan - Checkpoint 07	21	49d	Wed 11/04/01	Tue 29/05/01
25	Supervisor Acknowledge		0d	Tue 05/06/01	Tue 05/06/01
26	Intermediate Viva Preparation	25	4d	Tue 05/06/01	Fri 08/06/01
27	Second Interim Report to UCL		0d	Mon 11/06/01	Mon 11/06/01
28	**Project Planning - Phase III**	**13**	**98d**	**Tue 12/06/01**	**Mon 17/09/01**
29	Work Progress Control Plan - Checkpoint 08		0d	Wed 13/06/01	Wed 13/06/01
30	Work Progress Control Plan - Checkpoint 09	29	7d	Thu 14/06/01	Wed 20/06/01
31	Work Progress Control Plan - Checkpoint 10	30	7d	Thu 21/06/01	Wed 27/06/01
32	External Examiner Meeting		0d	Thu 28/06/01	Thu 28/06/01
33	Work Progress Control Plan - Checkpoint 11	31	5d	Fri 29/06/01	Tue 03/07/01
34	Interferometry Module - Version 1.0	18	10d	Mon 02/07/01	Wed 11/07/01
35	Intermediate Viva		0d	Wed 04/07/01	Wed 04/07/01
36	Work Progress Control Plan - Checkpoint 12	33	7d	Thu 05/07/01	Wed 11/07/01
37	Work Progress Control Plan - Checkpoint 13	36	6d	Thu 12/07/01	Tue 17/07/01
38	Range Profile Module - Version 1.0		5d	Thu 12/07/01	Mon 16/07/01
39	Manual Results - Progress Demonstration	38	0d	Mon 16/07/01	Mon 16/07/01
40	Work Progress Control Plan - Checkpoint 14	37,39	7d	Wed 18/07/01	Tue 24/07/01
41	Major Reprogramming - Results Automation	39	13d	Tue 17/07/01	Sun 29/07/01
42	FFT Completion - ISAR Image Results	41	0d	Tue 31/07/01	Tue 31/07/01
43	Work Progress Control Plan - Checkpoint 15	42	0d	Tue 31/07/01	Tue 31/07/01
44	Work Progress Control Plan - Checkpoint 16	40	8d	Wed 25/07/01	Wed 01/08/01
45	Interferometry Software-Algorithm Testing	34,38	30d	Tue 17/07/01	Wed 15/08/01
46	ISAR Software-Algorithm Testing	38	30d	Tue 17/07/01	Wed 15/08/01
47	Draft Final Report Authoring		15d	Wed 01/08/01	Wed 15/08/01
48	Draft Final Report to Supervisor	47	0d	Wed 15/08/01	Wed 15/08/01
49	Experiments based on derived Ship Model		23d	Mon 20/08/01	Tue 11/09/01
50	Final Report Authoring		92d	Tue 12/06/01	Tue 11/09/01
51	Supervisor Acknowledge		0d	Tue 11/09/01	Tue 11/09/01
52	**Final Report to UCL**		**0d**	**Fri 21/09/01**	**Fri 21/09/01**
53	Viva Preparation		5d	Mon 10/09/01	Fri 14/09/01

UNIVERSITY COLLEGE LONDON - Interferometric Inverse Synthetic Aperture Radar (InISAR)
T. KOSTIS MSc Microwaves & Optoelectronics 9011874.

ID	Task Name	Duration	Start	Finish	Predecessors
1	**The FB16 Project**	**305 days**	**Fri 17/11/00**	**Mon 17/09/01**	
2	First Report	60 days	Fri 17/11/00	Mon 15/01/01	
3	Second Report	190 days	Fri 17/11/00	Fri 25/05/01	
4	Final Report	305 days	Fri 17/11/00	Mon 17/09/01	
5	**Project Planning - Phase I**	**73 days**	**Fri 17/11/00**	**Sun 28/01/01**	
6	Initial Research & Goal Setting	18 days	Fri 17/11/00	Mon 04/12/00	
7	Requirements Analysis	19 days	Tue 05/12/00	Sat 23/12/00	6
8	Feasibility Analysis	12 days	Mon 11/12/00	Fri 22/12/00	6
9	Interim Report Authoring	17 days	Sat 23/12/00	Mon 08/01/01	8
10	Supervisor Acknowledge	0 days	Wed 10/01/01	Wed 10/01/01	9
11	First Interim Report to UCL	0 days	Mon 29/01/01	Mon 29/01/01	10
12	MOE0 Final Exam	0 days	Wed 17/01/01	Wed 17/01/01	
13	**Project Planning - Phase II**	**134 days**	**Mon 29/01/01**	**Mon 11/06/01**	**5**
14	Work Progress Control Plan - Checkpoint 0	0 days	Mon 29/01/01	Mon 29/01/01	
15	Work Progress Control Plan - Checkpoint 01	16 days	Mon 29/01/01	Tue 13/02/01	14
16	Work Progress Control Plan - Checkpoint 02	13 days	Wed 14/02/01	Mon 26/02/01	15
17	Work Progress Control Plan - Checkpoint 03	14 days	Tue 27/02/01	Mon 12/03/01	16
18	Software-Algorithm Design	53 days	Tue 13/03/01	Fri 04/05/01	17
19	Work Progress Control Plan - Checkpoint 04	14 days	Tue 13/03/01	Mon 26/03/01	17
20	Work Progress Control Plan - Checkpoint 05	0 days	Fri 30/03/01	Fri 30/03/01	19
21	Work Progress Control Plan - Checkpoint 06	12 days	Fri 30/03/01	Tue 10/04/01	20
22	Final Exams Preparation	25 days	Wed 25/04/01	Sat 19/05/01	
23	Last Draft to both Supervisors	0 days	Tue 29/05/01	Tue 29/05/01	
24	Work Progress Control Plan - Checkpoint 07	49 days	Wed 11/04/01	Tue 29/05/01	21
25	**Supervisor Acknowledge**	**0 days**	**Tue 05/06/01**	**Tue 05/06/01**	
26	Intermediate Viva Preparation	4 days	Tue 05/06/01	Fri 08/06/01	25
27	Second Interim Report to UCL	0 days	Mon 11/06/01	Mon 11/06/01	
28	**Project Planning - Phase III**	**98 days**	**Tue 12/06/01**	**Mon 17/09/01**	**13**
29	Work Progress Control Plan - Checkpoint 08	0 days	Wed 13/06/01	Wed 13/06/01	
30	Work Progress Control Plan - Checkpoint 09	7 days	Thu 14/06/01	Wed 20/06/01	29
31	Work Progress Control Plan - Checkpoint 10	7 days	Thu 21/06/01	Wed 27/06/01	30
32	External Examiner Meeting	0 days	Thu 28/06/01	Thu 28/06/01	
33	Work Progress Control Plan - Checkpoint 11	5 days	Fri 29/06/01	Tue 03/07/01	31
34	Interferometry Module - Version 1.0	10 days	Mon 02/07/01	Wed 11/07/01	18
35	Intermediate Viva	0 days	Wed 04/07/01	Wed 04/07/01	
36	Work Progress Control Plan - Checkpoint 12	7 days	Thu 05/07/01	Wed 11/07/01	33
37	Work Progress Control Plan - Checkpoint 13	6 days	Thu 12/07/01	Tue 17/07/01	36
38	Range Profile Module - Version 1.0	5 days	Thu 12/07/01	Mon 16/07/01	
39	Manual Results - Progress Demonstration	0 days	Mon 16/07/01	Mon 16/07/01	38
40	Work Progress Control Plan - Checkpoint 14	7 days	Wed 18/07/01	Tue 24/07/01	37,39
41	Major Reprogramming - Results Automation	13 days	Tue 17/07/01	Sun 29/07/01	39
42	FFT Completion - ISAR Image Results	0 days	Tue 31/07/01	Tue 31/07/01	41
43	Work Progress Control Plan - Checkpoint 15	0 days	Tue 31/07/01	Tue 31/07/01	42
44	Work Progress Control Plan - Checkpoint 16	8 days	Wed 25/07/01	Wed 01/08/01	40
45	Interferometry Software-Algorithm Testing	30 days	Tue 17/07/01	Wed 15/08/01	34,38
46	ISAR Software-Algorithm Testing	30 days	Tue 17/07/01	Wed 15/08/01	38
47	Draft Final Report Authoring	15 days	Wed 01/08/01	Wed 15/08/01	
48	Draft Final Report to Supervisor	0 days	Wed 15/08/01	Wed 15/08/01	47
49	Experiments based on derived Ship Model	23 days	Mon 20/08/01	Tue 11/09/01	
50	Final Report Authoring	92 days	Tue 12/06/01	Tue 11/09/01	
51	Supervisor Acknowledge	0 days	Tue 11/09/01	Tue 11/09/01	
52	Final Report to UCL	0 days	Fri 21/09/01	Fri 21/09/01	
53	Viva Preparation	5 days	Mon 10/09/01	Fri 14/09/01	

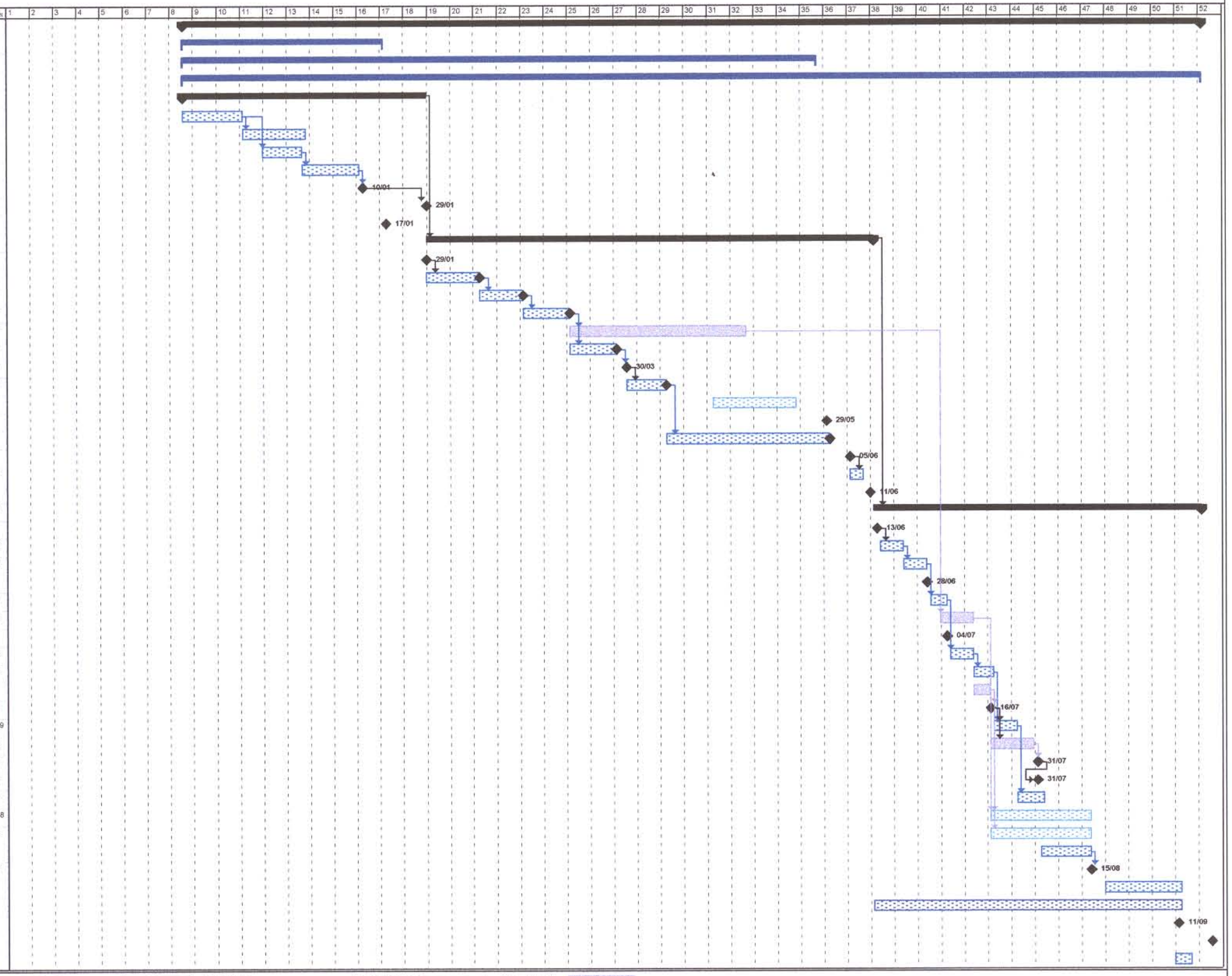

Project: Deadlines
Date: Wed 26/02/03

Task	Progress	Summary	Rolled Up Split	Rolled Up Progress	Project Summary
Split	Milestone	Rolled Up Task	Rolled Up Milestone	External Tasks	

Interferometric Inverse Synthetic Aperture Radar

Work Progress Control Plan - Final Project Report - 17th September 2001

Basics	Radar Power	Antenna	HRR	SAR	ISAR	Optics	Software	3D	InISAR	Final
Preliminary	The Radar Equation	Antenna Theory	Range Resolution	Analytical Model	Analytical Model	Physical Optics Theory	Data Collection Aperture	3D InISAR Imagery	Research Setup	First Interim
Range Resolution	Radar Cross Section	Antenna Characteristics	Pulse Compression	Geometry	Geometry	Interferometry	Software Authoring	In Height Ship Profile	Interferometry = Height	Second Interim
Angular Resolution	Antenna Effective Area	Two-Element Array	Analog Linear FM	System Overview & Operation	Resampling	Antenna Baseline	Testing Process	In Top View Ship Profile	ISAR = 2D Plane	Software Authoring
Pulse Repetition Frequency	Receiver Noise Power	Auto-Correlation Effect	Digital Barker Codes	Synthetic Aperture Imaging	Linear Interpolation	Interferogram	White Box Testing	ISAR Height Ship Profile	Coupling In to ISAR (InISAR)	Software Testing
Maximum Unambiguous Range	Signal to Noise Ratio	N-Element Array	Matched Filter	SAR Ground Mapping	Polar to Cartesian	Height Estimation	Black Box Testing	ISAR Top View Ship Profile	Problems Outline	Ship Imaging
Scanning Radar : Azimuth	Maximum Detection Range	Beam Steering Techniques	Ambiguity Function	Resolutiion Cells	ISAR Model Analysis	Range Estimation	Stress Testing	Comparisons	Computer Programs	Experiments on Model
$cosec^2$ Antenna Pattern	Integration Gain	Null Steering Techniques	Linear Frequency Modulation	Moving Target Errors	Radar Aspect Angle	Phase Unwrapping	Time Testing	In Rotation Vector	Rotation Vector Scaling	Results
Doppler Effect	Power-Aperture Product	Digital Signal Processing	Linear Period Modulation	Spotlight Mode (Strip-Hybrid)	Ship Targets (Fresnel)	Digital Elevation Model	Error Input Testing	ISAR Scaling	Height Comparisons	Supervisor Acknowledge
Radar-Sonar Tutorials	Pulse Properties	Shannon's Theorem	Paper Reading	SAR-ISAR Duality	Point Targets Approach	First Stage Results	Supervisor Acknowledge	Image Formation	Automatic Target ID	Final Conclusions
Bibliography Reading	Bibliography Reading	Bibliography Reading	Bibliography Reading	Paper Reading	Paper Reading	Paper Reading	System Overview & Operation	Results	Results	Further Suggestions
Foundation Theory I	Foundation Theory II	Foundation Theory III	High Resolution Radar	ISAR Theory	ISAR Equations	Interferometry Equations	InISAR Software	Research	Interferometric ISAR	Final Report

Work Breakdown Structure Legend Note : Main tasks are inside grey boxes.

UCL 9011874

12. APPENDICES

12.1. CONTENTS

12.2. Interferometry Simulation with a Stationary Five Prominent Points Target.

12.2.1. Interferometric Operation Top-Down Design - Five Scatterers.

```
% Interferometric Operation Top-Down Design - Five Scatterers.
%
% Purpose : Calculates and plots the interferometric results.
% FINAL PLOTTING WORKING VERSION
% Plot of Real Target Height vs Radar Estimated Target Height
%
% General :    lamda Wavelenght
%                  B Baseline
%
% Input   :        R Ground Range.
%                 R1 Range to target from lower antenna.
%                 R2 Range to target from higher antenna.
%                  h Height from lower antenna to ground.
%              zreal Real target height.
%                  a Baseline angle (a=0 Vertical interferometer).
%
%
% Output  :      phi Phase difference between corresponding pixels in the two images.
%              theta Angle between height and R1.
%                  z Estimated Target height.
%                  y Estimated Ground range.
%             Deltaz Height error for short range hi-res aircraft interferometry.

% General Parameters

lamda = 0.003; % VHF 150MHz 2 - L 1.300000040 0.23076923 - X 10GHz 0.03 - Ka
35.000035Ghz 0.00857142
% EXP 100GHz 0.003

a=0; % Baseline angle (a=0 Vertical interferometer).

R=1000000; % 1.Range [m].

B=1; % 2. Baseline [m].

h=2000; % 3.Radar Height [m].

zreal=50; % 4. Target Height [m]. Height of first scatterer closer to the ground.

fprintf('Data Explanation : [i] [h] [R1] [R2] [phi] [theta] [zreal] [z] [R] [y]\n');

% Computational Part.
% Makes a database holding details of a target's prominent points.

for i=1:5
% Increases the scatterer height by 1m making five scatterers off the ground.

% R2=R1+(phi*lamda/2); -------------------------------------------------------------

R1=sqrt(((h-zreal).^2)+(R.^2)); % Registration of the two images

R2=sqrt((((h+B)-zreal).^2)+(R.^2)); % will reveal the phase difference phi.

phi=((2.*pi)/lamda).*(R2-R1);       % Phase Difference computed.

% costheta -----------------------------------------------------------------------

thetainsidevalue = ((R2.^2-B.^2-R1.^2)/(2.*B.*R1))-a; % The value of thetainsidevalue.

thetarads = acos(thetainsidevalue); % The value of theta in rads.

theta = thetarads.*(180./pi); % The value of theta in degrees.

costheta=cos(thetarads); % The value of costheta in degrees.

z=h-(R1.*(costheta)); % The value of z (Estimated Target Height).

y=sqrt((R1.^2)-((h-z).^2)); % The value of y (Estimated Ground range).

% Radar InterFerometer (RIF) Array
RIF(i).h=h;
RIF(i).R1=R1;
RIF(i).R2=R2;
RIF(i).phi=phi;
RIF(i).theta=theta;
RIF(i).zreal=zreal;
```

```
RIF(i).z=z;
RIF(i).R=R;
RIF(i).y=y;

%fprintf('%-+6.2f %-+6.2f %-+6.6f %-+6.6f %-+6.6f %-+6.6f %-+6.10f %-+6.10f %-
+6.10f\n',
%h, R1, R2, phi, theta, zreal, z, R, y);

fprintf('%1d %-+6.2f|%-+6.2f|%-+6.2f|%-+6.10f|%-+6.6f|%-+6.2f|%-+6.10f|%-+6.2f|%-
+6.10f\n', ...
 i,RIF(i).h, RIF(i).R1, RIF(i).R2, RIF(i).phi, RIF(i).theta, RIF(i).zreal, RIF(i).z,
RIF(i).R, RIF(i).y);

zreal=zreal+1;

end

% Plotting Vectors

zrealplot = [RIF(1).zreal RIF(2).zreal RIF(3).zreal RIF(4).zreal RIF(5).zreal];
phiplot   = [RIF(1).phi   RIF(2).phi   RIF(3).phi   RIF(4).phi   RIF(5).phi   ];
zplot     = [RIF(1).z     RIF(2).z     RIF(3).z     RIF(4).z     RIF(5).z     ];

plot(zrealplot,zplot,'bo-');

axis([RIF(1).zreal-1 RIF(5).zreal+1 RIF(1).z-1 RIF(5).z+1]);
title ('Plot of Real Target Height vs Radar Estimated Target Height');
xlabel ('Plot of Real Target Height');
ylabel('Radar Estimated Target Height');
grid on;
```

```
Data Explanation : [i] [h] [R1] [R2] [phi] [theta] [zreal] [z] [R] [y]
1 +2000.00|+1000001.90|+1000001.90|+4.0851097422|+89.888273|+50.00|+50.0000610350|+1000000.00|+1000000.0000001190
2 +2000.00|+1000001.90|+1000001.90|+4.0830155749|+89.888331|+51.00|+51.0000000000|+1000000.00|+1000000.0000000000
3 +2000.00|+1000001.90|+1000001.90|+4.0809211639|+89.888388|+52.00|+51.9999389648|+1000000.00|+999999.9999998810
4 +2000.00|+1000001.90|+1000001.90|+4.0788267528|+89.888445|+53.00|+52.9999999999|+1000000.00|+999999.9999999998
5 +2000.00|+1000001.89|+1000001.90|+4.0767323418|+89.888503|+54.00|+53.9999999999|+1000000.00|+999999.9999999998
```

Listing 12.2.1.L1. Five Static Scatterers.

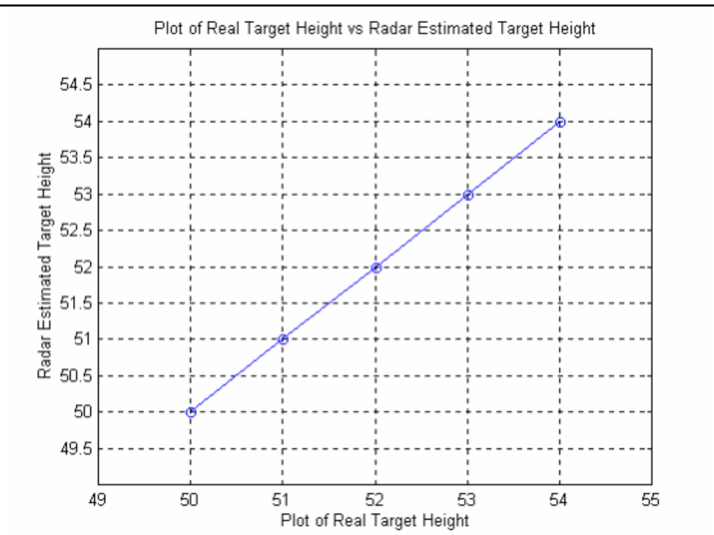

Figure 12.2.1.F1. Plot of Real Target Height vs Estimated Target Height.

12.2.2. Interferometric Operation Program Design - Five Scatterers.

There follows the flowchart for multiple reflectors within the same coordinates. The difference from section 12.2.1. is that the RIF function is now employed.

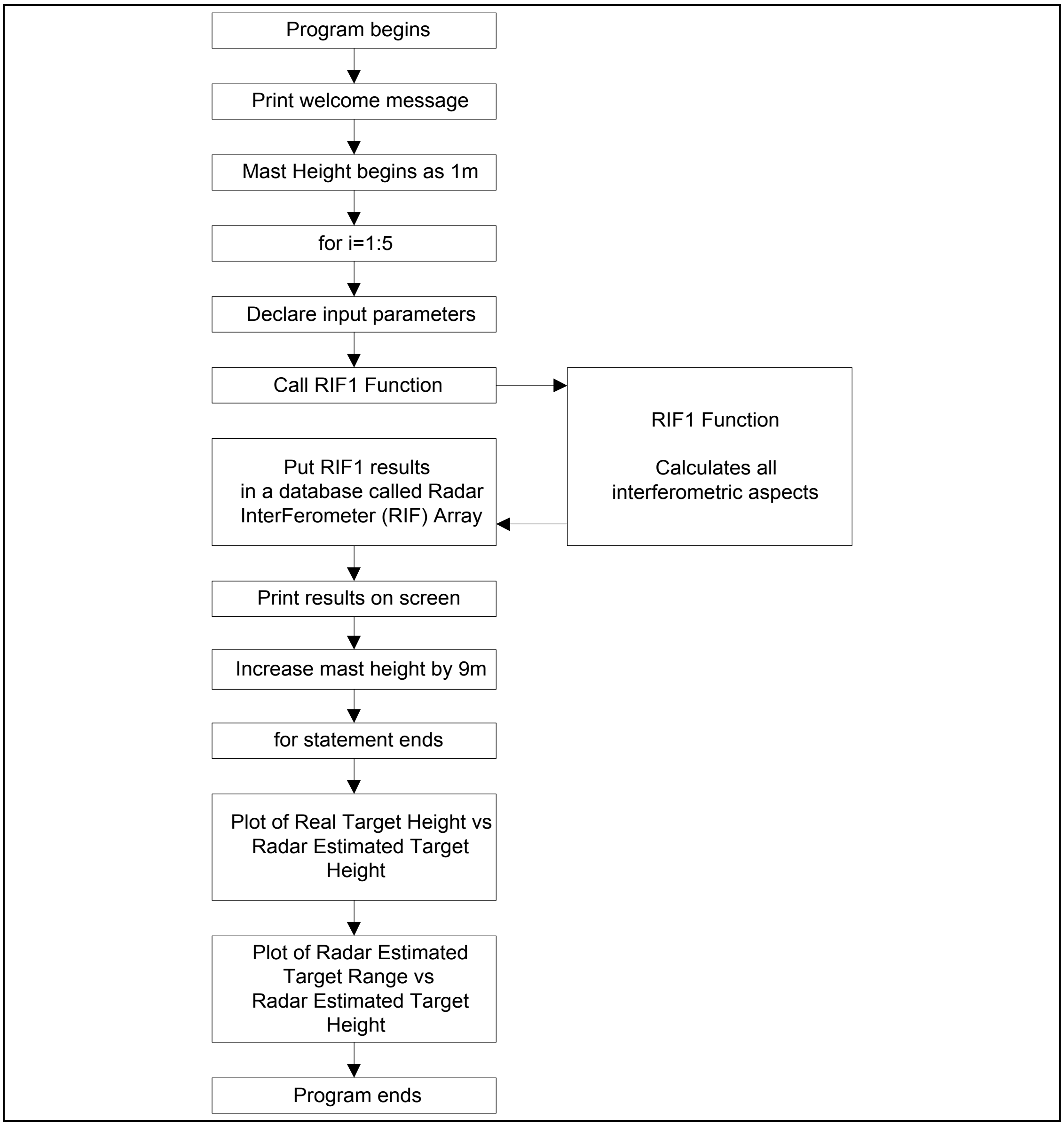

Figure 12.2.2.F1. Flowchart for multiple reflectors within the same coordinates.

```
% InFNCRIF : Interferometric Operation Calling Program - Five Scatterers.
% UNIVERSITY COLLEGE LONDON @2001 - 9011874.
%
% Purpose : Calculates and plots the interferometric results.
% FINAL PLOTTING WORKING VERSION
% Plot of Real Target Height vs Radar Estimated Target Height
%
% General :     lamda Wavelenght
%                   B Baseline
%
% Input   :         R Ground Range.
%                  R1 Range to target from lower antenna.
%                  R2 Range to target from higher antenna.
%                   h Height from lower antenna to ground.
%               zreal Real target height.
%                   a Baseline angle (a=0 Vertical interferometer).
%
%
% Output  :       phi Phase difference between corresponding pixels in the two images.
%               theta Angle between height and R1.
%                   z Estimated Target height.
%                   y Estimated Ground range.
%              Deltaz Height error for short range hi-res aircraft interferometry.

% Bismarck Mast Dimensions - Zero Height is sea level.

fprintf('UNIVERSITY COLLEGE LONDON @2001 FINAL PLOTTING WORKING VERSION -
9011874.\n');
fprintf('Data Explanation : [i] [h] [R1] [R2] [phi] [theta] [zreal] [z] [R] [y]\n');

zreal=1;

for i=1:5;

% Function Input Parameters : lamda (f=5GHz), a, R, B, h, zreal
[h, R1, R2, phi, theta, zreal, z, R, y] = RIF1(0.06,0,15000,0.5,2000,zreal);

% Radar InterFerometer (RIF) Array
RIF(i).h     = h;
RIF(i).R1    = R1;
RIF(i).R2    = R2;
RIF(i).phi   = phi;
RIF(i).theta = theta;
RIF(i).zreal = zreal;
RIF(i).z     = z;
RIF(i).R     = R;
RIF(i).y     = y;

%fprintf('%-+6.2f %-+6.2f %-+6.6f %-+6.6f %-+6.6f %-+6.6f %-+6.10f %-+6.10f %-
+6.10f\n',
%h, R1, R2, phi, theta, zreal, z, R, y);

fprintf('%1d %-+6.2f|%-+6.2f|%-+6.2f|%-+6.10f|%-+6.6f|%-+6.2f|%-+6.10f|%-+6.2f|%-
+6.10f\n', ...
 i,RIF(i).h, RIF(i).R1, RIF(i).R2, RIF(i).phi, RIF(i).theta, RIF(i).zreal, RIF(i).z,
RIF(i).R, RIF(i).y);

zreal=zreal+9;

end

% Plotting Vectors

zrealplot = [RIF(1).zreal RIF(2).zreal RIF(3).zreal RIF(4).zreal RIF(5).zreal];
phiplot   = [RIF(1).phi   RIF(2).phi   RIF(3).phi   RIF(4).phi   RIF(5).phi   ];
zplot     = [RIF(1).z     RIF(2).z     RIF(3).z     RIF(4).z     RIF(5).z     ];

plot(zrealplot,zplot,'bo-');

axis([RIF(1).zreal-1 RIF(5).zreal+1 RIF(1).z-1 RIF(5).z+1]);
title ('Plot of Real Target Height vs Radar Estimated Target Height');
xlabel ('Real Target Height');
ylabel('Radar Estimated Target Height');
grid on;

Rplot     = [RIF(1).R     RIF(1).R     RIF(1).R     RIF(1).R     RIF(1).R     ];
yplot     = [RIF(1).y     RIF(2).y     RIF(3).y     RIF(4).y     RIF(5).y     ];

figure;
plot(yplot,zplot,'bo-');
```

```
axis([RIF(1).y-1 RIF(5).y+1 RIF(1).z-1 RIF(5).z+1]);
title ('Plot of Radar Estimated Target Range vs Radar Estimated Target Height');
xlabel ('Radar Estimated Target Range ');
ylabel('Radar Estimated Target Height');
grid on;
```

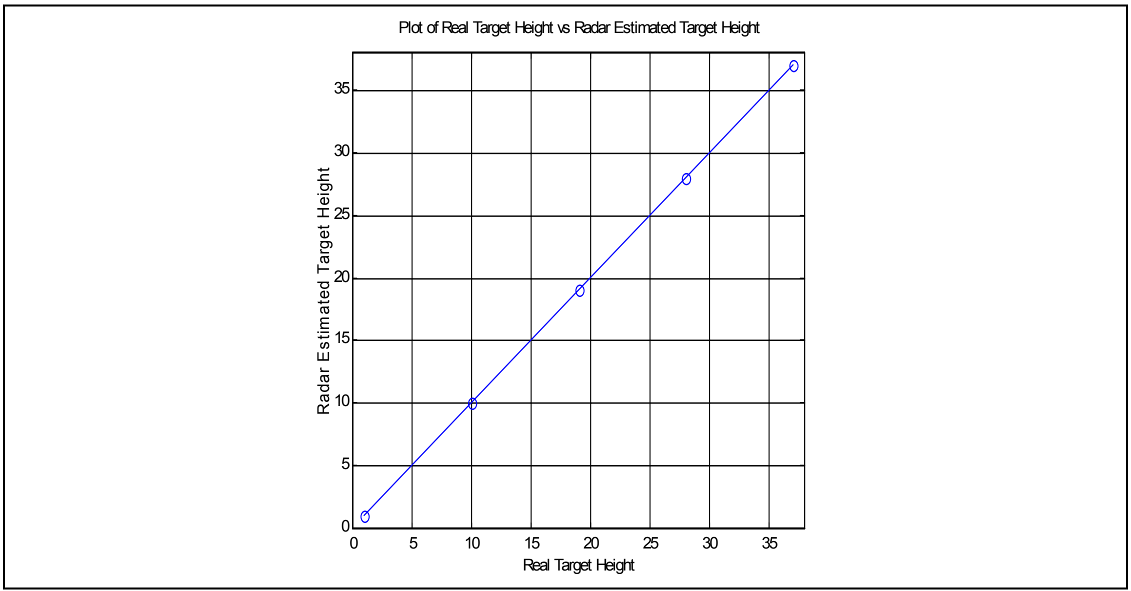

Figure 12.2.2.F1. Plot of Real Target Height vs Estimated Target Height.

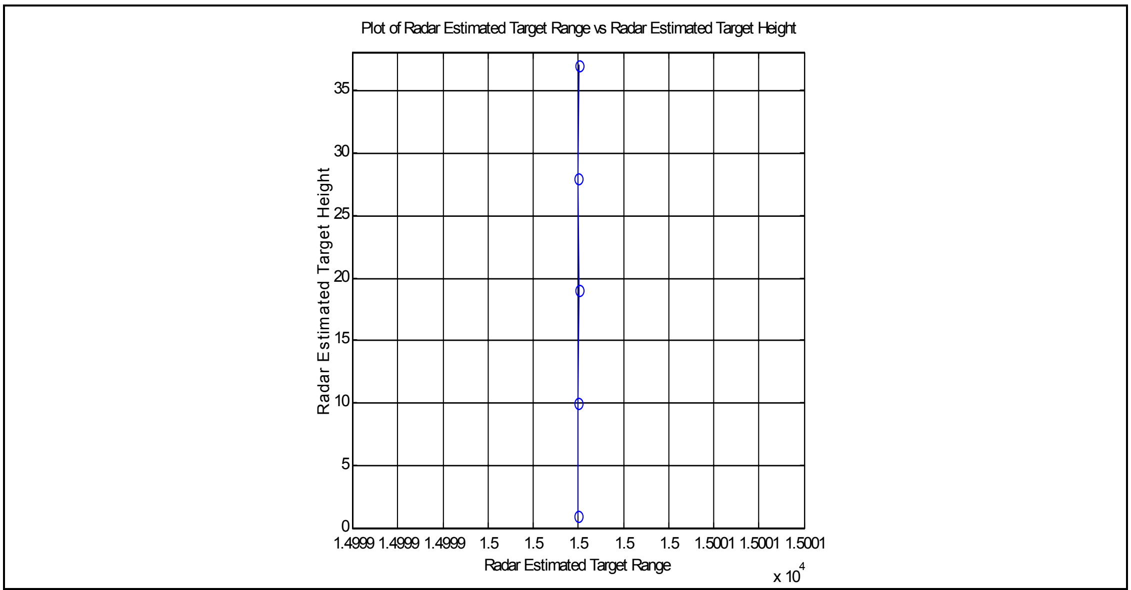

Figure 12.2.2.F2. Plot of Estimated Target Range vs Estimated Target Height.

RIF1 Function Input Parameters

λ	Wavelength
α	Antenna Tilt
R	Range
B	Baseline
H	Radar Height
zreal	Target Height

$$R_1 = \sqrt{R^2 + (H - z)^2}$$

Calculate R1 from the geometry of Figure 5.4.F1.

$$R_2 = \sqrt{R^2 + ((H + B) - z)^2}$$

Calculate R2 from the geometry of Figure 5.4.F1.

$$\phi = \frac{2\pi}{\lambda}(R_2 - R_1)$$

Calculate the phase difference φ from the geometry of Figure 5.4.F1.

$$\theta = \cos^{-1}\left(\frac{R_2{}^2 - R_1{}^2 - B^2}{2BR_1}\right) - a$$

Calculate the angle θ between R1 and H from the geometry of Figure 5.4.F1.

$$z = H - R_1 \cos\theta$$

Calculate Radar Estimated Target Height z from the geometry of Figure 5.4.F1.

$$y = \sqrt{R_1{}^2 - (H - z)^2}$$

Calculate Radar Estimated Target Range y from the geometry of Figure 5.4.F1.

RIF1 Function Output Parameters

H	Radar Height
R1	R1 Range
R2	R2 Range
φ	Phase Difference
θ	Angle
zreal	Real Target Height
z	Radar Estimated Target Height
R	Actual Ground Range to Target
y	Radar Estimated Target Range

Figure 12.2.2.F3. Interferometric Function Description.

```
function [h, R1, R2, phi, theta, zreal, z, R, y] = RIF (lamda, a, R, B, h,zreal)
% RIF1 Version 1.0 April 2001  - UNIVERSITY COLLEGE LONDON 9011874.
% Interferometric Operation Function - Five Scatterers.
%
% Purpose : Calculates and plots the interferometric results.
%
% General :     lamda Wavelenght
%                   B Baseline
%
% Input   :         R Ground Range.
%                  R1 Range to target from lower antenna.
%                  R2 Range to target from higher antenna.
%                   h Height from lower antenna to ground.
%               zreal Real target height.
%                   a Baseline angle (a=0 Vertical interferometer).
%
%
% Output  :       phi Phase difference between corresponding pixels in the two images.
%               theta Angle between height and R1.
%                   z Estimated Target height.
%                   y Estimated Ground range.
%              Deltaz Height error for short range hi-res aircraft interferometry.

% General Parameters

%lamda = 0.003; % VHF 150MHz 2 - L 1.300000040 0.23076923 - X 10GHz 0.03 - Ka
35.000035Ghz 0.00857142
% EXP 100GHz 0.003

%a=0; % Baseline angle (a=0 Vertical interferometer).

%R=1000000; % 1.Range [m].

%B=1; % 2. Baseline [m].

%h=2000; % 3.Radar Height [m].

%zreal=50; % 4. Target Height [m]. Height of first scatterer closer to the ground.

%fprintf('RIF Version 1.0 Radar InterFerometric Function invoked.\n');
%fprintf('Data Explanation : [i] [h] [R1] [R2] [phi] [theta] [zreal] [z] [R] [y]\n');

% Computational Part.
% Makes a database holding details of a target's prominent points.

%for i=1:5
% Increases the scatterer height by 1m making five scatterers off the ground.

% R2=R1+(phi*lamda/2); -------------------------------------------------------------

R1=sqrt(((h-zreal).^2)+(R.^2)); % Registration of the two images

R2=sqrt((((h+B)-zreal).^2)+(R.^2)); % will reveal the phase difference phi.

phi=((2.*pi)/lamda).*(R2-R1);       % Phase Difference computed.

% costheta -------------------------------------------------------------------------

thetainsidevalue = ((R2.^2-B.^2-R1.^2)/(2.*B.*R1))-a; % The value of thetainsidevalue.

thetarads = acos(thetainsidevalue); % The value of theta in rads.

theta = thetarads.*(180./pi); % The value of theta in degrees.

costheta=cos(thetarads); % The value of costheta in degrees.

z=h-(R1.*(costheta)); % The value of z (Estimated Target Height).

y=sqrt((R1.^2)-((h-z).^2)); % The value of y (Estimated Ground range).

%fprintf('RIF Version 1.0 Radar InterFerometric Function ended.\n');
```

```
UNIVERSITY COLLEGE LONDON @2001 FINAL PLOTTING WORKING VERSION - 9011874.
Data Explanation : [i] [h] [R1] [R2] [phi] [theta] [zreal] [z] [R] [y]
1 +2000.00|+15132.61|+15132.61|+0.0000138333|+82.409088|+1.00 |+0.9943246841|+15000.00|+14999.9992436685
2 +2000.00|+15131.43|+15131.43|+0.0000137722|+82.442869|+10.00|+9.9946260452|+15000.00|+14999.9992870544
3 +2000.00|+15130.25|+15130.25|+0.0000137109|+82.476770|+19.00|+19.0247297287|+15000.00|+15000.0032659521
4 +2000.00|+15129.07|+15129.07|+0.0000136497|+82.510448|+28.00|+27.9952287674|+15000.00|+14999.9993727412
5 +2000.00|+15127.90|+15127.90|+0.0000135884|+82.544302|+37.00|+37.0104312897|+15000.00|+15000.0013651044
```

Listing 12.2.2.L1. Five Static Scatterers.

12.3. Interferometry Simulations

12.3.1. Introduction - Interferometry Simulation with a Moving Target.

```
% InFNCRIF5 : Moving Interferometric Operation - One Moving Scatterer.
% UNIVERSITY COLLEGE LONDON @2001 - 9011874.
%
% Purpose : Calculates and plots the interferometric results.
%
% General :     lamda Wavelenght
%                   B Baseline
%
% Input   :         R Ground Range.
%                  R1 Range to target from lower antenna.
%                  R2 Range to target from higher antenna.
%                   h Height from lower antenna to ground.
%               zreal Real target height.
%                   a Baseline angle (a=0 Vertical interferometer).
%
%                MovR Reducing Range as mast approaches radar.
%               MovMH Changing Mast Height.
%
% Output  :       phi Phase difference between corresponding pixels in the two images.
%               theta Angle between height and R1.
%                   z Estimated Target height.
%                   y Estimated Ground range.
%              Deltaz Height error for short range hi-res aircraft interferometry.
%
% Bismarck Mast Dimensions - Zero Height is sea level.

lamda = 0.06;
SampleTime = 1E-1; % Radar Sample Time set at 2sec

MovR(1)=15000.855168; %zero u
MovR(2)=15000.855168;
MovR(3)=15000.641390;
MovR(4)=15000.427600;
MovR(5)=15000.213802;
MovR(6)=15000.000000;
MovR(7)=14999.786198;
MovR(8)=14999.572400;
MovR(9)=14999.358610;
MovR(10)=14999.144832;
MovR(11)=14999.144832; %zero u
MovR(12)=14999.358610;
MovR(13)=14999.572400;
MovR(14)=14999.786198;
MovR(15)=15000.000000;
MovR(16)=15000.213802;
MovR(17)=15000.427600;
MovR(18)=15000.641390;
MovR(19)=15000.855168;
MovR(20)=15000.855168; %zero u

MovMH(1)=48.99253706; %zero u
MovMH(2)=48.99253706;
MovMH(3)=48.99580205;
MovMH(4)=48.99813423;
MovMH(5)=48.99953356;
MovMH(6)=49.00000000;
MovMH(7)=48.99953356;
MovMH(8)=48.99813423;
MovMH(9)=48.99580205;
MovMH(10)=48.99253706;
MovMH(11)=48.99253706; %zero u
MovMH(12)=48.99580205;
MovMH(13)=48.99813423;
MovMH(14)=48.99953356;
MovMH(15)=49.00000000;
MovMH(16)=48.99953356;
MovMH(17)=48.99813423;
MovMH(18)=48.99580205;
MovMH(19)=48.99253706;
MovMH(20)=48.99253706; %zero u

%ms = 0.135*pi % Mast Speed
MH=49; % Mast Height is 49 meters.

R=15000; % Range when Mast is vertical is 15Km.
```

```
for i=1:20;

%fprintf('Input Value was = %6.6f\n', MovMH);

%fprintf('Input Value was = %6.6f\n', MovR);
% Function Input Parameters : lamda (f=5GHz), a (0m), R (15Km), B (1m), h (2Km), Mast
Height (49m)
[h, R1, R2, phi, theta, zreal, z, R, y] = RIF1(0.06,0,MovR(i),1,2000,MovMH(i));
%fprintf('Data Explanation : [i] [h] [R1] [R2] [phi] [theta] [zreal] [z] [R] [y]\n');

% Radar InterFerometer (RIF) Array
%i=1; % RIF Index
RIF(i).h     = h;
RIF(i).R1    = R1;
RIF(i).R2    = R2;
RIF(i).phi   = phi;
RIF(i).theta = theta;
RIF(i).zreal = zreal;
RIF(i).z     = z;
RIF(i).R     = R;
RIF(i).y     = y;

%fprintf('%-+6.2f %-+6.2f %-+6.6f %-+6.6f %-+6.6f %-+6.6f %-+6.10f %-+6.10f %-
+6.10f\n',
%h, R1, R2, phi, theta, zreal, z, R, y);

fprintf('%1d %-+6.2f|%-+6.2f|%-+6.2f|%-+6.10f|%-+6.6f|%-+6.8f|%-+6.8f|%-+6.8f|%-
+6.8f\n', ...
 i,RIF(i).h, RIF(i).R1, RIF(i).R2, RIF(i).phi, RIF(i).theta, RIF(i).zreal, RIF(i).z,
RIF(i).R, RIF(i).y);


end;

fprintf(' k   HorVector [m]    VerVector[m]    Magnitude[m]  Velocity[m/sec]
Velocity[Km/h]    Doppler[Hz]\n');

for k = 1:19;
HorVector = RIF(k).y-RIF(k+1).y; % Horizontal Length Vector Component
VerVector = RIF(k+1).z-RIF(k).z; % Horizontal Length Vector Component
Magnitude = sqrt((HorVector^2)+(VerVector^2));
Velocity  = HorVector/SampleTime;
Velocityk = Velocity*3.6;
DV   = 2*Velocity/lamda; % Doppler wrt Velocity
VDF(k).DV = DV; % Velocity Doppler Frequency Array

fprintf('|%d| |%-+6.10f| |%-+6.10f| |%-+6.10f| |%-+6.10f| |%-+6.10f| |%-+6.10f|\n',
...
   k, HorVector, VerVector, Magnitude, Velocity, Velocityk, DV);

end;

% Plotting Vectors
% ---------------------------------------------------------------------------
%zrealplot = [RIF(1).zreal RIF(2).zreal RIF(3).zreal RIF(4).zreal RIF(5).zreal
RIF(5).zreal];
%phiplot   = [RIF(1).phi   RIF(2).phi   RIF(3).phi   RIF(4).phi   RIF(5).phi   ];
z1plot     = [RIF(1).z RIF(2).z RIF(3).z RIF(4).z RIF(5).z  RIF(6).z RIF(7).z RIF(8).z
RIF(9).z RIF(10).z];
y1plot     = [RIF(1).y RIF(2).y RIF(3).y RIF(4).y RIF(5).y  RIF(6).y RIF(7).y RIF(8).y
RIF(9).y RIF(10).y];


plot(y1plot,z1plot,'b>-');

%axis([RIF(1).y-1 RIF(9).y+1 RIF(1).z-1 RIF(9).z+1]);
title ('Moving Interferometer - Towards Radar');
xlabel ('Radar Estimated Target Range');
ylabel('Radar Estimated Target Height');
grid on;

% ---------------------------------------------------------------------------

z2plot     = [RIF(11).z RIF(12).z RIF(13).z RIF(14).z  RIF(15).z RIF(16).z RIF(17).z
RIF(18).z RIF(19).z];
y2plot     = [RIF(11).y RIF(12).y RIF(13).y RIF(14).y  RIF(15).y RIF(16).y RIF(17).y
RIF(18).y RIF(19).y];

figure;
plot(y2plot,z2plot,'b<-');
```

```
%axis([RIF(1).y-1 RIF(9).y+1 RIF(1).z-1 RIF(9).z+1]);
title ('Moving Interferometer - Away from Radar');
xlabel ('Radar Estimated Target Range');
ylabel('Radar Estimated Target Height');
grid on;

% ----------------------------------------------------------------------------

sampleinstance = [1 2 3 4 5 6 7 8 9 10 11 12 13 14 15 16 17 18 19];
dopplerv       = [VDF(1).DV  VDF(2).DV  VDF(3).DV  VDF(4).DV  VDF(5).DV  VDF(6).DV
VDF(7).DV  VDF(8).DV  VDF(9).DV VDF(10).DV ...
                  VDF(11).DV VDF(12).DV VDF(13).DV VDF(14).DV VDF(15).DV VDF(16).DV
VDF(17).DV VDF(18).DV VDF(19).DV];

figure;
plot(sampleinstance,dopplerv,'b>-');
title ('Moving Interferometer - Doppler Frequency');
xlabel ('Radar Sample Instance');
ylabel('Radar Doppler Frequency');
grid on;

% ----------------------------------------------------------------------------
```

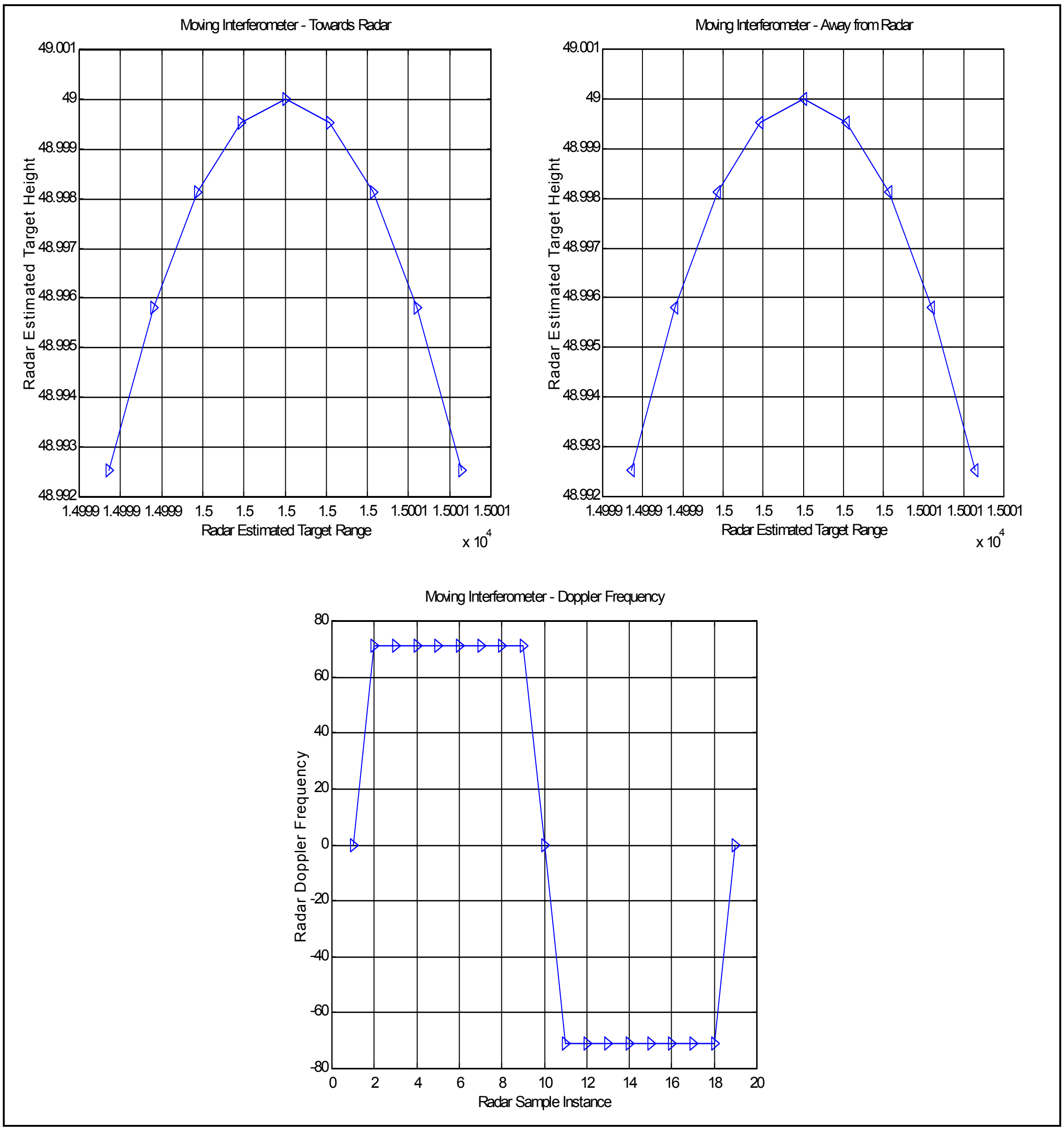

Figure 12.3.1.F1. Moving Interferometer Demonstration Simulation.

12.3.2. Interferometric ISAR Routine

The following routine tracks the movement of the ship target every 1 millisecond.

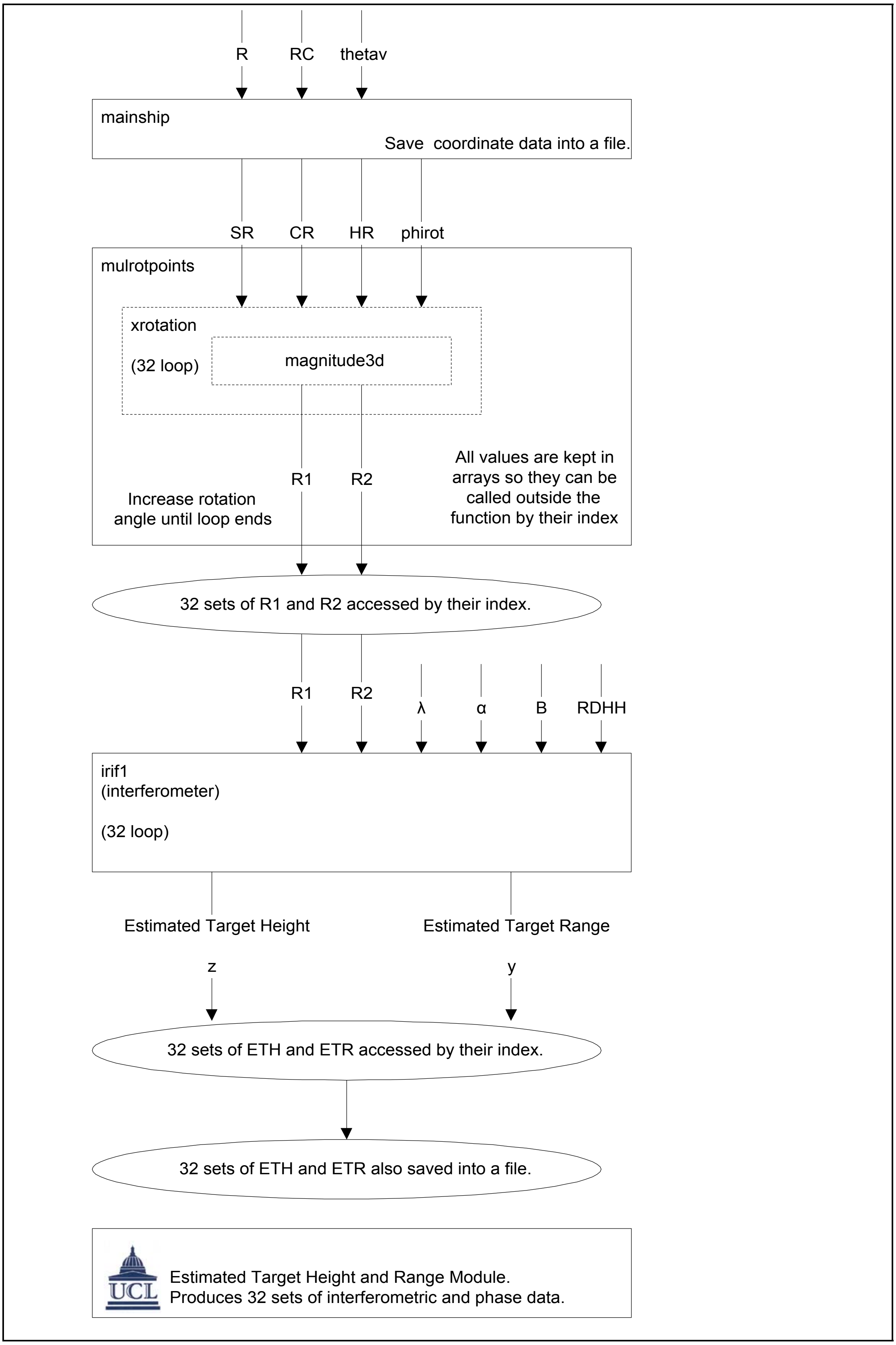

Figure 12.3.2.F1. Height Interferometric Profiles Generator Module.

This simulation uses a different Radar Interferometer approach from the previous section which is detailed in figure 12.3.2.F2. below.

IRIF1 Function Input Parameters

R1	R1 Range
R2	R2 Range
λ	Wavelength
α	Antenna Tilt
B	Baseline
H	Radar Height

$$\phi = \frac{2\pi}{\lambda}\left(R_2 - R_1\right)$$

Calculate the phase difference φ from the geometry of Figure 5.4.F1.

$$\theta = \cos^{-1}\left(\frac{R_2{}^2 - R_1{}^2 - B^2}{2BR_1}\right) - a$$

Calculate the angle θ between R1 and H from the geometry of Figure 5.4.F1.

$$z = H - R_1 \cos\theta$$

Calculate Radar Estimated Target Height z from the geometry of Figure 5.4.F1.

$$y = \sqrt{R_1{}^2 - \left(H - z\right)^2}$$

Calculate Radar Estimated Target Range y from the geometry of Figure 5.4.F1.

RIF1 Function Output Parameters

H	Radar Height
R1	R1 Range
R2	R2 Range
φ	Phase Difference
θ	Angle
z	Radar Estimated Target Height
y	Radar Estimated Target Range

Figure 12.3.2.F2. IRIF Function.

12.4. ISAR Simulation

The ISAR software was done in two parts. First the results we acquired with a non-automatic method so their validity could be checked. And then a major reprogramming task followed to automate the FFT procedures that follow the slant range profiles. Finally the ISAR simulation listings are found in the accompanying cd rom.

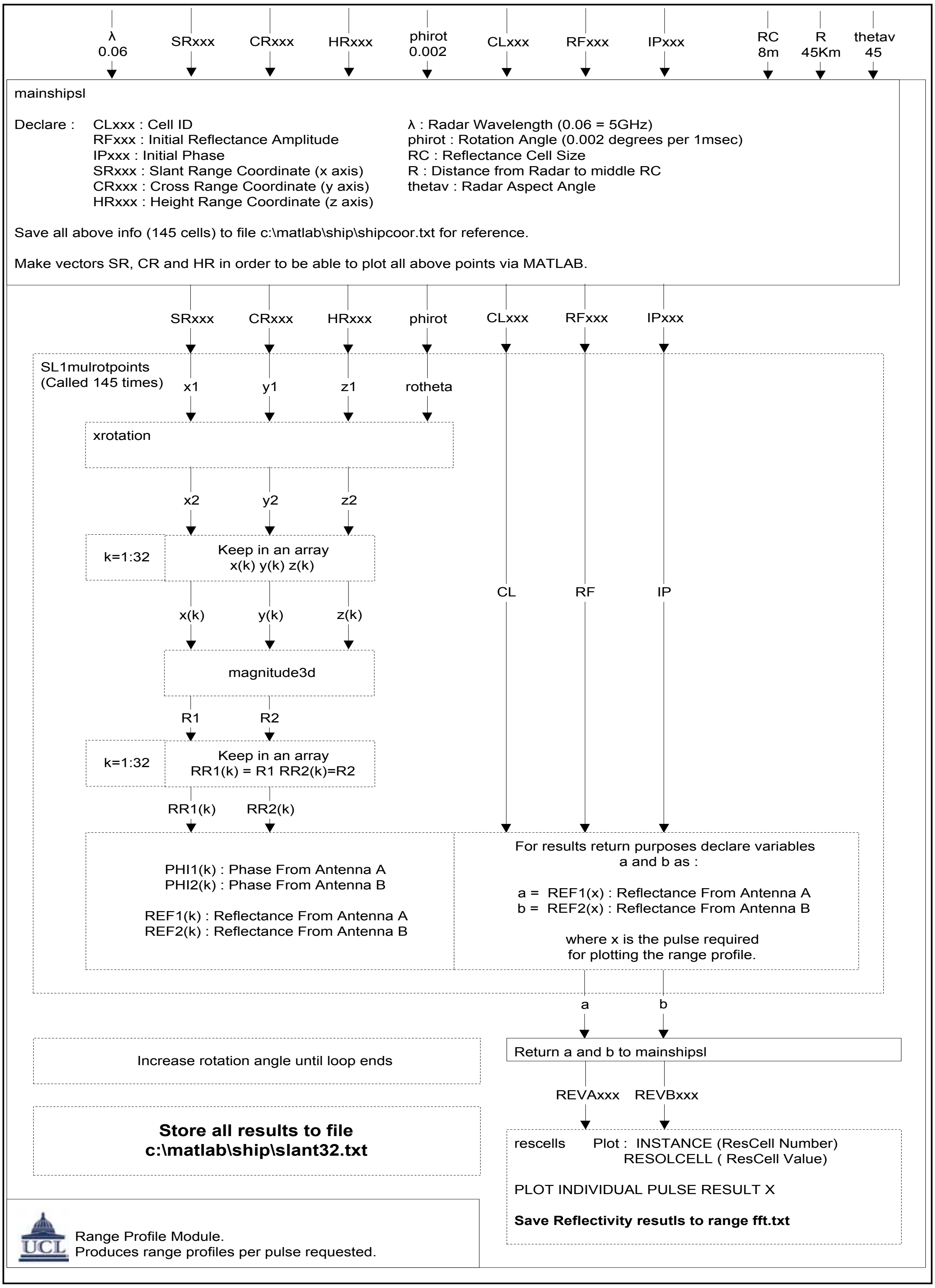

Figure 12.4.F1. Range Profiles Generator Module - Non-Automatic Results Procedure.

Now the following software automates the steps shown in figure 12.4.F1. The movement processing steps are the same and are shown in figure 12.4.F2.

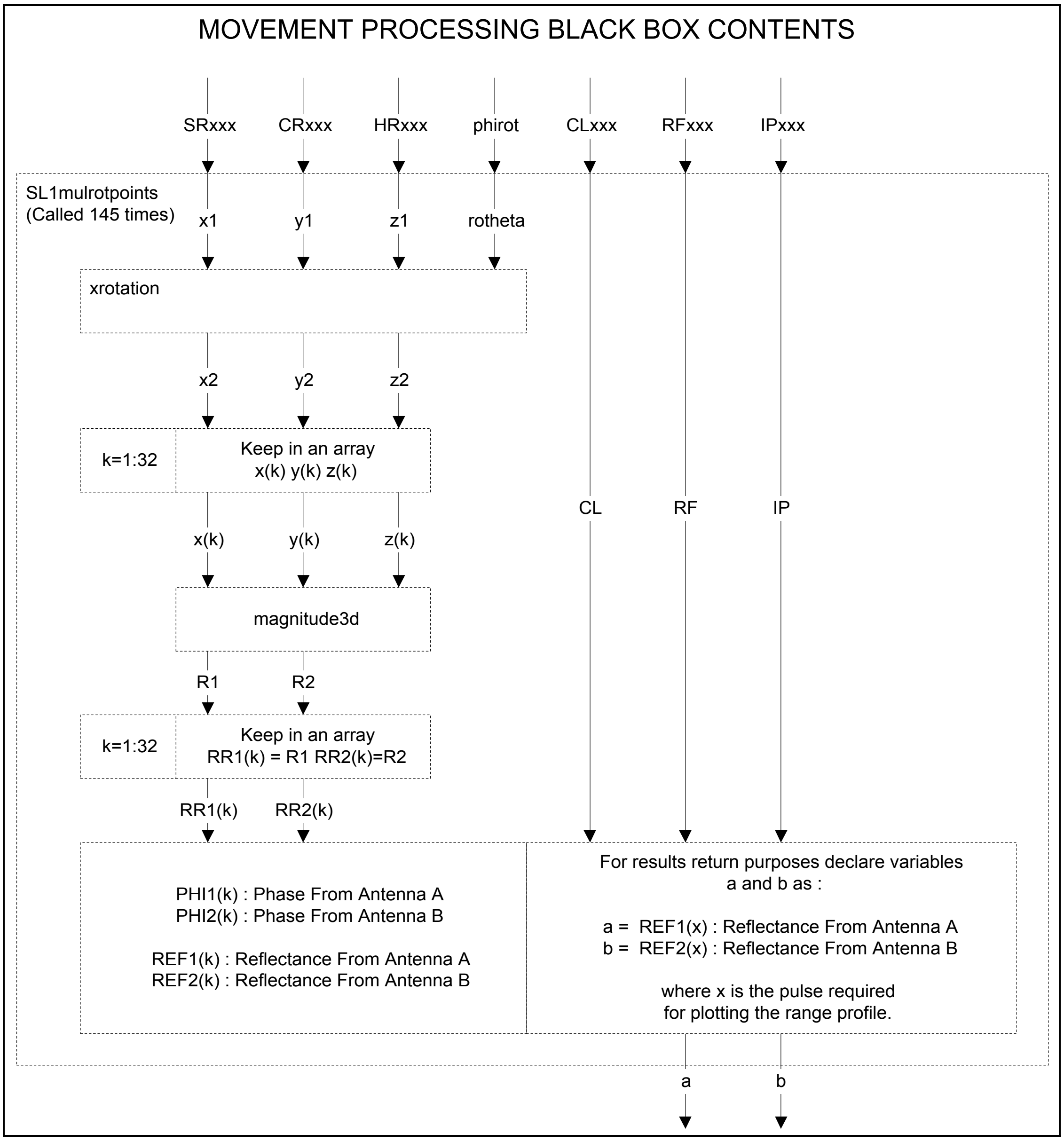

Figure 12.4.F2. Movement Processing Black Box Contents.

Now the process was automated as shown in figure 12.4.F3.

λ 0.06 | SRxxx | CRxxx | HRxxx | phirot 0.002 | CLxxx | RFxxx | IPxxx | RC 8m | R 45Km | thetav 45

mainshipsl

Declare :
CLxxx : Cell ID
RFxxx : Initial Reflectance Amplitude
IPxxx : Initial Phase
SRxxx : Slant Range Coordinate (x axis)
CRxxx : Cross Range Coordinate (y axis)
HRxxx : Height Range Coordinate (z axis)

λ : Radar Wavelength (0.06 = 5GHz)
phirot : Rotation Angle (0.002 degrees per 1msec)
RC : Reflectance Cell Size
R : Distance from Radar to middle RC
thetav : Radar Aspect Angle

Save all above info (145 cells) to file c:\matlab\ship\shipcoor.txt for reference.

Make vectors SR, CR and HR in order to be able to plot all above points via MATLAB.

SRxxx | CRxxx | HRxxx | phirot | CLxxx | RFxxx | IPxxx

MOVEMENT PROCESSING BLACK BOX
Note : Contents are shown separately

Increase rotation angle until loop ends

a01 ... a32 | b01 ... b32

Now ALL a and b return to mainshipsl and are assigned to diffent variables before they change for the next point

ANTENNA 1 : a01 = PxxxAyy, where xxx is the Point ID (ie 001) and yy is the movement profile (ie 01, 02, ...,32)

ANTENNA 2 : b01 = PxxxByy, where xxx is the Point ID (ie 001) and yy is the movement profile (ie 01, 02, ...,32)

Now the REFLECTANCE MAP is initiated.

Group all points that have common yy (ie Points P001A01 ... P145A01). (mainshipslb groups all common B points)

Pass them through to the radar beam function ResCellsANT1

mainshipsla	mainshipslb
ANTENNA 1 : a01 = PxxxAyy, where xxx is the Point ID (ie 001) and yy is the movement profile (ie 01, 02, ...,32)	ANTENNA 2 : b01 = PxxxByy, where xxx is the Point ID (ie 001) and yy is the movement profile (ie 01, 02, ...,32)

PxxxAyy
[xxx = 001 to 145]
[yy = 01 ...32]

PxxxByy
[xxx = 001 to 145]
[yy = 01 ...32]

ResCellsANT1

REVAxxx

NOTE : The prefix ANT1 is used by both antennas.

NOTE : The prefix REVA is used by both antennas.

REVAxxx

SLRnnVmm
[nn=01...32]
[mm=01...33]

NOTE : The processes for the two antennas are not parallel - they are performed by two files (mainshipsla - mainshipslb).

SLRnnVmm
[nn=01...32]
[mm=01...33]

Now the SLANT RANGE PROFILES are in mainshipsl.

Make vectors SLRnnV that represent the 32 slant range profiles.
Plot SLRnnV vs Resolution Cell ID (1...33)

Make vectors VmmANT1 that represent the 33 vertical cut of the SRP.
Make associated vectors DFTAVmm that are the fft of the VmmANT1 vectors.
Plot DFTAVmm vs Resolution Cell ID (1...33)

Range Profile Module- Automated Processing.
Produces Slant Range Profiles and ISAR Height Information per pulse requested.

Figure 12.4.F3. Range Profiles Generator Module - Automatic Results Procedure.

12.4.1. Test procedure for verifying correctness of reflectance values

The MAINSHIPSL program was first fed with all reflectance values set to 1 and all initial phases set to 0. The SL1MulRotPoints routine shown in Listing 10.4.L1. was modified to include only the initial values and phases. Modifications are shown in enlarged bold characters. The result is shown in Figure 10.4. which is the expected correct result for a 45 degrees radar viewing angle.

```
for k = 1:32;

[x2,y2,z2] = xrotation (x1,y1,z1,rotheta);

x(k) = x2;
y(k) = y2;
z(k) = z2;

% fprintf('Rotated  Coords %d %6.6f %6.6f %6.6f \n', k, x2, y2, z2);

% Call the coordinate function and calculate the distances from the radar to the new
point.

[R1,R2] = Magnitude3D(x(k),y(k),z(k));

% fprintf('R1 = %6.6f R2 = %6.6f \n', R1, R2);

% Turn R1 R2 into arrays

RR1(k) = R1;
RR2(k) = R2;

%PHI1(k) = IP + ( (2*pi/lamda)*(2*RR1(k)) );
%PHI2(k) = IP + ( (2*pi/lamda)*(2*RR2(k)) );

PHI1(k) = IP; % + ( (2*pi/lamda)*(2*RR1(k)) );
PHI2(k) = IP; % + ( (2*pi/lamda)*(2*RR2(k)) );

REF1(k) = RF * ( cos(PHI1(k)) + i*sin(PHI1(k)) ) ;
REF2(k) = RF * ( cos(PHI2(k)) + i*sin(PHI2(k)) ) ;

%fprintf(fid,'%6.6f %2.0d %6.6f %6.6f %6.6f %6.6f %6.6f %6.6f \n', CL, k, RR1(k),
RR2(k), PHI1(k), PHI2(k), REF1(k), REF2(k) );

rotheta = rotheta + 0.00003490658504; % 0.002 degrees.

end;
```

Listing 12.4.1.L1. Part of SL1MulRotPoints Routine modified for test purposes.

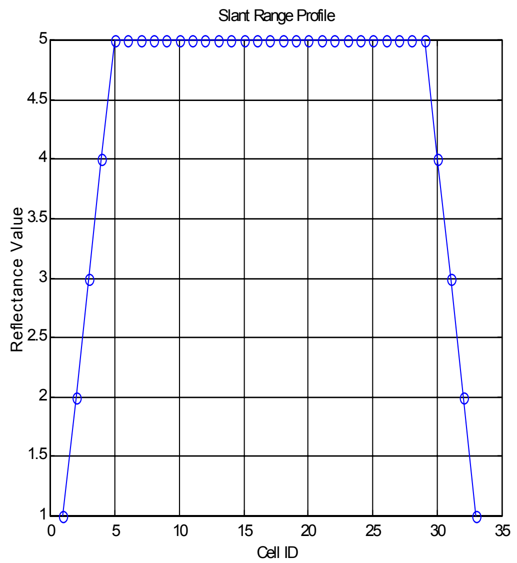

Figure 12.4.1.F2. Test Reflectance Map (initial reflectance values 1 and initial phases 0).

12.4.1.1. Basic Permutation 1.

1 TEST MODEL - INITIAL PHASE 0 ONLY NOT DEPENDENT ON RADAR RANGE

Setting all amplitudes to 1 and all initial phases to 0 the following two graph pairs are acquired :

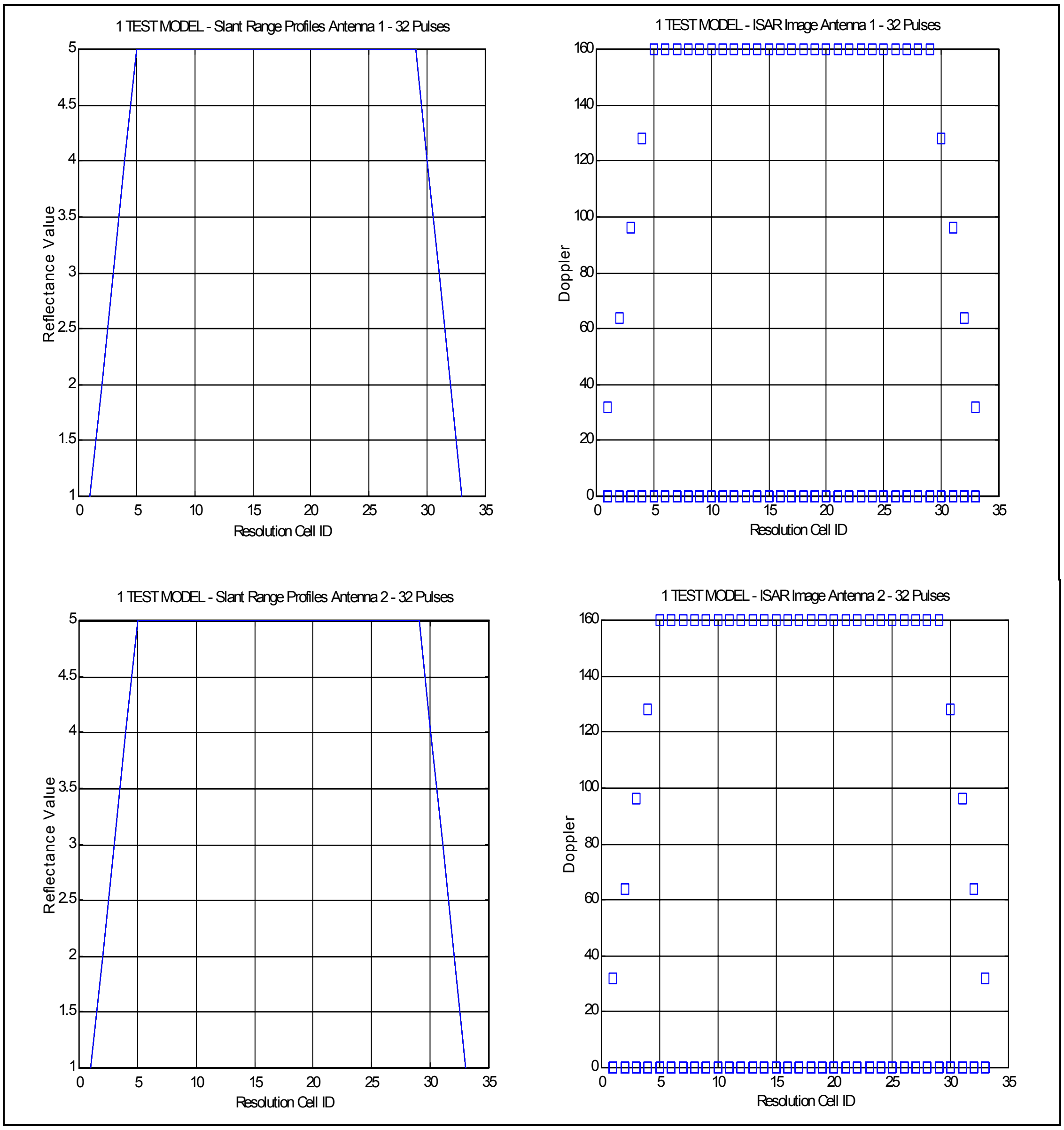

Figure 12.4.1.1.F1. Permutation 1 Test Model - Not dependent on range from radar.

12.4.1.2. Basic Permutation 2.

2 TEST MODEL - DEPENDENT ON DISTANCE RELATED PHASE

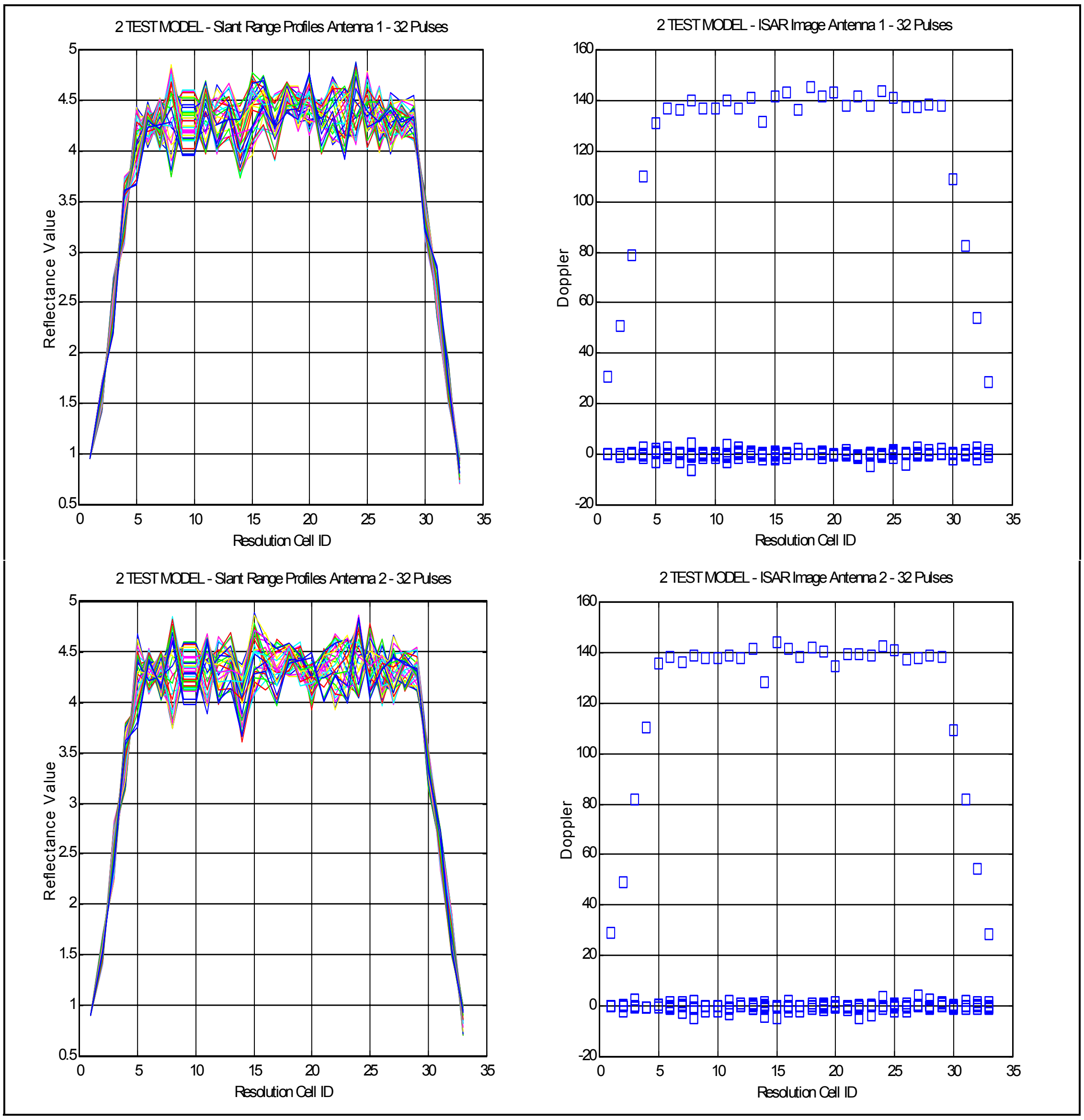

Figure 12.4.1.2.F1. Permutation 2 Test Model - Dependent on range from radar.

12.4.1.3. Basic Permutation 3.

3 MORE REALISTIC MODEL - COMPLETE WITH PHASES - DEPENDENT ON RADAR RANGE

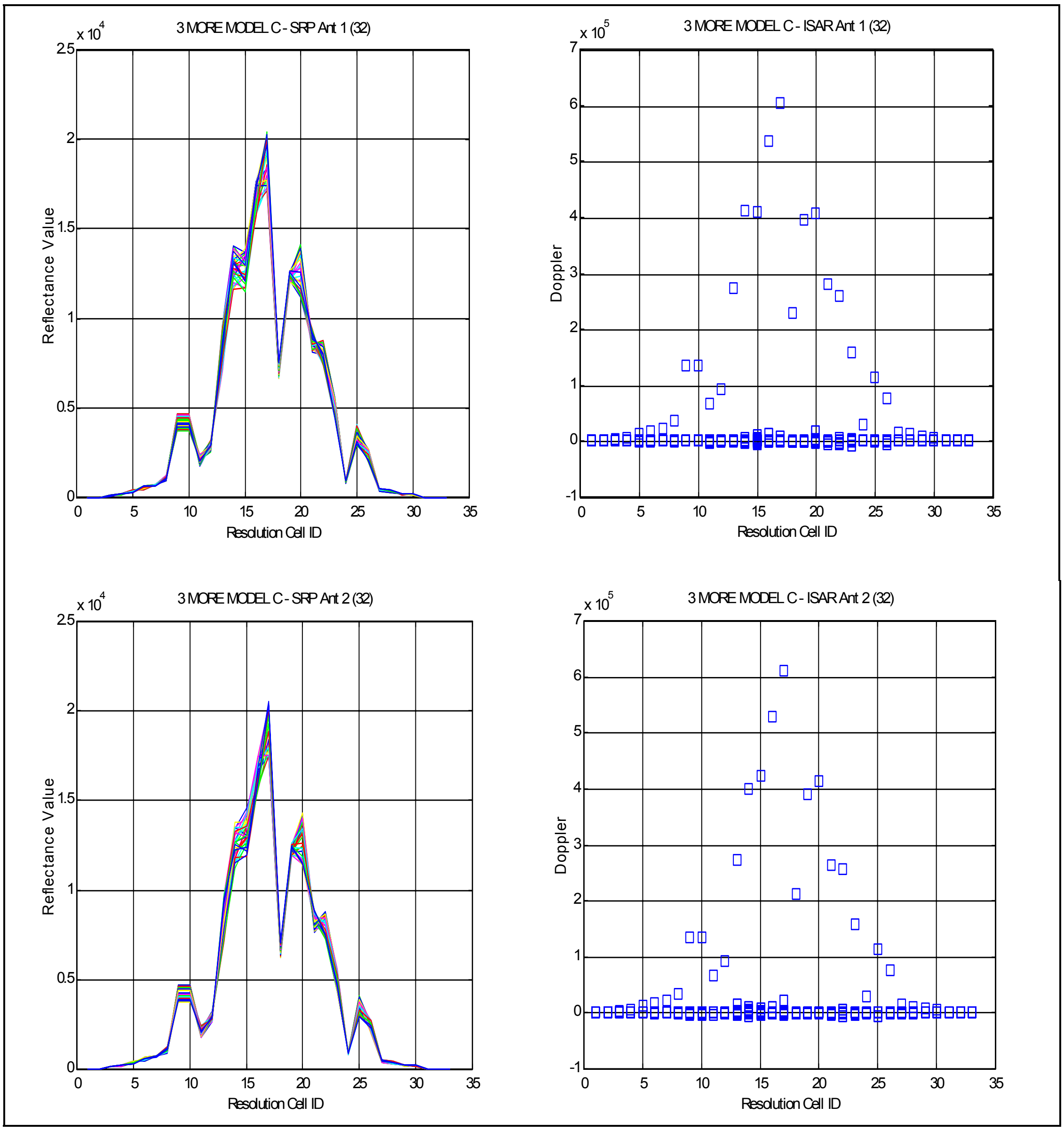

Figure 12.4.1.3.F1. Permutation 3 More Model Complete - Dependent on range from radar.

12.4.1.4. Basic Permutation 4.

4 MORE REALISTIC MODEL - ALL INITIAL PHASES 0 - DEPENDENT ON RADAR RANGE

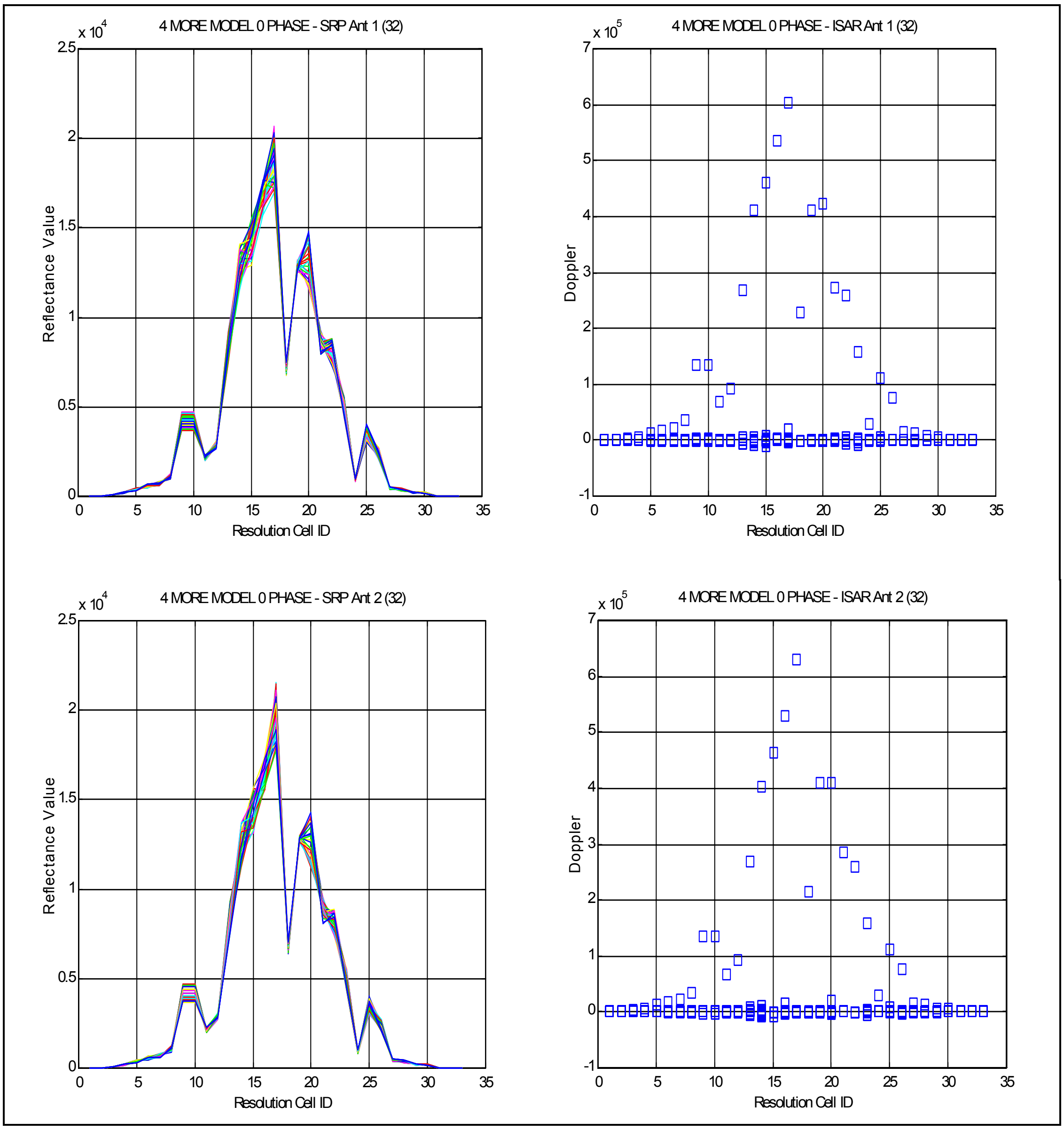

Figure 12.4.1.4.F1. Permutation 4 More Model Zero Initial Phases - Dependent on range.

12.5. Experiments based on the Derived Ship Model

12.5.1. E1 MULTILAYER SHIP MODEL

The logical description of this model is found in section 6.3.3.5.

The results are shown in section 7.1.1.

The ISAR simulation listings for the Multi-Layer Model are called multsla and multslb and are found in the accompanying cd rom.

Also another model was created that had high value reflectance in lower heights ship coordinates. These are the results for this model.

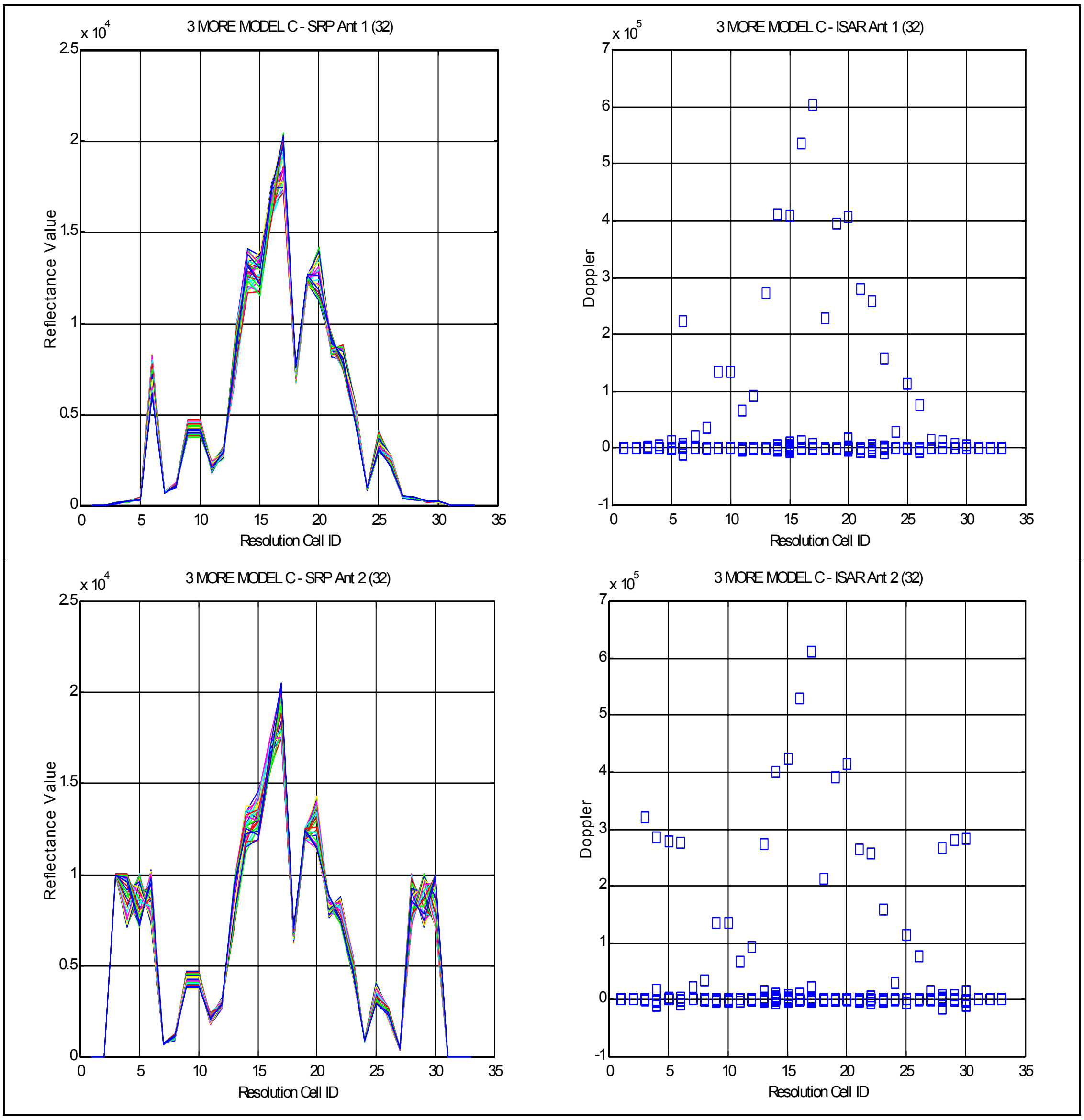

Figure 12.5.2.F1. Bright -End Reflectors in Lower Height Coordinates.

There follows the flow control of the Multi-Layer Model as shown in figure 12.5.1.F1.

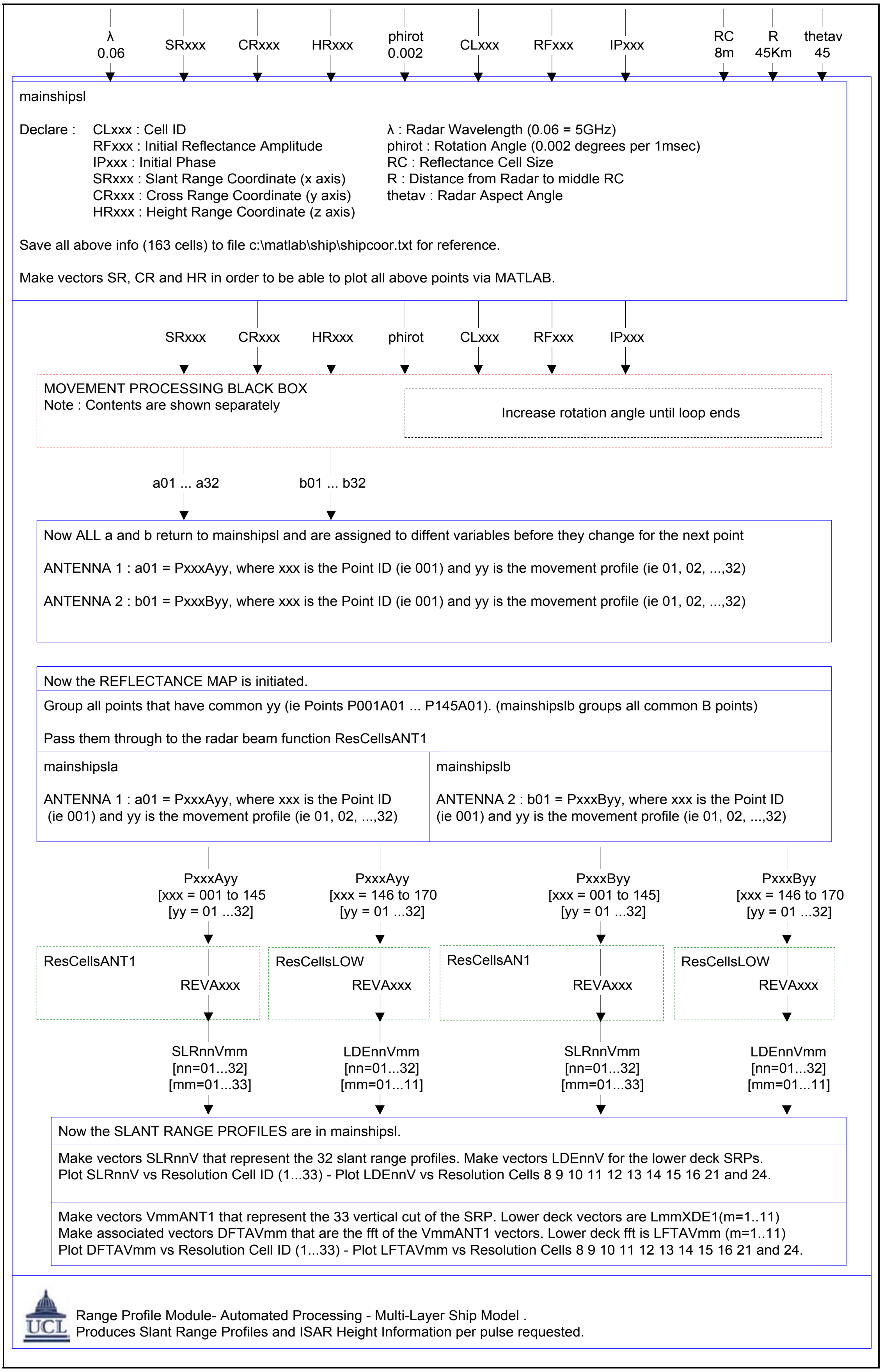

Figure 12.5.F1. Multi-Layer Range Profiles Generator Module - Automatic Results Procedure.

12.5.2. E2 NOISE CONSIDERATIONS

12.5.2.1. Noise levels at 15dB

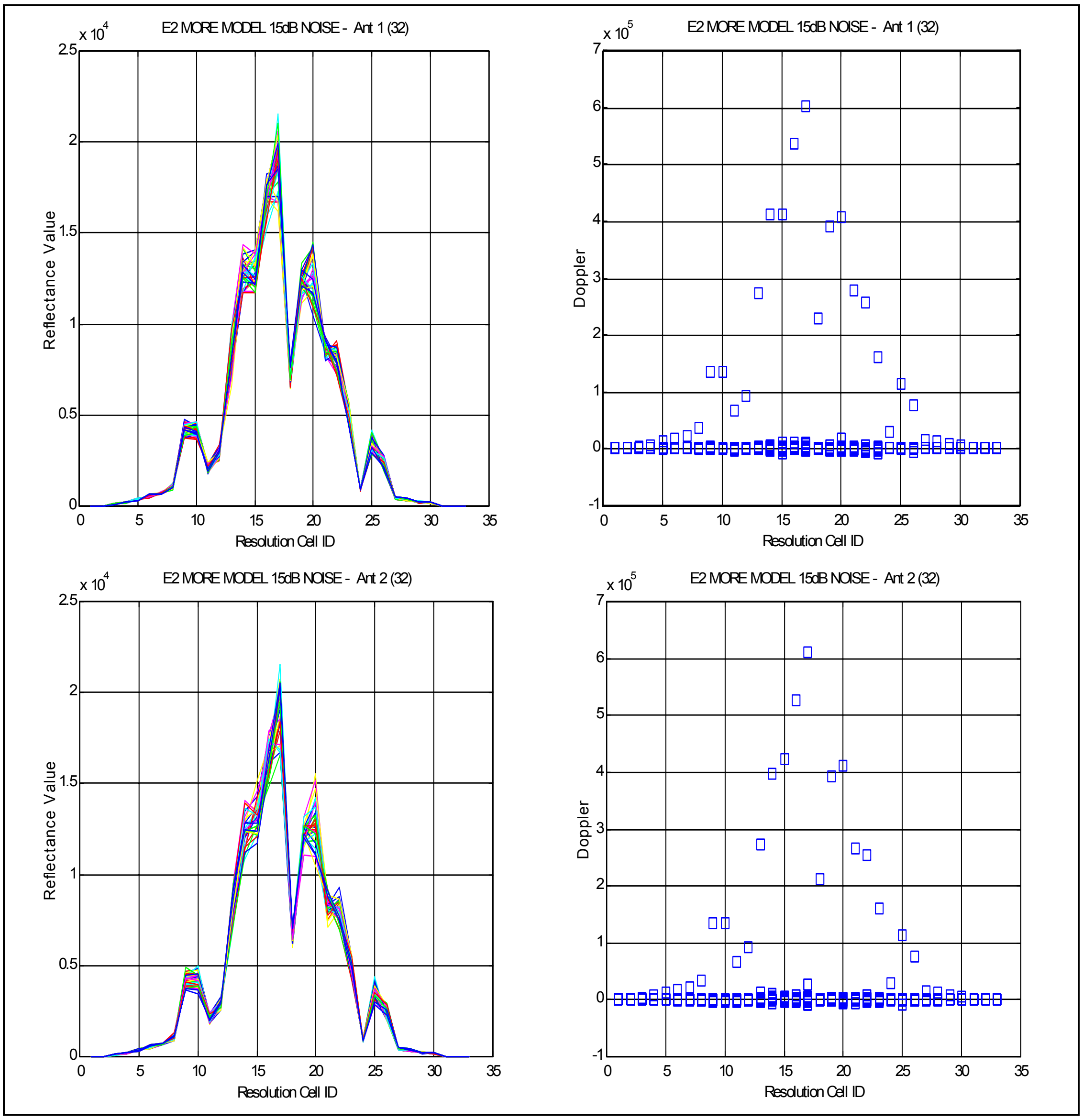

Figure 12.5.2.1.F1. Noise levels results at 15dB.

12.5.2.2. Noise levels at 20dB

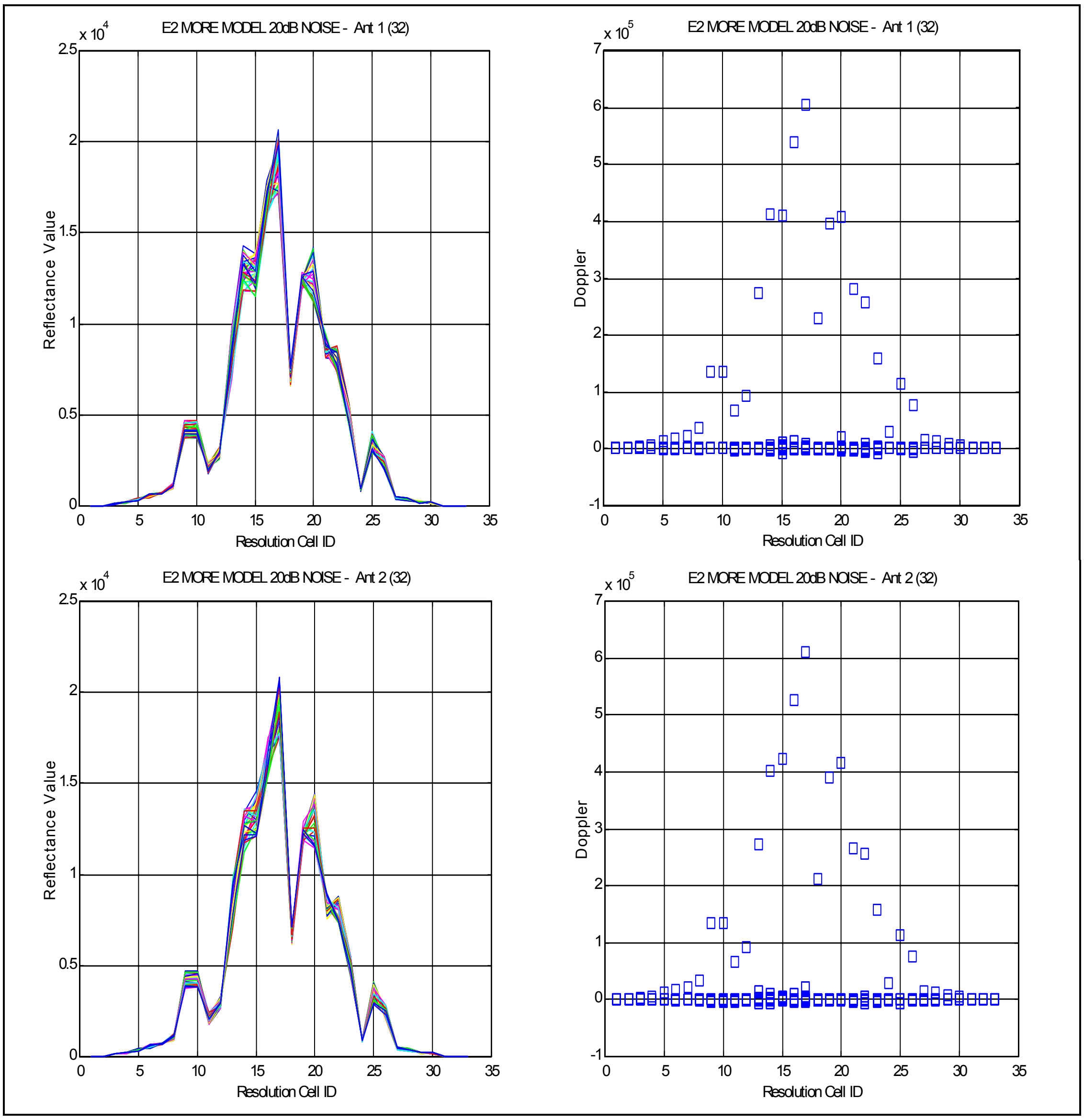

Figure 12.5.2.2.F1. Noise levels results at 20dB.

12.5.3. E3 ISAR INTENSITY COLOUR CODING

There is no additional information for this section as of the submission date.

12.5.4. E4 INTERFEROMETRY & ISAR HEIGHT COMPARISONS

There is no additional information for this section as of the submission date.

12.5.5. E5 ROTATION VECTOR MEASUREMENT

There is no additional information for this section as of the submission date.

12.5.6. E6 ORIENTATION & SCALING OF THE ISAR IMAGE

There is no additional information for this section as of the submission date.

12.5.6.1. ISAR CORRECTION IN 3D SPACE

There is no additional information for this section as of the submission date.

12.5.7. E7 TRANSLATIONAL MOTION

12.5.7.1. Translational Motion at 05 Knots

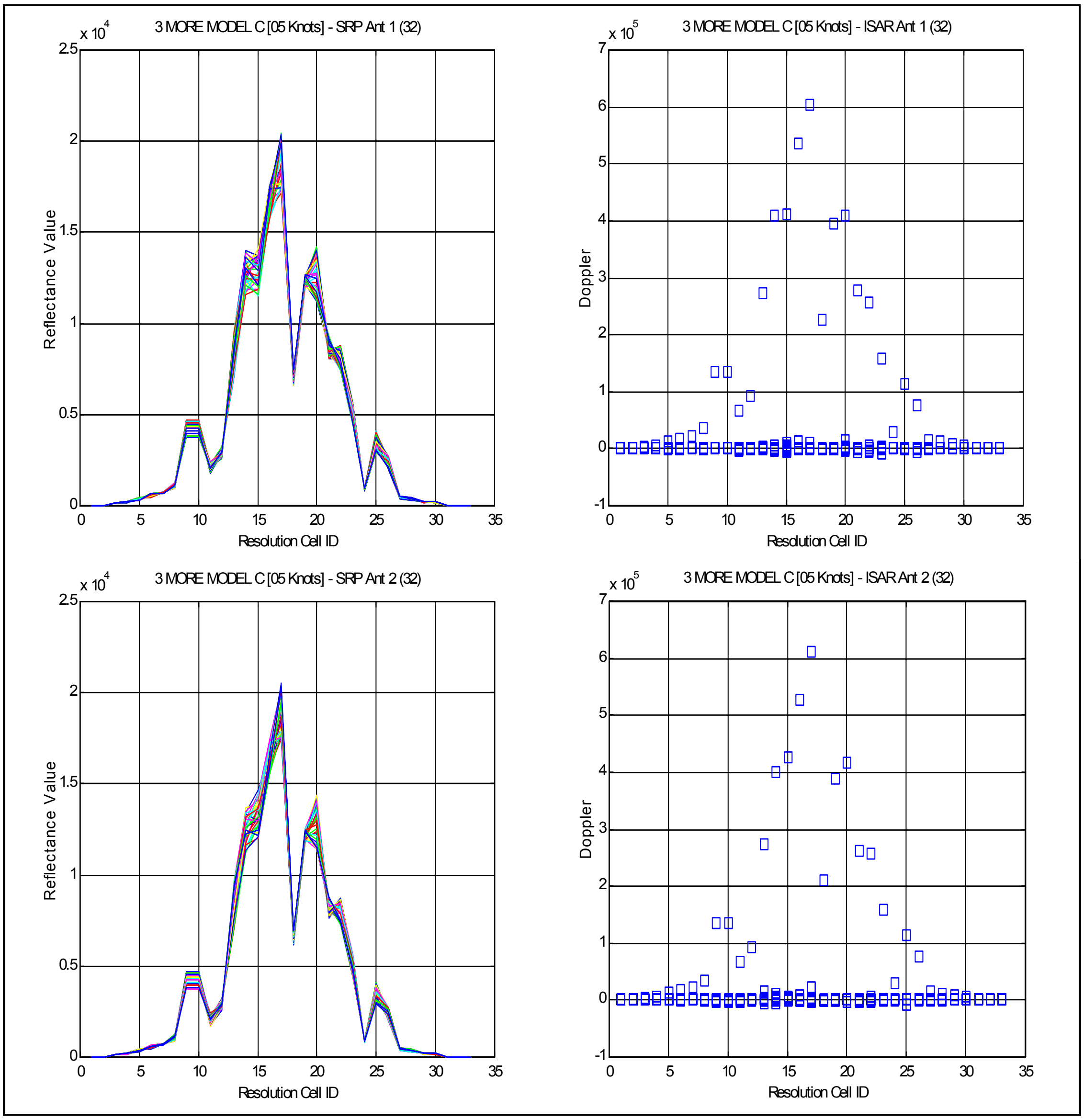

Figure 12.5.7.1.F1. Translational motion results at 05 Knots.

12.5.7.2. Translational Motion at 15 Knots

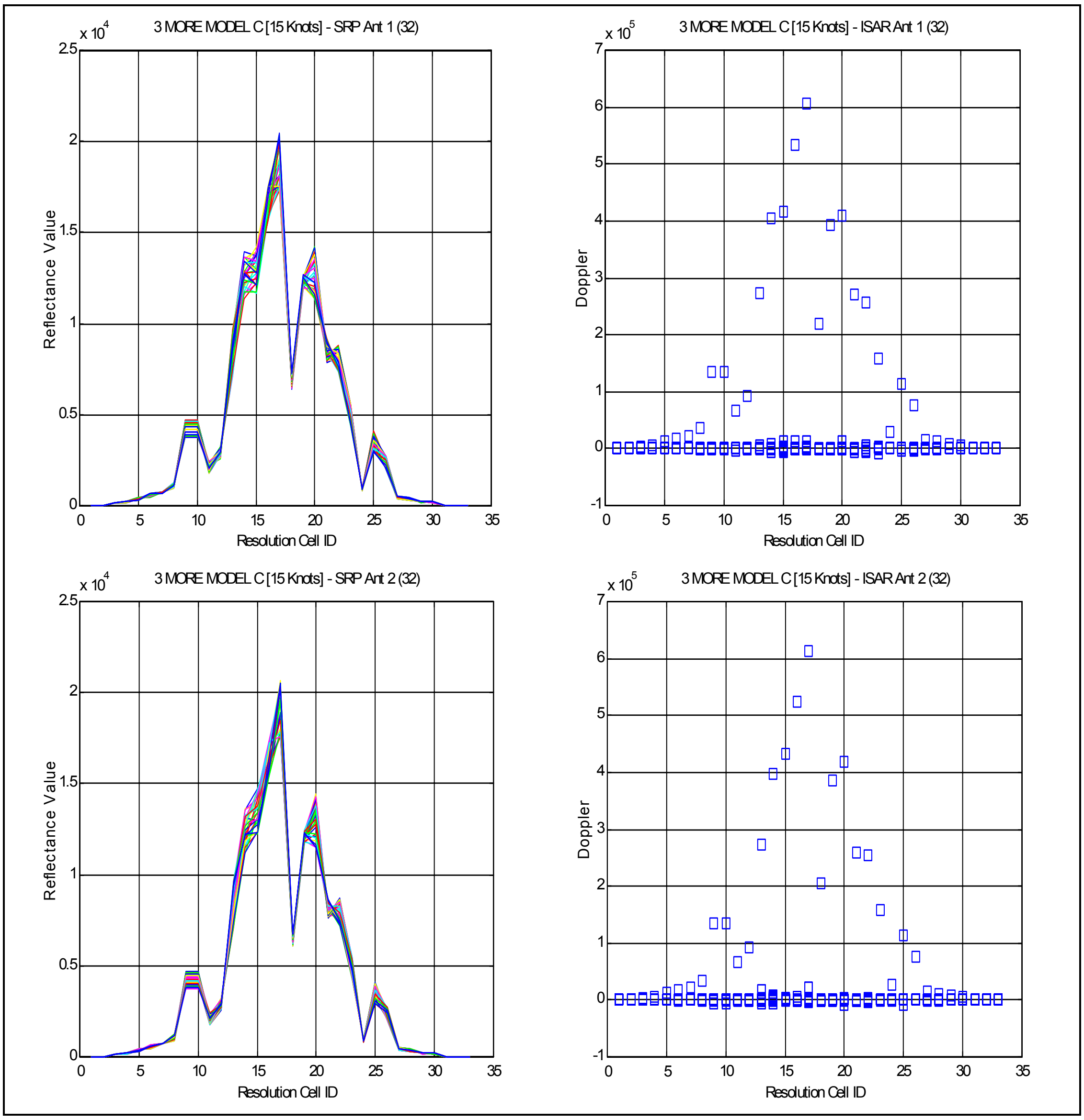

Figure 12.5.7.2.F1. Translational motion results at 15 Knots.

12.6. MATLAB Created Text Data Files

The following files produced text files with results that helped to develop the automatic processes. All files are saved during execution in subdirectory c:\matlab\ship\<filename>.txt

---

1. SHIPCOOR.TXT

Function	Filename						
mainshipsl	shipcoor	CLxxx	RFxxx	IPxxx	SRxxx	CRxxx	HRxxx

Saves all ship coordinates and attributes from the main calling program.

CLxxx : Cell ID
RFxxx : Point Scatterer Reflectivity Amplitude
Ipxxx : Point Scatterer Initial Phase
SRxxx : Slant Range
CRxxx : Cross Range
HRxxx : Height Range

---

2. XROTATION.TXT

Function	Filename							
xrotation	coords	x1	y1	z1	x2	y2	z2	rotheta

Saves the starting coordinates and the rotated coordinates together with the corresponding rotation angle.

---

3. SLANT32.TXT

Function	Filename								
SL1MulRotPoints	slant32	CL	k	RR1 (k)	RR2 (k)	PHI1 (k)	PHI2 (k)	REF1 (k)	REF2 (k)

Saves the cell number and the instance that corresponds to the following information :

RR1 : Distance from point scatterer on vessel to Lower Radar Antenna.
RR2 : Distance from point scatterer on vessel to Higher Radar Antenna.
PHI1 : Point scatterer phase (initial value and distance from Lower Radar Antenna).
PHI2 : Point scatterer phase (initial value and distance from Higher Radar Antenna).
REF1 : Point scatterer reflectivity (initial value and phase from Lower Radar Antenna).
REF2 : Point scatterer reflectivity (initial value and phase from Higher Radar Antenna).

---

4. RANGEFFT.TXT

Function	Filename		
ResCellsA	rangefft	resindex	RESOLARRAY(resindex)

Saves the resolution cell index (1 to 33) together with the corresponding reflectivity.

12.7. KMS BISMARCK

Figure 12.6.F1. KMS Bismarck Crest.

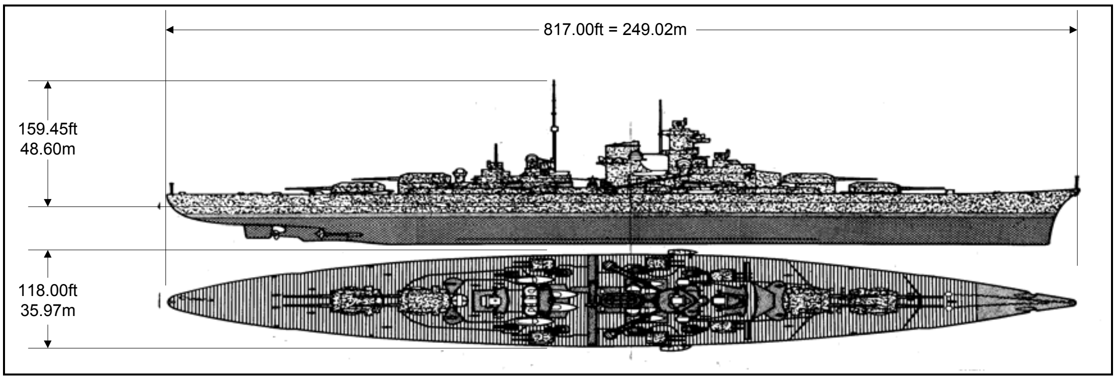

Figure 12.6.F1. KMS Bismarck blueprint.

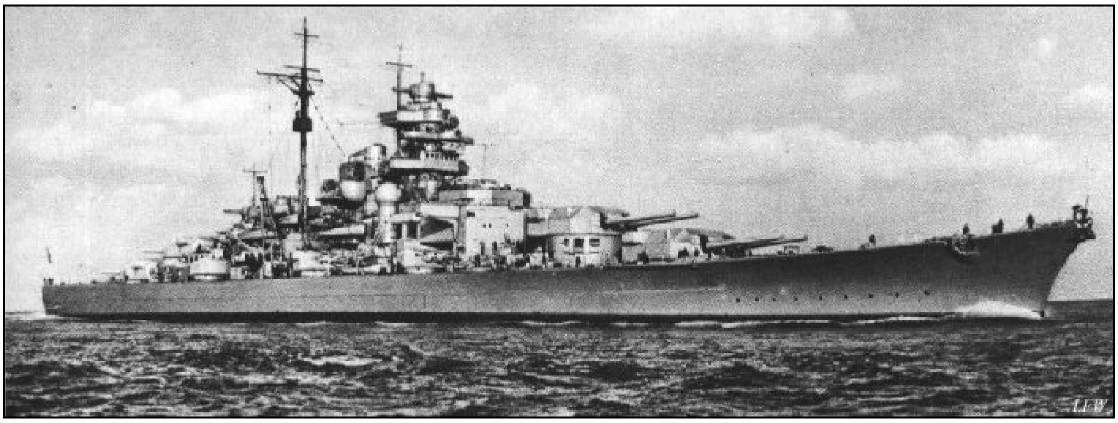

Figure 12.6.F2. Deutsche KriegsMarine Schlachtschiff Bismarck.

Type of Vessel : Battleship	Launched : February 14, 1939 Blohm & Voss Shipyards, Hamburg
Commissioned: August 24, 1940	First military operation: May 18, 1941
Length: 817' (249.02m)	Breadth: 118' (35.97m)
Maximum speed: 30.8 knots	Displacement: 50,950 tons
Hull: Clad with thick armour plate	Armaments: Four giant double 38cm gun turrets capable of 36Km hit range.
Sank: May 27, 1941 (Atlantic Ocean)	Crew onboard: 2,091

CD Theme
The lower part of the CD cover features the firing of a devastating salvo from KMS Bismarck which was capable of an operating range of thirty-six kilometers. And the top-part features some of the InISAR process results obtained while observing the target at the relatively safe distance of forty-five kilometers.

T. KOSTIS UCL 9011874

September 2001.
Printed & Bound in England.